THESIS ON MECHANICAL AND INSTRUMENTAL ENGINEERING E60

Duplex Treatment of Steel Surface

ANDREI SURZHENKOV

TUT PRESS

TALLINN UNIVERSITY OF TECHNOLOGY
Faculty of Mechanical Engineering
Department of Materials Engineering

Dissertation was accepted for the defence of the degree of Doctor of Philosophy in Engineering on April 19th, 2011.

Supervisor: Prof. Priit Kulu, Faculty of Mechanical Engineering, Department of Materials Engineering, Tallinn University of Technology

Opponents: Prof. Jakob Kübarsepp, Faculty of Mechanical Engineering, Department of Materials Engineering, Tallinn University of Technology

Prof. Petri Vuoristo, Department of Materials Science, Faculty of Automation, Mechanical and Materials Engineering, Tampere University of Technology

Defense of the thesis: June 13th, 2011 at 14:00
Room No.: V-215
Tallinn University of Technology
Ehitajate tee 5, 19086 Tallinn, Estonia

Declaration:
Hereby I declare that this doctoral thesis, my original investigation and achievement submitted for the doctoral degree at Tallinn University of Technology has not been submitted for any academic degree.

/Andrei Surženkov/

Euroopa Liit
Euroopa Sotsiaalfond
Eesti tuleviku heaks

ISSN: 1406-4758
ISBN: 978-9949-23-115-7 (publication)
ISBN: 978-9949-23-116-4 (PDF)

MASINA- JA APARAADIEHITUS E60

Terase pinna duplekstöötlus

ANDREI SURZHENKOV

TTÜ KIRJASTUS

CONTENTS

LIST OF ABBREVIATIONS AND SYMBOLS

ABBREVIATIONS

ABRW – Abrasive Block on Ring Wear
AEW – Abrasive Erosive Wear
AIW – Abrasive Impact Wear
ASTM – American Standards for Materials Testing
BoP – Ball-on-Plate
BoR – Block-on-Ring
CI – Cyclic Indentation
CoF – coefficient of friction
CS – Carbon Steel
CVD – Chemical Vapor Deposition
CWTS – Cold Work Tool Steel
DLC – Diamond Like Carbon
EDS – Energy Dispersive Spectroscopy
HSS – High Speed Steel
HV- Vickers Hardness
HVOFS – High Velocity Oxy-Fuel Spray
IW – Impact Wear
LH – Laser Hardening
LHZ – Laser Hardened Zone
LT – Laser Treatment
NS – Nitriding Steel
OM – Optical Microscope
PN – Plasma Nitriding
PS – Plasma Spray
PVD – Physical Vapor Deposition
RW – Rubber Wheel
SEM – Scanning Electron Microscope
TS – Thermal Spray

SYMBOLS

E – modulus of elasticity (GPa)
F - normal load (N)
FR – Failed Area Ratio (%)
H – nanohardness of coating (GPa)
I_v – volumetric wear (mm^3/kg)
k – wear coefficient (mm3/Nm)

q – quantity of the abrasive (kg)
r – radius of the ring (m)
t – time of experiment (s)
v – speed of rotation (min^{-1})
Δm – mass loss (kg)

Greek symbols

δ- indentation depth (mm)
σ – indentation stress (GPa)
ρ – density (kg/m^3)

PREFACE

The selection of the appropriate coating for specific application depends on the coating's functional properties, such as fatigue, cracking, wear and frictional resistance. Traditional hard PVD coatings (TiN, Ti(C,N), etc.) and thermal sprayed coatings (hardmetal based, self-fluxing alloy based, etc.) are widely used to increase the wear resistance of steel surfaces in many industrial fields.

Duplex treatment can significantly improve the fatigue, cracking and wear resistance of a material's surface, either uncoated or coated, what may enhance the lifetime of a component up to several times. Among the others, thermal and thermochemical treatments of a coating, applied before or after one's deposition, are one of the most versatile and efficient ways of both thin and thick coatings' modification. However, data is either lacking or controversial in literature about the certain combinations of coating processes and supplementary treatments. This work considers the questions of thin PVD coatings on plasma nitrided (pre-treated) steels, laser hardening of thin PVD coatings on different steel substrates, as well as laser treatment of thick thermal sprayed coatings of various materials. The opportunities of all processes are discussed in the light of variations of coatings' materials, substrates and parameters of treatments. Recommendations are given for the usage of proposed duplex treatments, and future research is planned.

Acknowledgements

I would like to express my sincere gratitude to my supervisor Prof. Priit Kulu of the Department of Materials Engineering of TUT, for providing me the topic of my work, priceless guidance, advice, support and encouragement. I would also like to thank Prof. Renno Veinthal, Head of the Department of Materials Engineering for his support during my work's preparation.

I would like to thank my colleagues from the Department of Materials Engineering for unlimited technical support and consultations, especially PhD Fjodor Sergejev, PhD Mart Saarna, PhD Vitali Podgurski, PhD student Eron Adoberg, PhD student Heikki Sarjas, MSc Dmitri Goljandin, DSc Priit Põdra, DSc Mats-Maidu Nanits and PhD Alina Sivitski from the Department of Mechatronics, MSc Mykola Semeniuk from the Department of Machinery.

I owe great gratitude to Prof. Toomas Pihl from the Tallinn University of Applied Sciences and to PhD Andre Gregor for the versatile co-operation. I would especially like to thank Dr. Habil. Günter Köhler and other collegues from the Günter-Köhler-Institut für Fügetechnik und Werkstoffprüfung (Jena, Gemany), particularly to Dr.Habil.-Eng. Hartmut Müller, Jörg Körner and Steffen Dahms for their priceless help and guidance during my stay in Jena. I am very grateful to Prof. Petri Vuoristo and PhD Jyrki Latokartano from the Tampere University of Technology for the fruitful collaboration and consulting.

I would like to express my gratitude to workers of Reneko Ltd. (Tallinn, Estonia), especially to MSc Vyacheslav Kastyushin for the help and consultations. I thank Andrey Tatmianin from Korund Ltd. (Maardu, Estonia) for his help and guidance.

Finally, I thank my parents, Gennady and Ljubov, for their support and advice during this work's preparation, as well as other relatives and friends for their support and patience.

This work would not have been possible without the support from the Estonian Ministry of Education and Research in the form of projects SF0142505s03 and SF0140091s08. I would like to thank Archimedes Foundation, Doctoral School of "Functional Materials and Technologies".

LIST OF PUBLICATIONS

The current PhD thesis is based on the following papers, referred in the text by their Roman numerals I–V.

I. Surzhenkov, A., Kulu, P., Gregor, A., Vuoristo, P., Latokartano, J., Rupponen, M. (2008). Laser Treatment of PVD Coated Carbon Steels and Powder Steels. *Materials Science (Medžiagotyra)*, 14 (4), 301 – 305.

II. Surzhenkov, A., Allikas, G., Gregor, A., Zimakov, S., Kulu, P., Müller, H. (2008). Laser Treatment of Surfaces of Tool and PM steels and Steels with Coatings. In: *Proceedings of the 6th International Conference of DAAAM Baltic "Industrial Engineering"*: 24–26th April, 2008, Tallinn, Estonia. (Ed.) R. Kyttner. Tallinn University of Technology, 2008, 555 – 560.

III. Surzenkov, A., Kulu, P., Tarbe, R., Mikli, V., Sarjas, H., Latokartano, J. (2009). Wear resistance of laser remelted thermally sprayed coatings. *Estonian Journal of Engineering*, 15(4), 318 – 328.

IV. Kulu, P., Saarna, M., Sergejev, F., Gregor, A., Surženkov, A. (2010). Selection of coating systems and processes for different wear conditions. In: *Proceedings of 14th Nordic Symposium on Tribology*, NORDTRIB 2010, Storforsen, Sweden. Lulea University of Technology, 2010, 1 – 8.

V. Surzhenkov, A., Põdra, P., Adoberg, E., Sergejev, F., Saarna, M., Viljus, M., Mikli, V., Kulu, P (2011). Comparative analysis of the duplex I–III generation PVD coatings. *Materials Science (Medžiagotyra)* (accepted for publication).

Author's contribution

Author of the current thesis was responsible for planning and processing of experiments (Papers I–III and V, Paper IV – part, concerning HVOFS specimens), also further analysis of experimental data (Papers I-III and V). In Paper I, III and V principle analysis was made by the author. Other authors were consulted. The list of publications, not included in the current work, is shown below. However, the intellectual merit is the result of the framework, where the contribution of every author should not be underestimated.

List of publications, not included in the doctoral thesis

I. Podgursky, V., Nisumaa, R., Adoberg, E., Surzhenkov, A., Sivitski, A., Kulu, P. (2010). Comparative study of surface roughness and tribological behavior during running-in period of hard coatings deposited by lateral rotating cathode arc. *Wear*, 268(5–6), 751 – 755.

II. Surzhenkov, A., Kulu, P., Viljus, M., Vallikivi, A., Latokartano, J. (2010). microstructure and wear resistance of the laser hardened PM tool steel Vanadis 6. In: *Proceedings of 7th International Conference of DAAAM Baltic Industrial Engineering*: Tallinn, Estonia, 22–24 April 2010. (Ed.) R. Küttner. Tallinn University of Technology, 2010, 486 – 491.

III. Lille, H., Kõo, J., Ryabchikov, A., Toropov, S., Veinthal, R., Surzhenkov, A. (2010). Comparative analysis of residual stresses in flame-sprayed and electrodeposited coatings using substrate deformation and hole-drilling methods. In: *Proceedings of the 7th International Conference of DAAAM Baltic Industrial Engineering*, Tallinn, Estonia, April 22–24, 2010. (Ed.) R. Kyttner. Tallinn University of Technology, 2010, 474 – 479.

IV. Surzhenkov, A.; Pihl, T.; Viljus, M.; Latokartano, J.; Vallikivi, A. (2010). Abrasive wear resistance of the laser treated electroplated coatings. In: *Proceedings of the 1st International Conference on Manufacturing Engineering & Management*, Prešov, Slovak Republic, 25–26 November 2010. (Ed.) V. Modrak, S. Hloch. Czestochowa, Slovak Republic: Udulibri, 2010, 5 – 8.

V. V. Podgurski, E. Adoberg, A. Surženkov, E. Kimmari, M. Viljus, V. Mikli, M. Hartelt, R. Wäsche, M. Šima (2011). Dependence of the friction coefficient on roughness parameters during early stage fretting of (Al,Ti)N coated surfaces. *Wear*, In press (corrected proof).

Approbation at the international conferences

1. 18th International Baltic Conference „Engineering Materials and Tribology BALTMATTRIB-2009", Tallinn, Estonia, October 22–23, 2009.
2. 1st Mediterranean Conference on Heat Treatment and Surface Engineering, Sharm El-Sheikh, Egypt, December 1–3, 2009.
3. 19th International Baltic Conference „Materials Engineering & Balttrib-2010", Riga, Latvia, October 28–29,2010.

1 INTRODUCTION

1.1 Background

Duplex treatment (sometimes called hybrid treatment) is a way of modification of a metal alloy's surface, when two or more established surface treatments are sequentially applied to form a surface layer, which has properties higher than obtainable through the individual surface treatment [1–4]. Duplex treatment is often meant to be a hard coating, carried onto a treated surface [4–7]. Sometimes the term *duplex treatment* is understood in a more specific way – as a combination of a thermochemical treatment of the substrate and a hard wear-resistant coating [8–14]. The concept of duplex treatment was proposed in 1979 by Brainard and Weeler [15]. The first deeper studies were brought out in the 1980s by Bell and co-workers and independently by Zlatanovic and Münz [16, 17], the first attempts to apply it in industry refer to the beginning of the 1990s [16]. At the beginning the duplex treatment comprised low or high-pressure plasma nitriding and PVD coating deposition, applied to a tool steel [18]. This modification of duplex treatment still remains the most widely used in the industry [16].

The typical division of tasks in the duplex system is represented in Fig. 1.1. Casually, different treatments are implemented to improve the properties of the substrate and of the surface layer or coating.

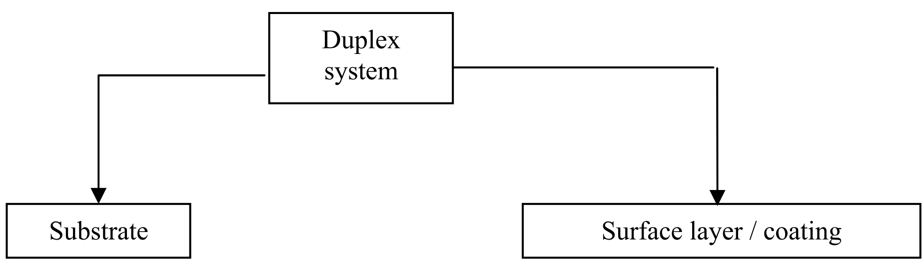

1. Load support
2. Stress gradient
3. Adhesion
4. Bulk strength
5. Fracture toughness

1. Hardness
2. Wear resistance
3. CoF
4. Corrosion resistance
5. Thermal resistance

Figure 1.1 Tasks of the substrate and the surface layer / coating in a duplex system

It can be noted that thinner coatings, obtained by different PVD or CVD methods, are subjected to mechanical [19], thermal [20–24] treatments and ion implantation [25], while thicker coatings, obtained by thermal spraying, electrodeposition and cladding methods, are subjected to thermo(chemical) [26–31] and thermal [22, 32–46] treatments. It can be also noted that substrate is modified prior to thinner coatings' deposition.

Among other surface treatment technologies, thermal treatment seems to be most universal in the light of coatings' modification, as it allows treating both thinner and thicker coatings. Among other types of thermal treatment, laser and electron beam surface hardening seems to be most appropriate in the case of thinner coatings, as it causes low distortion [21, 23] and can be applied as a finishing treatment [21]. According to [21, 23, 24], laser and electron beam hardening can enhance the surface hardness by 1.2 – 2.3 times (see Fig. 1.2) and the adhesion – by 1.2 – 3.3 times (see Fig. 1.3 and 1.4), whereas the biggest increase is observed in the case of plain carbon and low-alloy steels. The distortion values depend on the chemical composition of the basic material [23]; for example, for the steel 42CrMo4 it equalled to 13 μm, for the steel 153CrMoV12 – to 18 μm and for the steel X100CrMoV5-1 – to 21 μm.

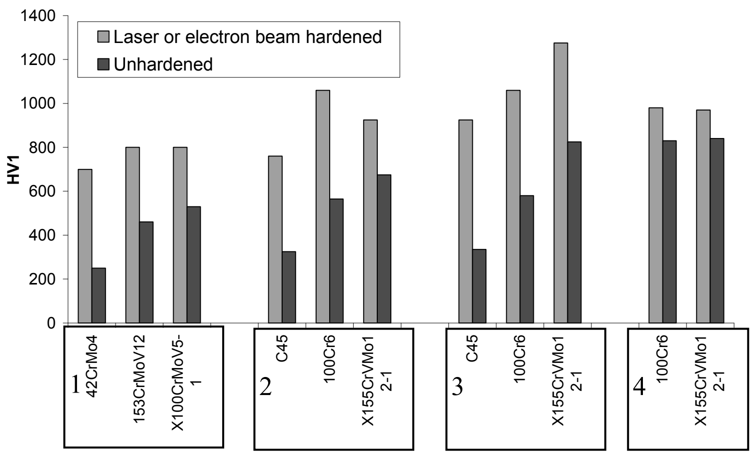

Figure 1.2 Surface hardness of laser or electron beam hardened and PVD or CVD coated steels: 1 – CVD TiN coating; 2 – PVD TiN coating; 3 – PVD Ti(C,N) coating; 4 – CVD DLC coating [23, 24]

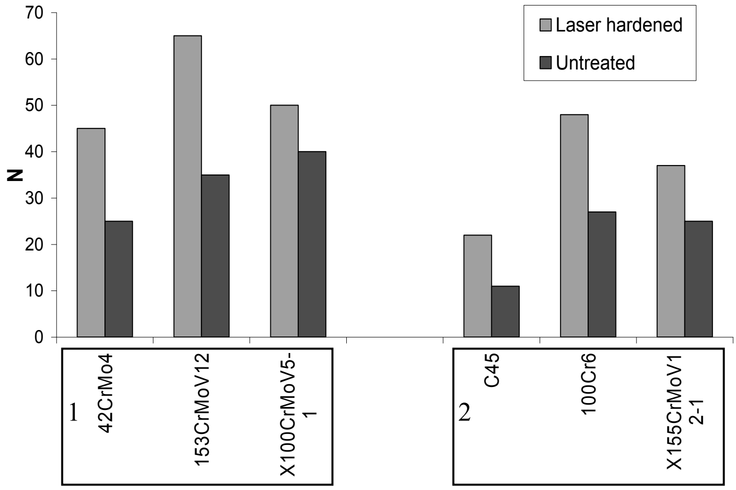

Figure 1.3 Adhesion of laser hardened CVD and PVD coated steel: 1 – CVD TiN; 2 – PVD Ti(C,N)[21, 24]

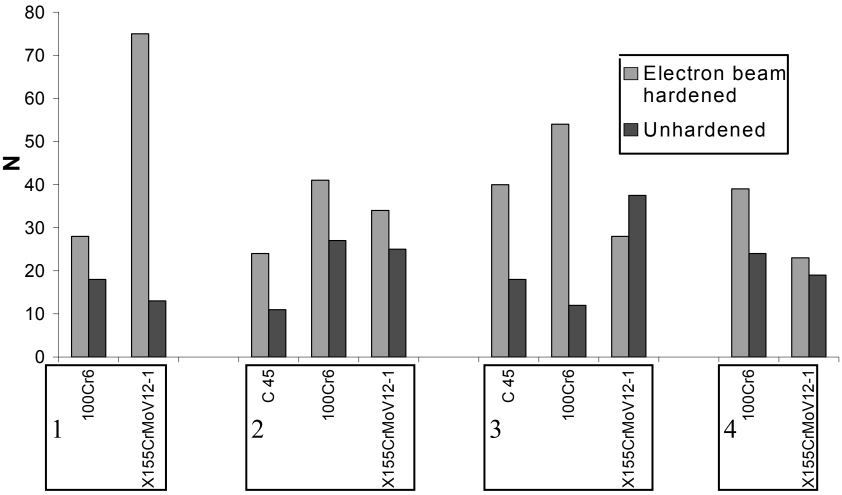

Figure 1.4 Adhesion of electron beam hardened CVD and PVD coated steels: 1 – PVD TiN;, 2 – PVD Ti(C,N); 3 – PVD (Ti,Al)N; 4 – CVD DLC [23, 24]

In its turn, laser (electron beam) treatment (remelting) of thicker coatings, especially thermal sprayed ones, has been successfully applied to decrease their porosity [32, 35, 37–42, 44, 45] and increase the homogeneity of these coatings [36–42, 44]. Laser remelting of thermal sprayed coatings leads to the 1.05 – 1.25 times increase in the adhesion values, whereas smaller rise is shown by hardmetal coatings, namely 75/25 Cr_2C_3/NiCr [39] and WC-Co [41] coatings, and higher one – by ceramic coatings (Al_2O_3 – TiO_2 and pure Al_2O_3 [42]).

However, the situation with hardness and wear resistance is not that definite. The self-fluxing NiCrSiB alloys, sprayed by different methods, demonstrate as a 1.2 decrease in the microhardness values [33], as 1.2 – 2.2 increase after laser treatment [37, 43]. Plasma sprayed and laser remelted NiCrAlY and Ni_3Al alloys show the 65 % and 10 % decrease in hardness values in respect to the as-sprayed condition [44]. WC and Cr_2C_3-based hardmetals generally exhibit a 1.2 – 1.9 rise in the hardness values after the laser remelting, except for [34], where the 1.2 – 1.3 decrease in the microhardness' values of the laser remelted coatings is observed in comparison with the as-sprayed ones. The composite NiCrSiB-WC coating demonstrated the 2 times rise in the microhardness values after the laser remelting [43]. Composite Al_2O_3-TiO_2 coatings showed as an increase of microhardness by 1.0 – 2.3 times [40], as a slight decrease by 1.03 times [42] in the laser remelted coatings in comparison with the as-sprayed condition. Pure laser remelted Al_2O_3 coatings exhibited the small increase in the microhardness values, being compared with the unremelted coatings.

Several authors have reported an increase in the sliding wear resistance of laser remelted hardmetal coatings [34, 41]. In the case of abrasive wear, both increase and decrease of the wear resistance were reported. In [34], the 1.8 and 1.3 decrease in the abrasive wear resistance was observed in the case of laser remelted WC-Co coatings, produced applying conventional and nanoscale powders, respectively. However, the 2.7 times higher abrasive wear resistance was observed in [45] for the WC-24Cr_2C_3-6Ni laser remelted coating in comparison with the as-sprayed one. NiCrSiB-WC composite coating demonstrated the 1.4 times lower abrasive wear resistance after laser remelting, although pure NiCrSiB showed the 2 times increase in the wear resistance after laser remelting [43].

Electron beam remelted detonation gun sprayed coatings show a 3.4 times increase in coating adhesion, 3 times increased microhardness and 20 times increased wear resistance [22]. The same authors have reported that plasma jet remelted detonation gun sprayed coatings showed only 1.1 times increase in adhesion and 2 times increase in wear resistance, but the 5 times increase in microhardness (in Ni-based coating).

However, the most widely applied duplex treatment remains the combination of a coating and a thermochemical treatment. In the majority of cases it means the application of plasma nitriding or nitrocarburizing, less frequently carburising or boronizing and a modification of a PVD or CVD process, applied to steels and titanium alloys.

The nitrided/nitrocarburized layer is supposed to enhance the load carrying capacity of the surface [4, 47–51] that should prevent the plastic deformation of the substrate and subsequent delamination of thin and brittle coating [4, 48, 49, 52] and provide the proper hardness [4, 49, 51, 53] and stress [4, 54] gradients between the coating and the substrate. The coating, in its turn, should provide high anti-wear and anti-corrosion properties, comprising of low coefficient of friction and high hardness [4, 48]. The subsequent application of these technologies provides an increased adhesion and susceptibility to the cracking of the coating, as well as sliding, abrasive, erosive, impact wear and corrosion resistance of the composite together with the decrease in coefficient of friction.

Depending on the coating and the substrate, nitridining can enhance the adhesion of the coating by 1.2 – 19 times, as it can be seen at Fig. 1.5.

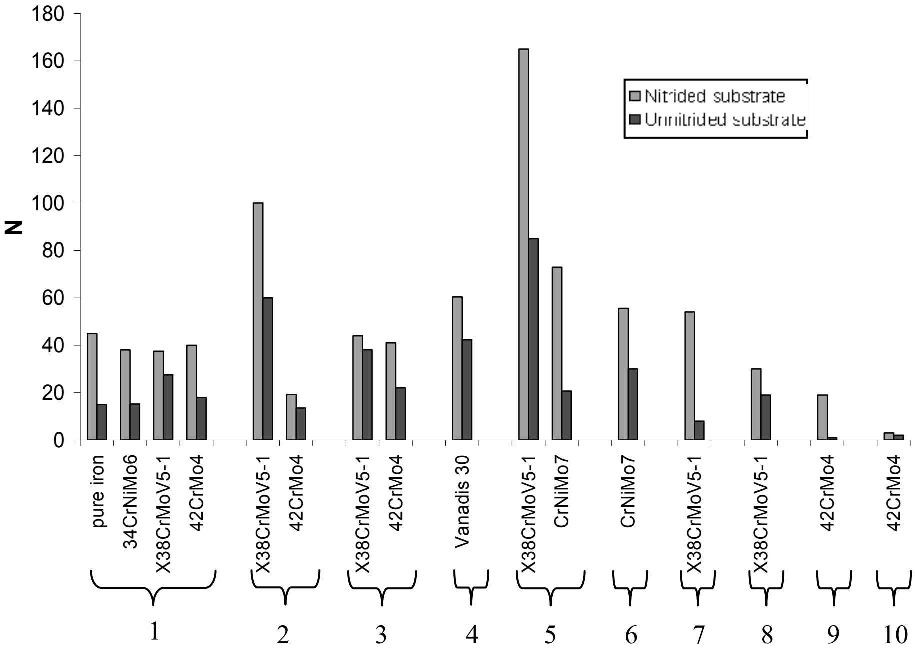

Figure 1.5 Adhesion of PVD and CVD coatings on the nitrided substrates, PVD: 1 –TiN; 2 –CrN; 3 –TiAl;, 4 –TiAlCrYN; 5 - Balinit® Futura-TiN/TiAlN; 6 –TiAlN/VN; CVD: 7 –TiB2; 8 –TiBN; 9 – a:C:H:S;, 10 – ta-C [3, 12, 50, 55 – 60]

Plasma nitriding of the substrate allows avoiding the adhesive failure of PVD TiAlN, TiN and CrN coatings, leading only to the cohesive failure and radial cracking in the case of duplex TiN coating after 5×10^4 impacts [3, 54]. No failure of duplex (plasma nitriding and PVD) CrN coating was observed [55] after 5×10^4 impacts. Also no cracking of the same type duplex CrN coating was found in contrast to the single coating [56]. Electroless nitrocarburizing of the substrate prior to the DLC coating allowed the 2.3 times decrease in the size of the impact wear scar after 10^4 strokes in reference with the non-duplex DLC [61].

The application of nitriding or nitrocarburising together with the CVD or PVD coating generally allows to increase the wear resistance up to hundreds of percents. The specific values depend on the coating parameters, such as thickness, hardness, modulus of elasticity, etc., as well as on substrate type, thermochemical treatment, material of the counterbody, etc. For example, the PVD TiN coating, applied to a nitrided substrate, can enhance the wear resistance by 1.8 – 4.9 times in comparison with the non-duplex TiN coating [62–64]. The wear (mass loss) of the plasma nitrided and CVD coated steel 40Cr decreased by 8.3 – 10.8 times depending on the applied normal load in reference to the nitrided only steel [65]. The deposition of TiAlN coating onto plasma nitrided steel allows to reach the enhancement in the wear resistance by 3.4 – 5 times [63, 64], the combination of plasma nitriding and PVD CrN coating lead to the 11.6 times decrease in the wear volume [66]. Duplex treatment, consisting of plasma nitriding and PVD TiN-MoS_x coating, allowed improving the wear rate by the factor of 1.6 [67], compared with the non-duplex coating. The corresponding treatment with the PVD CrN/NbN coating improved the wear resistance of the S154 steel by more than two orders of magnitude [57]. The application of duplex (plasma nitrided and PVD coated) TiCN/TiN coating lead to the increase in the wear resistance by 9.2 times [68]. However, some worsening of the wear resistance was observed for the PVD TiAlN/VN (1.6 – 3.7 times depending on the load) and TiAlCrYN (1.5 times) coatings, deposited onto plasma nitrided P20 steel as against the single coatings [69].

The application of ta-C coating to the nitrided steel AISI 4140 lead to the 4 – 6 times lower wear rate [63, 70]. The application of DLC coating and nitriding/nitrocarburizing can lead to the increase in the wear resistance from 1.4 to two orders of magnitude [61, 67, 71]. The combination of plasma nitriding and the CN_x film can improve the wear resistance of the Ti6Al4V alloy by 5.7 – 19.8 [72]. However, in [73] slightly worse wear resistance was demonstrated by the duplex treated (plasma nitrided and DLC coated) Ti6Al4V alloy.

The big variations in the characteristics of the duplex treated and single PVD coatings in different cases are caused by various factors, such as experimental conditions, substrate steels, etc. Also the fact, that described PVD coatings belong to different generations, on the grounds of the coatings' architecture (I generation – single layer coatings; II generation – multilayer or multicomponent coatings; III generation – gradient or nanocomposite coatings; IV generation – adaptive coatings [74]), should not be underestimated.

1.2 Conclusions on the chapter and objectives of the study

On the basis of the overview the following conclusions may be drawn:

1. Laser and electron beam hardening can remarkably enhance the surface hardness of PVD and CVD coated steels without their deterioration.
2. Laser and electron beam hardening can sufficiently improve the adhesion of thin PVD and CVD coatings to the steel substrate, whereas the effect is more pronounced in the case of plain carbon and low alloy steels.

3. Laser and electron beam treatment (remelting) decreases the porosity, improves homogeneity and adhesion of thermal sprayed coatings.
4. Laser treatment can increase or decrease the hardness and wear resistance of TS ceramics based coatings, whereas more positive results are obtained for self-fluxing alloy based coatings.
5. Nitriding and nitrocarburizing sufficiently improve the adhesion and wear resistance of the I–II generation PVD coatings, except for some multilayer coatings.

The objectives of the study

The main aim of the current work is to offer ways to improve the functional properties of hard PVD and thermal sprayed coatings. The following objectives of the study were formulated:

1. Study of the duplex treatment of the PVD coated CWTS and CS by laser hardening.
2. Comparative study of the duplex treatment of the I–III generations' PVD coatings by the application of the preliminary nitriding of the steel substrate
3. Study of the duplex treatment of hardmetal and composite 'self-fluxing alloy – hardmetal' coatings by laser treatment (remelting).

2 EXPERIMENTAL

2.1 Substrate steels, surface treatments and coatings.

For production of different coatings, three various types of non-heat resistant hardening and tempering and tool steels – non-alloy carbon steel (C45), low-alloy nitriding steel (42CrMo4) and cold work tool steel (Vanadis 6) – were used as the substrate materials. Two types of wear resistant coatings – thin (2 – 3 μm) hard PVD coatings (TiN, Ti(C,N), (Ti,Al)N-ML, (Al,Ti)N-G, FiVIc®) and thick (200 – 300 μm) thermal sprayed (plasma sprayed and high velocity oxy-fuel sprayed) coatings were selected.

Laser hardening and plasma nitriding were used as the supplementary technologies in the case of PVD coatings. The properties of substrates, coatings and their deposition parameters are shown in Table 2.1 and Table 2.2.

Table 2.1 Chemical composition and initial hardness of used substrate steels

Substrate type	Steel grade	Chemical composition, wt%	Condition	Initial hardness, HV
Carbon steel (C45)	C45	0.42 – 0.50 C; 0.50 – 0.80 Mn; 0.02 – 0.04 Si; 0.045 P; 0.045 S; ≤ 0.40 Cr; ≤ 0.10 Mo; ≤ 0.10 % Ni	Annealed	200 – 235
Nitradable steel (NS)	42CrMo4	0.38 – 0.45 C; 0.60 – 0.90 Mn; ≤ 0.40 Si; 0.035 P; 0.035 S; 0.90 – 1.20 Cr; 0.15 – 0.30 Mo	Hardened and tempered	315 – 345
Cold work tool steel (CWTS)	Vanadis 6	2.60 C; 0.40 Mn; 1.00 Si; 6.50 Cr; 1.50 Mo; 5.40 V	Annealed	245 – 320

Laser treatment was applied in the case of thermal sprayed coatings. Two different thermal spraying methods were used – high velocity oxy-fuel spraying (HVOFS) and plasma spraying (PS). For the first process, commercial hardmetal powder was applied, for the second process the composite powder, based on self-fluxing alloy and recycled (produced by mechanical milling) hardmetal was used. Tables 2.3 and 2.4 specify the main characteristics of the powders, applied for TS, and of the technological processes, respectively.

Table 2.2 Surface technologies (thin coatings)

Coating's type and substrate	Main technology and parameters	Supplementary treatment and parameters
PVD TiN (CWTS, CS), Ti(C,N), (Al,Ti)N (CS)	TiN on Vanadis 6: cathodic arc current 80 A, substrate bias 300 V. TiN, Ti(C,N), (Al,Ti)N on C45: cathodic arc current 50 – 125 A, bias voltage (–60) – (–150) V	Laser hardening (LH): TiN on CWTS: laser beam power 350 W, scan speed 1200 mm/min, spot size Ø 0.96 mm TiN, (Al,Ti)N on CS: laser beam power 500 W, Ti(C,N) – 600 W, scan speed – 300 mm/min, spot size 4 × 8 mm
PVD TiN, (Ti,Al)N-ML, (Al,Ti)N-G, FiVIc® (NS).	PVD: TiN, Ti(C,N), (Ti,Al)N-ML, (Al,Ti)N-G, FiVIc®): cathodic arc current 50 – 125 A, bias voltage (–60) – (–150) V	Plasma nitriding (PN): Standard process by Bodycote OY (500 – 520 ºC, 1 – 10 mbar).

Table 2.3 Applied thick coatings and related surface technologies

Powder (substrate)	Method and parameters of the spraying process	Supplementary treatment and parameters
WC-17Co (C45)	HVOFS, O_2 pressure 14 bar, O_2 flow 56634 l/min, N_2 pressure 3.5 bar, N_2 flow 651.3 l/min, kerosene pressure 11.75 bar, kerosene flow 0.38 l/min	Laser treatment (LT): Laser beam power 495 W, scan speed 300 mm/min, spot size Ø 0.96 mm
75 wt% NiCrSiB + 25 wt% WC-12Co (recycled[1]) (C45) 75 wt% FeCrSiB + 25 wt% WC-12Co (recycled[1]) (C45)	PS, current 380 A, voltage –150 V, powder feed rate 30 g/min, spray distance 100 mm, Ar flow rate 135 l/min, H_2 flow rate 90 l/min	Laser treatment (LT): Laser beam power 1750 W (I series), 1500 W (II series), scan speed 10 mm/min, spot size 4 × 8 mm.

[1)] Desintegrator milled at TUT.

Table 2.4 Powders, applied for thermal spraying

Powder grade	Chemical composition, wt%	Particle size
1343VM[1]	83 WC; 17 Co	(–45) – (+15) μm
1640-02[2]	7.5 Cr; 3.5 Si; 1.6 B; 0.25 C; 2.5 Fe; Ni – bal.	(–45) – (+15) μm
1660-02[2]	14.8 Cr; 4.3 Si; 9.1 B; 0.75 C; 3.7 Fe; Ni bal.	(–45) – (+15) μm
6AB[2]	13.7 Cr; 2.7 Si; 3.4 B; 2.1 C; 6.0 Ni; Fe bal.	(–45) – (+15) μm
WC-12Co (recycled)	75.6 WC; 11.5 Co; 12.9 Fe	(–63) μm (–63) – (+20) μm

1) Tafa Inc.

2) Höganas AB.

2.2 Testing procedure

2.2.1 Microstructural studies

Grinded and polished cross-sections of the specimens were etched with the 3 vol% nital solution and studied under the optical microscope (OM) AXIOVERT 25 (Carl Zeiss, Germany). Part of the thermal sprayed laser treated specimens' cross-sections were studied also under the electron scanning microscope (SEM) EVO MA15 (Carl Zeiss, Germany). The distribution of chemical elements in the laser treated TS coatings was determined by the means of energy dispersive spectroscopy (EDS).

2.2.2 Microhardness measurements

Vickers hardness (HV) was measured at the surface and at the polished cross-sections of all the specimens applying the microhardness tester Micromet 2001 (Buehler). The applied loads were 0.49 N and 2.94 N in the case of PVD coated specimens and 0.98 – 4.91 N in the case of thermal sprayed specimens. Surface hardness was measured at the fine grinded surface of the thermal sprayed coatings, except for the HVOF WC-17Co coating, applying the universal hardnessmeter 2.5/TS (Zwick, Germany) at the load of 0.98 N.

2.2.3 Indentation and wear testing.

The following indentation and wear testing methods of coated systems were used:

- cyclic indentation (CI) (cracking resistance test),
- impact wear (IW),
- sliding wear (ball-on-plate, BoP),

- abrasive wear (block-on-ring (rubber wheel), ABRW),
- abrasive erosive wear (AEW),
- abrasive impact wear (AIW).

The aim of cyclic indentation test was to determine the cracking resistance of a coating. Cracking resistance was estimated according to the qualitative evaluation criteria from 0 (very weak secondary radial cracks, emanated from the edge and around the corners) to VI (strong radial cracks and delamination of the coating around the corners of indent or perimeter) (see Paper IV for more details).

The aim of impact wear test was to determine the resistance to impact loads. The resistance was determined as the function of the indentation stress on the indentation depth in the case of PVD coatings and as the function of the failed area ratio on the number of cycles in the case of HVOFS coating.

To estimate the sliding wear of PVD coatings, the depths of wear scars' cross-sections were measured applying the Mahr profilomeeter.

In the ABRW test, wear coefficient was calculated as

$$k = \frac{\Delta m}{\rho F t v r} \tag{1}$$

where Δm – mass loss (kg),
ρ – density (kg/m^3),
F – normal load (N),
t – time of experiment (s),
v – speed of rotation (min^{-1}),
r – radius of the ring.

In the AEW and AIW tests, the volumetric wear was calculated as

$$I_v = \frac{\Delta m}{\rho q} \tag{2}$$

where Δm – mass loss (kg),
ρ – density (kg/m^3),
q – quantity of abrasive per specimen (kg).

The schemes and parameters of the tests are illustrated in Table 2.5.

.

Table 2.5 Applied indentation and wear tests

Test method	Testing scheme	Testing parameters
Cyclic indentation (CI) test	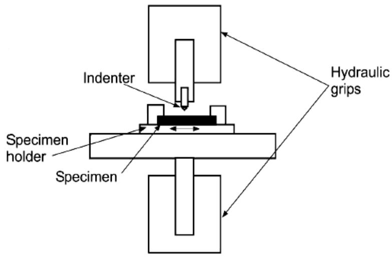	Load 50 N Frequency 50 Hz 1,000 – 10,000 indents
Impact wear (IW) test	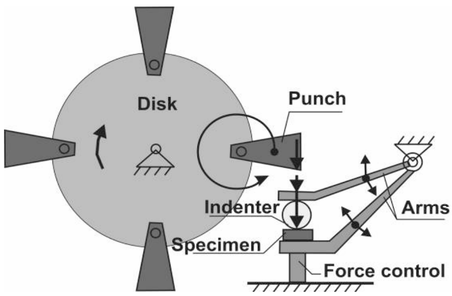	Load 16 N Frequency 25 Hz Linear speed of hammers 2.75 m/s Number of strokes $10^4 – 10^7$
Sliding wear test (ball-on-plate, BoP)	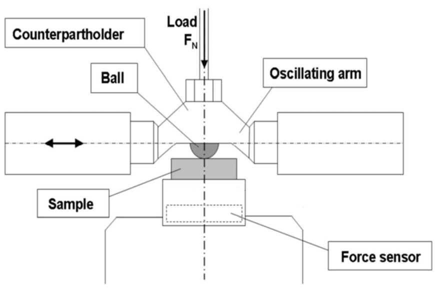 (75)	Load 10 N Ø 10 mm Al_2O_3 ball Frequency 5 Hz Amplitude 10 mm Duration of test 10 min

Table 2.5 (continued) Applied indentation and wear tests

Abrasive wear test (block-on-ring, rubber wheel; ABRW)	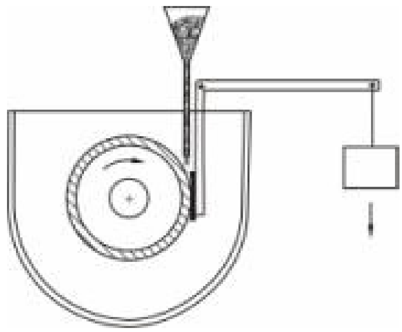	ASTM 65-00, 94 and ASTM B 611-85 Load 47 – 222 N Diameters of wheels Ø 80 and 228.6 mm Speed of rotation 200.8 and 238 rpm Abrasive – quartz sand, 0.1 – 0.3 mm. Mass of abrasive 1 – 1.5 kg Duration of test 3 min
Abrasive-erosive wear (AEW) test	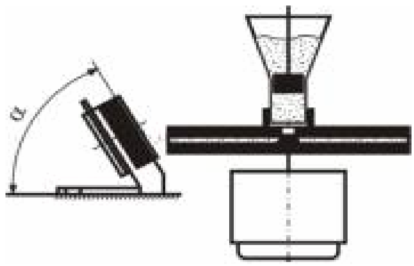	Abrasive particles' velocity 80 m/s Impact angle 30º / 90º Abrasive – quartz sand, 0.1 – 0.3 mm Mass of abrasive 3 kg
Abrasive-impact wear (AIW) test		Abrasive particles' velocity 80 m/s Abrasive – granite gravel, 4 – 5.6 mm Impact angle 90º

Due to the big number of tested coatings on different substrates and keeping in mind operating conditions, thin coatings were subjected to CI, IW and BoP tests, thick coatings – as a rule, to abrasive wear (ABRW, AEW and AIW) tests. The plan of indentation and wear testing experiments of different coatings is shown in Table 2.6.

Table 2.6 Testing procedures of duplex treated specimen

Duplex treatment	CI	IW	BoP	ABRW	AEW	AIW
PVD TiN, Ti(C,N), (Al,Ti)N (substrate C45) + LH	+	+	–	–	–	–
PN + PVD TiN, Ti(C,N), (Ti,Al)N-ML, (Al,Ti)N-G, FiVIc®	+	+	+	–	–	–
HVOFS WC–17Co + LT	+	+	–	+	–	–
PS NiCrSiB / FeCrSiB – WC-Co + LT	–	–	–	+	+	+

3 RESULTS AND DISCUSSION

3.1 Microstructure and hardness

3.1.1 Microstructure of the duplex treated steels

Substrate's microstructure observations show that the effect of laser hardening primarily depends on the type of coating and type of the laser that determines the absorption of the laser irradiation and affects heating of the coated steel through that. Laser beam power and scan speed seem to have a secondary importance. For example, the initial ferritic-pearlitic structure remained under the TiN and Ti(C,N) coatings on the steel C45 (Fig. 3.1, a and b), treated at the laser beam power values of 500 W and 600 W, respectively, and the scan speed of 300 mm/min. A quenching structure, consisting of remained austenite, ferrite and bainite has appeared under the (Al,Ti)N coating (see Fig. 3.1, c), treated at the similar set of parameters (500 W, 300 mm/min).

The depth of the hardened zone is approximately equal to 100 μm under the (Al,Ti)N coating. The incomplete dissolution of ferrite grains and the presence of the retained austenite witness the big rates of heating and cooling, characteristic for laser hardening.

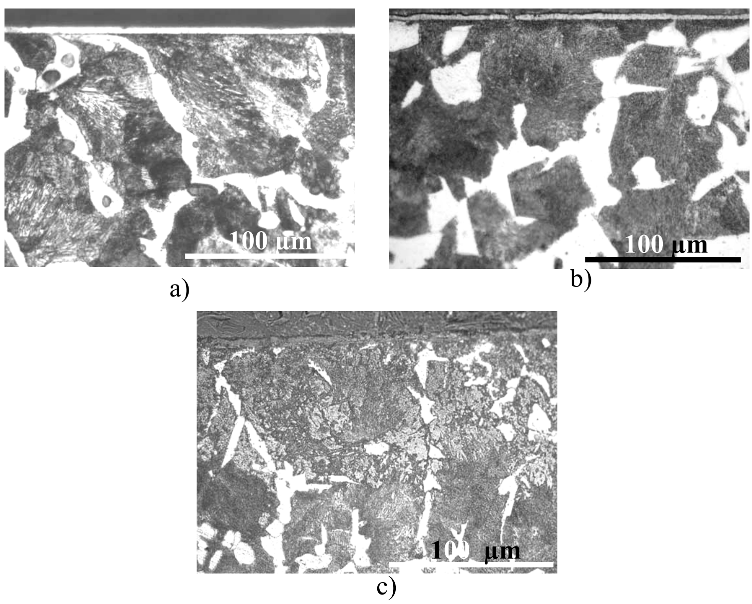

Figure 3.1 Microstructure of the PVD coated laser hardened carbon steel C45: a – TiN; b – Ti(C,N); c – (Al,Ti)N

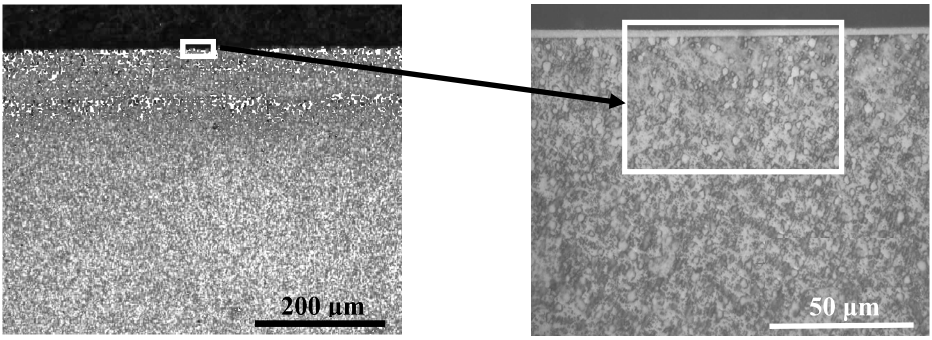

a) b)

Figure 3.2 Microstructure of the PVD coated laser hardened CWTS Vanadis 6:
a – general view; b – hardened zone

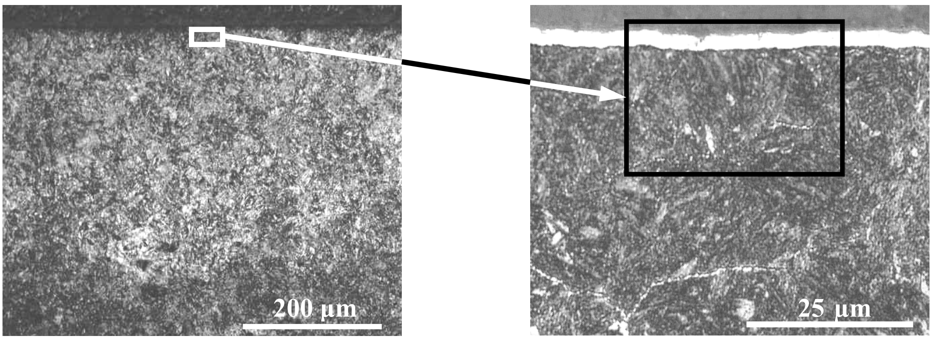

a) b)

Figure 3.3 Microstructure of the PVD coated plasma nitrided steel 42CrMo4:
a – general view; b – trostite - sorbite with the carbides' inclusions

A 100 µm in depth hardened zone is observed under the TiN coating in the laser hardened CWTS Vanadis 6, where partial dissolution of carbide particles can be seen at Fig.3.2 b. Neither martensitic nor sorbitic, or trostitic structures are present in the hardened zone. Its structure most probably consists of bainite, retained austenite and carbide particles.

Application of plasma nitriding to the substrate results in the formation of a hard layer with the average thickness of about 250 µm (Fig. 3.3 a). Microstructure observations (Fig. 3.3) demonstrate that the nitrided specimens have the eutectoid structure with the inclusion of carbide particles. Neither pores nor the compound $Fe_{2\text{-}3}N$ layer can be observed. Thus it can be concluded that the observed microstructure contains the α (Fe(N)) and γ' (Fe_4N) phases, with the presence of nitrides and carbonitrides of chromium and molybdenum, like CrN, MoN, Mo_2N [76].

The influence of laser hardening or plasma nitriding to the structure of PVD coatings was not observed during any of the treatments.

3.1.2 Microstructure of the thermal sprayed laser treated coatings

The microstructure of the thermal sprayed coatings is affected by laser treatment in different ways. While the literature sources [34, 38, 45] report the decrease in the porosity of the HVOFS laser treated hardmetal coatings, Fig. 3.4 a, b demonstrate the opposite. In addition to the increase in porosity, perpendicular cracks through the whole coating were observed. In principle, two zones can be observed in the laser treated coating, being depicted in Fig. 3.4 b and c, respectively. Both these zones are laid up by carbide particles, embedded in metal matrix, whereas no difference either in the size of the particles or in the amount of matrix can be seen. However, large pores and voids are present in the first zone (Fig. 3.4 b), whereas almost zero porosity is observed in the zone near the substrate (Fig. 3.4 c). As no other changes neither in the microstructure nor in the chemical composition of the coating were observed, the most probable

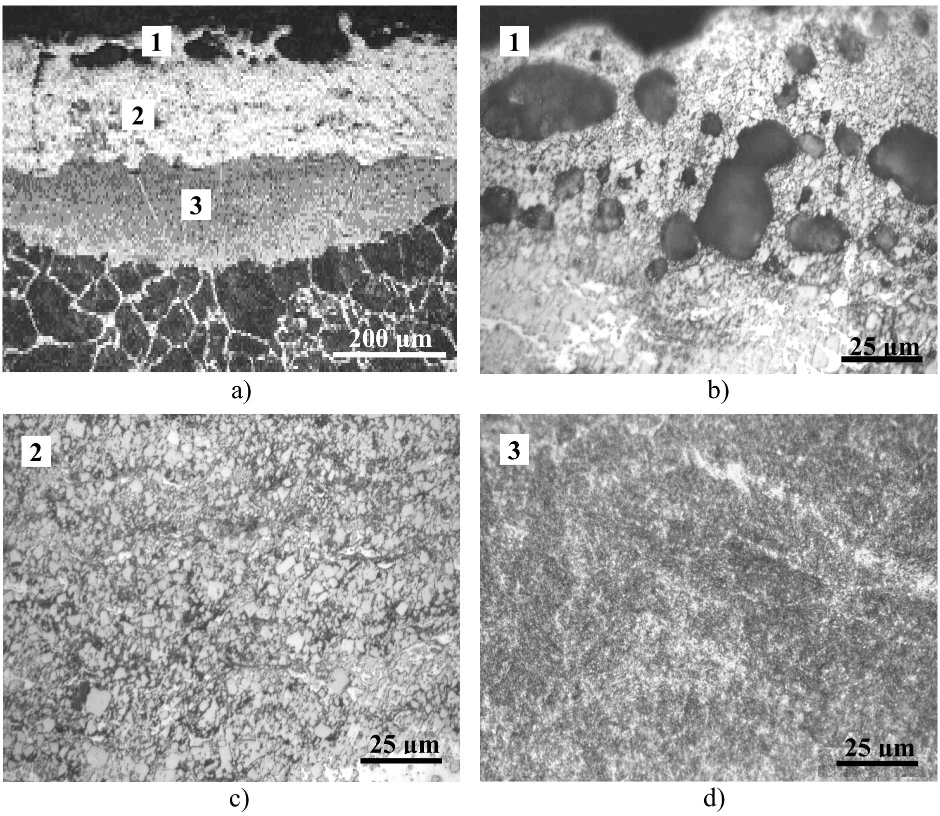

a) b)

c) d)

Figure 3.4 Microstructure of the WC–17Co HVOFS LT coating: a – general view; b – Zone 1 (high porosity); c – Zone 2 (low porosity); d – Zone 3 (hardened substrate – steel C45) reason for the voids' appearance is the loss of cohesion between carbide particles and the metal matrix. In its turn, it can also be caused by the big temperature gradients in the coating during the laser processing, appearing due to relatively big laser energy density and high scan speed (for details, see Paper II). The high cooling gradient is indirectly confirmed by the observation of a relatively big amount of retained austenite in the LHZ below the coating (Fig. 3.4 d). In addition to retained austenite, bainite and ferrite can be found in the LHZ zone.

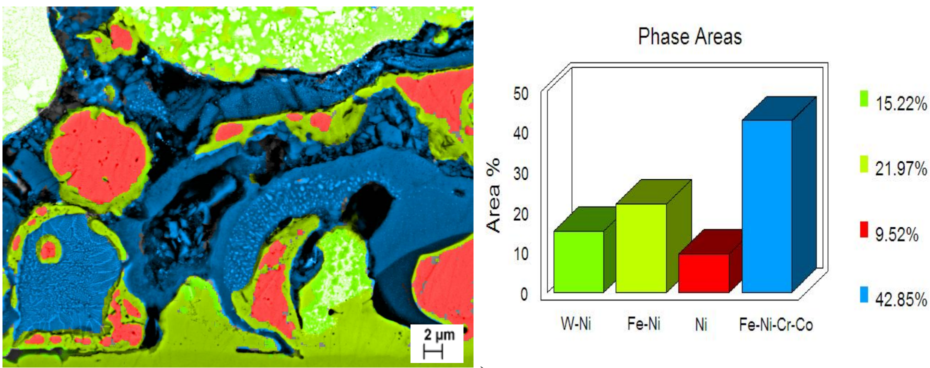

a)

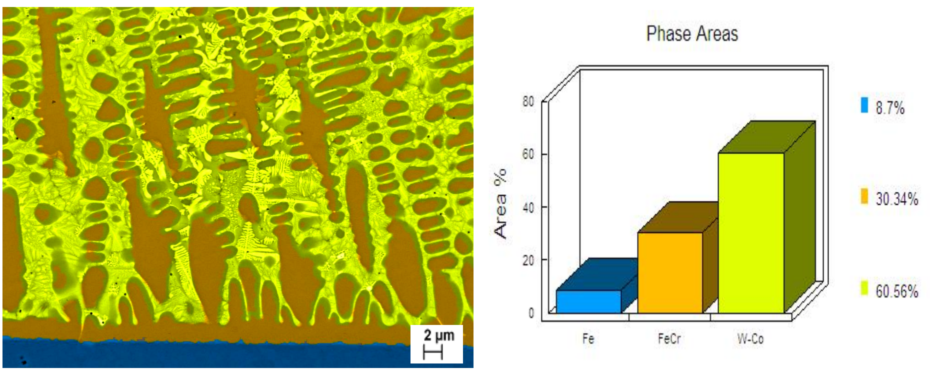

b)

Figure 3.5 Microstructure and chemical composition of the laser treated self-fluxing alloy based coating: a – NiCrSiB + 25% WC-Co; b – FeCrSiB + 25 % WC-Co

In contrast, dense porous free structures were obtained after laser treatment of coatings with the on Ni- or Fe-self-fluxing alloy matrix (Fig. 3.5 a and b). In both cases, the eutectic structure can be observed. However, in the case of Ni-alloy matrix, a notable inhomogeneity in the structure and in the chemical composition can be seen (Fig. 3.5 a). Also no hardmetal particles are present. The Fe-based alloy matrix coatings demonstrate the homogeneous dendritic structure, where some small hardmetal particles can be observed, although not evenly distributed (Fig. 3.5 b). This phenomenon needs further research.

3.1.3 Microhardness of the coatings and the substrates

The microhardness measurements of the PVD coated laser hardened steels indicate the presence of the 100 – 200 μm deep hardened zone under the (Al,Ti)N coating on the CS C45 and under the TiN coating (Fig. 3.6 a) on the CWTS Vanadis 6 (Fig. 3.6 b). No hardening effect was revealed under the TiN and Ti(C,N) coatings. It corresponds to the observations of the microstructure (Fig. 3.1 a – c). The possible reason for that is the relatively high reflection coefficient of these coatings in the case of ND:YAG laser.

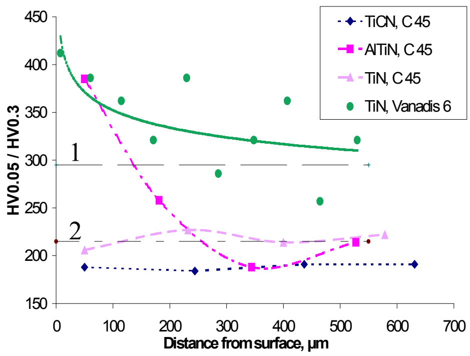

a

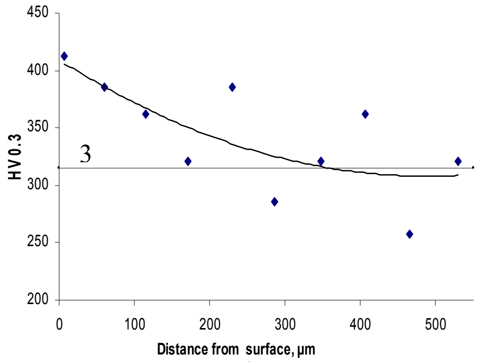

b

Figure 3.6 Microhardness distrubution of the PVD coated laser hardened steels: a - CS C45, b – NS 42CrMo4; 1 – average microhardness of Vanadis 6, 2 – average microhardness of C45, 3 – average microhardness of 42CrMo4

Table 3.1 Microhardness values of the thermally sprayed laser treated coatings

Type of coating	Composition	Hardness, HV0.1	
		Metal matrix	Reinforcement
HVOFS	WC-17Co	543 – 1200	
PS	NiCrSiB + 25 %WC-12Co	270 – 430	580 – 1880
PS	FeCrSiB + 25% WC-12Co	490 – 680	770 – 940

The hardened case in the case of the nitrided steel equaled to at least 250 μm. That complies with the microstructural studies and with the diffusion depth of the nitrogen, reported by the manufacturer [77].

The microhardness values of the thermally sprayed laser treated coatings are shown in Table 3.1. As it follows from the microhardness measurements, lower microhardness values in the HVOFS laser treated WC-17Co coatings were obtained near the coating's surface. It can be the effect of porous structure, observed earlier. The big variations in microhardness of the PS laser treated coatings may be explained by the large chemical and structural inhomogeneity.

3.2 Cracking resistance

The cracking resistance, determined during the indentation tests, was different for various coatings and various duplex treatments. The TiN and Ti(C,N) coatings on CS after laser hardening show multiple strong radial cracks (Fig. 3.7, a, b). That is characteristical for the coatings with a higher H/E ratio on a soft substrate [78], while weak radial cracks were observed at (Al,Ti)N coating. However, coating delamination at the edge of the impression can be observed (Fig. 3.7 c). It can be explained by the lower H/E ratio of the (Al,Ti)N coating in comparison with the TiN and Ti(C,N) coatings [78], as well as by the difference in the coefficients of thermal expansion of the steel C45 and (Al,Ti)N coating. This may lead to a decrease in the adhesion value between the coating and the substrate.

Except for the (Al,Ti)N-G coating, a ‘brittle’ failure (delamination of the coating without significant cracking) can be observed in the case of PVD coatings on nitrided steel (Fig. 3.8, a, c, d). At the (Al,Ti)N-G coating, small cone cracks were observed (Fig. 3.8, b). The possible reason for the best fatigue resistance of the (Al,Ti)N-G coating is the relative similarity between the coating’s and the substrate’s chemical composition [78]. However, this hypothesis needs further confirmation.

Indentation tests of HVOFS coatings demonstrated medium cracking resistance (Fig. 3.9, a, b). The increase in the number of cycles during the indentation testing leads to the formation and development of cone cracks in addition to the radial cracks. This confirms the sufficient susceptibility to plastic deformation of the coating and a relatively good resistivity to cyclic loads, as suggested in Paper IV.

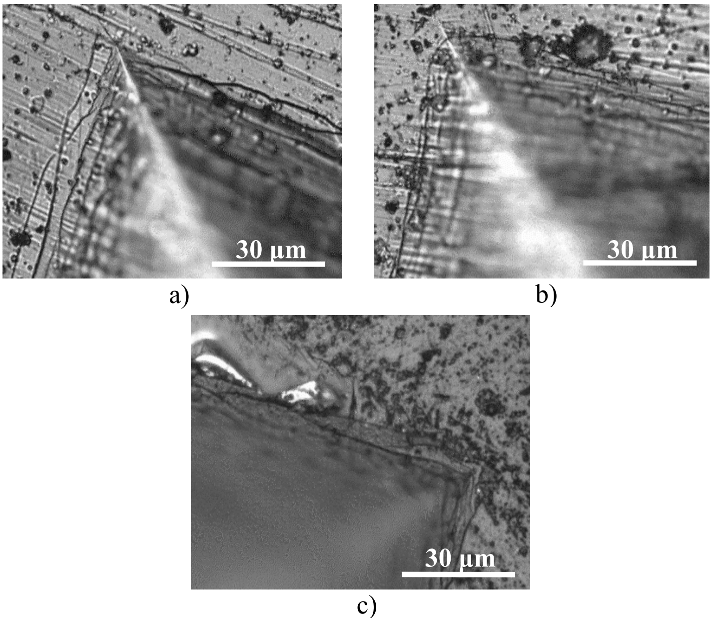

Figure 3.7 Impressions' corners on the PVD coated laser hardened steel C45, 10,000 cycles: a – TiN, IV criteria; b – Ti(C,N), IV criteria; c – (Al,Ti)N, III criteria with VI criteria

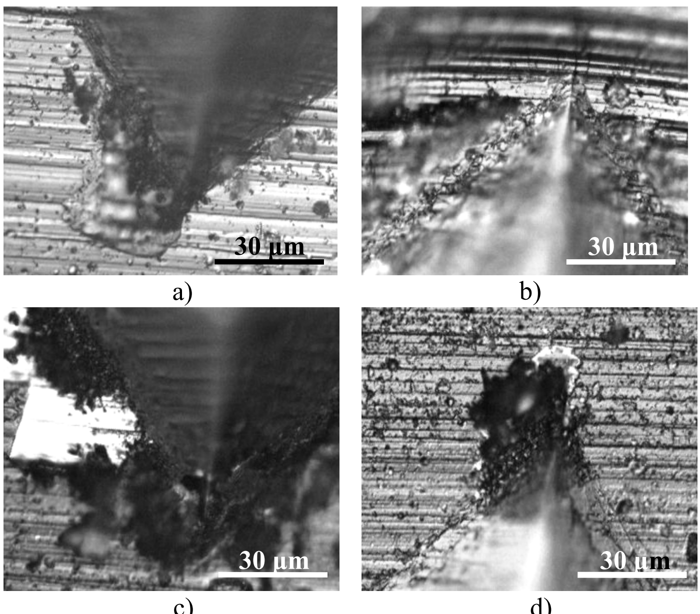

Figure 3.8 Impressions' corners on the PVD coated PN steel 42CrMo4, 10,000 cycles: a – TiN, VI criteria; b –(Al,Ti)N-G, II criteria; c – (Ti,Al)N-ML,VI criteria; d – FiVIc®, VI criteria

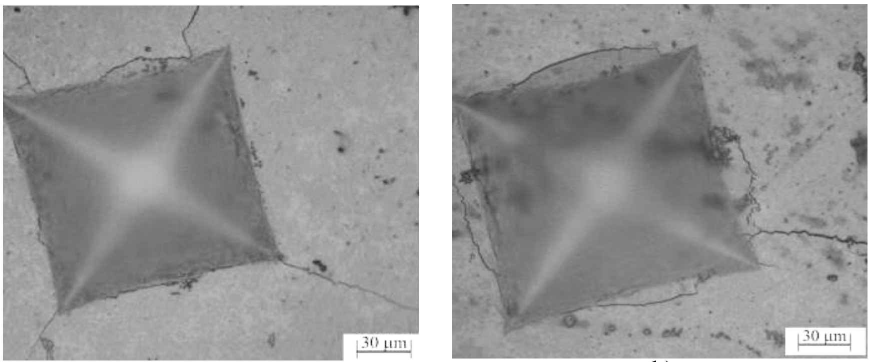

a) b)

Figure 3.9 Impression on the HVOFS WC-10%Co-4%Cr coating: a – after 1,000 cycles, III criteria; b – after 10,000 cycles, III criteria

3.3 Wear resistance

Wear resistance of different coatings was determined in different wear conditions: thin hard PVD coatings were subjected to sliding wear and impact wear tests, thick thermal sprayed coatings – to abrasion, abrasive-erosion and abrasive impact wear tests (see Table 2.6).

3.3.1. Impact wear

The results of the impact wear tests are presented at Fig. 3.10 – 3.12. The points on the curves in Fig. 3.10 and 3.11 correspond to the 10^4, 10^5, 10^6 and 10^7 impacts, as the indentation depth increases. As it is seen in Fig. 3.10, the best impact wear resistance is shown by (Al,Ti)N coating on the laser hardened steel C45, probably due to the better load support, provided by the hardened layer under the (Al,Ti)N-G coating (see Fig. 3.1 c).

In the case of plasma nitrided steel the I generation TiN coating demonstrates the best impact wear resistance (Fig. 3.11). The II–III generation PVD coatings show nearly the same results, whereas worse wear resistance was observed in the case of (Al,Ti)N-G coating. The most probable reason for that is the highest modulus of elasticity of the TiN coating in comparison with the other coatings [78], what allows the coating to resist to deformation during impact.

The HVOFS laser treated hardmetal coating demonstrates a good resistance to impact wear (Fig. 3.12). That shows a good resistance of the coating to the plastic deformation, as assumed in the Paper IV.

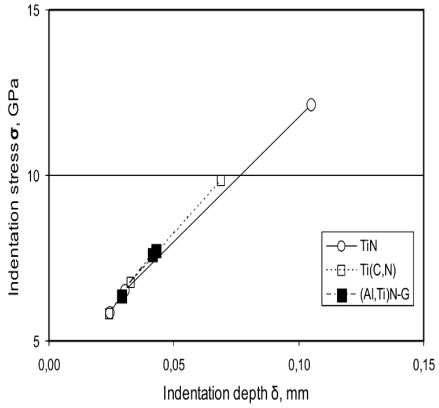

Figure 3.10 Impact wear of the PVD coated laser hardened steel C45

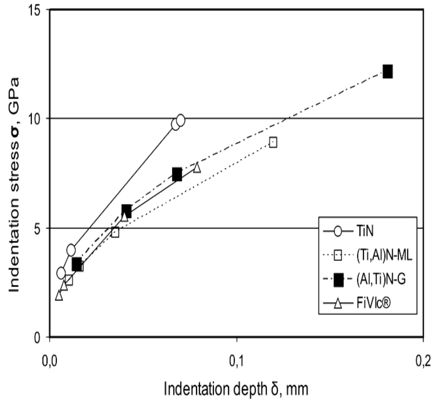

Fig. 3.11 Impact wear of the PVD coated nitrided steel 42CrMo4

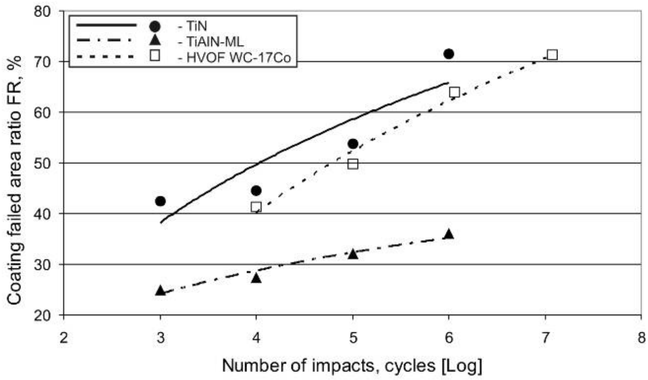

Fig. 3.12. Failed area ratio at different numbers of impacts

3.3.2 Sliding wear of duplex thin hard coatings

The I generation PVD TiN, II generation (Ti,Al)N-ML and III generation FiVIc® coatings on plasma nitrided steel specimens show slightly varying wear values with the lowest wear in the case of PVD FiVIc® coating (Fig. 3.13). This may be explained by the lowest CoF value of all observed coatings (see [78] for details). The highest wear in the case of the (Al,Ti)N-G coating can be explained by the highest Al content in this coating in comparison with the other ones. It can, taking into consideration the alumina counterbody, lead to a higher wear.

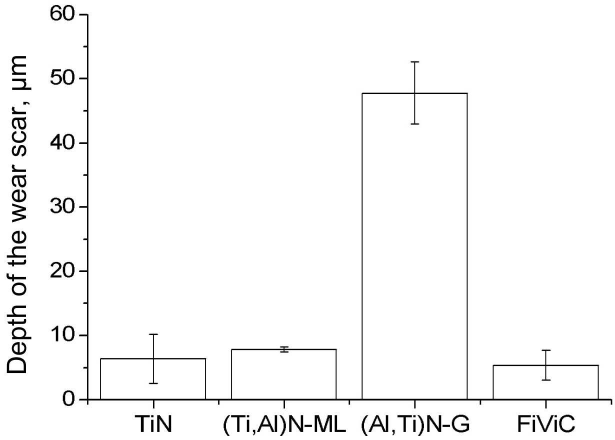

Figure 3.13 Depth of the wear track on the plasma nitrided PVD coated steel 42CrMo4

3.3.3 Abrasive wear of thick hard coatings

Abrasive wear resistance of all thermal sprayed laser treated coatings was lower in comparison with the reference materials (see Fig. 3.14). The lower wear resistance of the HVOFS laser treated coating is most probably caused by the big porosity of the near surface layer of the coating (see Fig. 3.4 b), and, as a consequence, lower microharness, as seen in Table 3.1.

Several reasons for the lower wear resistance of the PS laser treated coatings can be emphasized. The softer matrix (see Table 3.1) in comparison with the reference material, whose microharndess is in the range 490 – 510 HV0.1, can be responsible for that. Considering that the prevailing wear mechanism is the microcutting, the relatively soft matrix will lead to higher wear of the coatings in comparison with the reference material. This is confirmed by the study of the wear scars of the coatings, where deep grooves together with the pullout sites of the hard particles were observed (see Paper III for details).

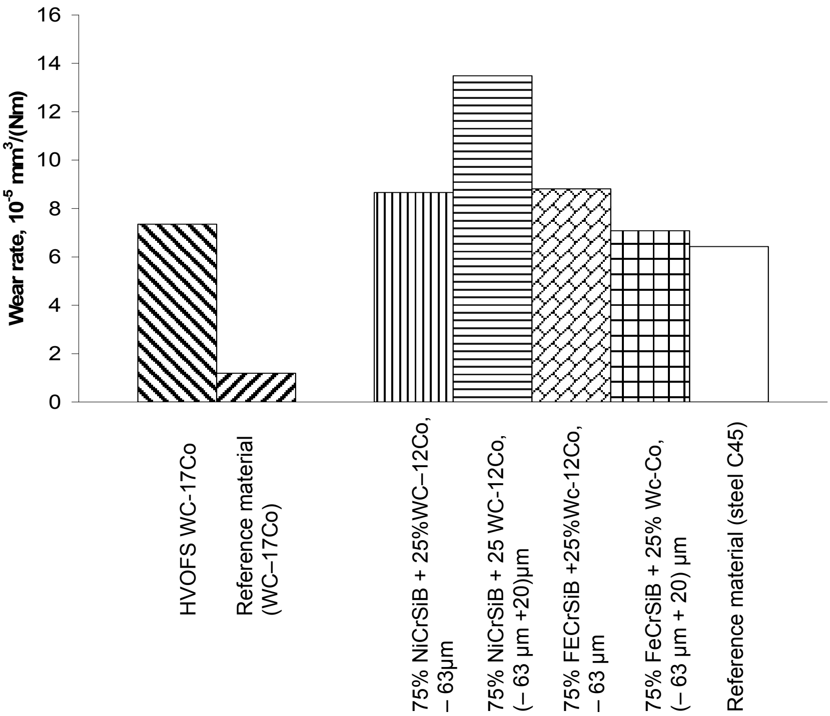

Figure 3.14 Abrasive wear rate of the HVOFS and PS laser treated coatings

The lower abrasive wear resistance of Ni-based self-fluxing alloy matrix coatings in comparison with the Fe-based self-fluxing alloy matrix ones can be explained by lower microhardness of the matrix of the former (270 – 430 HV0.1 against 490 – 680 HV0.1 of the matrix of the Fe-based self-fluxing alloy based coatings).

3.3.4 Abrasive-erosion wear

Results of abrasive-erosion tests are shown at Fig. 3.15. Compared to the reference material, Ni-based self-fluxing alloy matrix composite coatings show better abrasive-erosion wear resistance at the 90° impact angle and the Fe-based self-fluxing alloy matrix ones – at the 30° impact angle. The reason for that may be the differences in the wear mechanisms at different impact angles and by the different microhardness of the coatings' matrixes (see Table 3.1 for details). At the 30º impact angle, the wear mechanism is microcutting, at the 90º impact angle – the combination of microcutting and surface fatigue. As the Ni-based self-fluxing alloy matrix coatings have a softer matrix, than the Fe-based self-fluxing alloy matrix ones, due to the microcutting mechanism the former show higher wear rate at the 30º impact angle. However, as the Ni-based self-fluxing alloy matrix coatings are less brittle in comparison with the Fe-based self-fluxing alloy matrix ones, they are less susceptible to brittle fracture. This could make the Ni-based self-fluxing alloy matrix coatings more resistant at the surface impact conditions in comparison with the Fe-based self-fluxing alloy matrix ones.

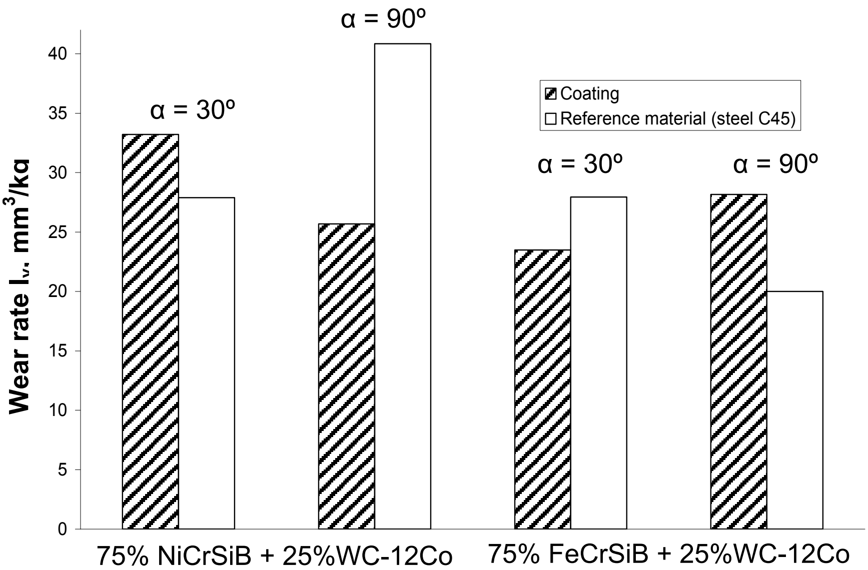

Figure 3.15 Abrasive-erosion wear rate of the PS laser treated coatings

3.3.5 Abrasive impact wear

The Fe-based self-fluxing alloy matrix composite coating shows the lowest wear (see Fig. 3.16), despite the fact that the main wear mechanism in the case of abrasive impact wear is the surface fatigue. It could be explained by the more even distribution of microhardness across the coating, indicating the less steep gradient of other mechanical properties. That may be more important in the case of coarser abrasive, used in the abrasive impact wear tests.

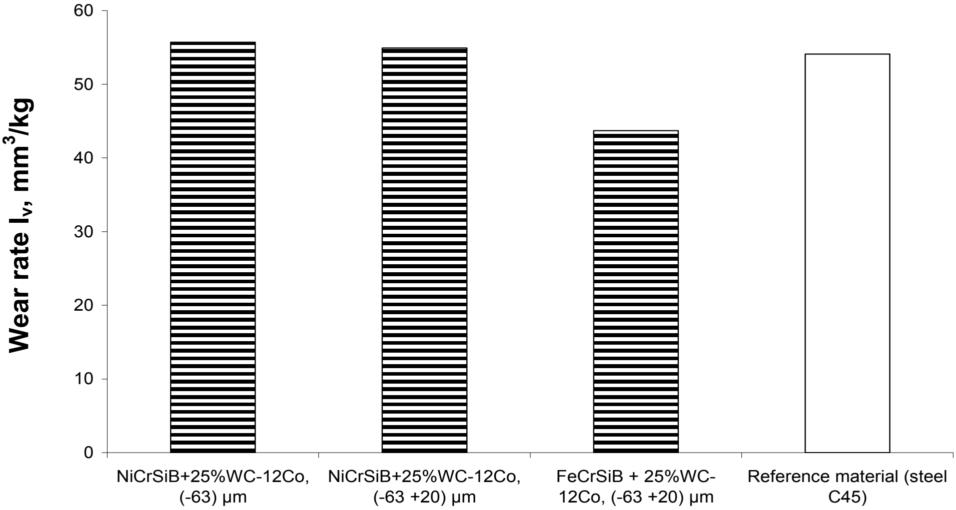

Figure 3.16 Abrasive impact wear rate of the PS laser treated coating

4 CONCLUSIONS

Based on the studies of duplex treatment – supplementary treatment (laser hardening/laser treatment and plasma nitriding) with a combination of coating technologies (physical vapour deposition and thermal spraying), of different steels (carbon steel, low-alloy nitrided steel, high-alloy cold work tool steel) for increasing their surface load capacity and wear resistance, the following principal conclusions can be drawn.

1. Pretreatment of steel (plasma nitriding, followed by PVD) or posttreatment of PVD coated constructional and tool steels allow to create, depending on treatment's type and steel grade, a 100 – 250 µm thick supportive layer with increased hardness under the coating. An increase in the microhardness values by 1.5 – 2 times can be obtained in a PVD coated laser hardened steel (up to 2 times for the constructional steel and up to 1.5 times for the tool steel).

2. Laser treatment of PS self-fluxing alloy based metal coatings allows obtaining a dense structure without pores. The Fe-based self-fluxing alloy based coating demonstrates the best results. Laser treatment of high velocity oxy-fuel sprayed hardmetal type coating is not advantageous, as it causes the porosity near the surface and cracks through the coating, leading to decrease in hardness and to a lower abrasive wear resistance.

3. Best cracking resistance was demonstrated by the duplex (Al,Ti)N-G coatings on laser hardened as well as on plasma nitrided substrates. Laser treatment of high velocity oxy-fuel sprayed coating demonstrates a medium resistance to cracking at cyclic impact loads.

4. Best impact wear resistance was shown by the I generation duplex (plasma nitrided and PVD) TiN coating due to the highest modulus of elasticity of the TiN coating. The II–III generation duplex (PN and PVD) coatings showed similar impact wear resistance. High velocity oxy-fuel sprayed laser treated coatings showed good impact wear resistance.

5. Sliding wear resistance of the duplex PVD coatings was found to be dependent on a combination of coating's and substrate's parameters. The best sliding wear resistance was demonstrated by the duplex IV generation PVD FiVIc® coating (the wear of it was 1.2 times lower than of the duplex I generation PVD TiN coating, 1.4 times lower than of the

duplex II generation PVD (Ti,Al)N-ML coating, 8.9 times lower than of the duplex IV generation (Al,Ti)N-G coating).

6. High velocity oxy-fuel sprayed laser treated hardmetal coating showed 6.2 times higher wear than the reference material. In the abrasive-erosion wear conditions plasma sprayed laser treated Fe-based self-fluxing alloy matrix composite coatings demonstrate the 1.1 – 1.9 times lower wear, than the Ni-based self-fluxing alloy ones. The exception is the abrasive-erosion wear at the impact angle of 90º, when the Ni-based self-fluxing alloy matrix composite coatings show the 1.1 times lower wear than the Fe-based self-fluxing alloy matrix ones.

7. The future research will be focused on the following:
   – study of the effect of duplex treatment (laser hardening or plasma nitriding) to adhesion and sliding wear resistance of physical vapour deposited coatings,
   – study of the effect of hard phase content and laser treatment parameters to the structure and properties of thermal sprayed duplex laser treated composite coatings,
   – choosing the potential application areas of duplex coatings on different steel substrates.

REFERENCES

1. **Fu, Y., Loh, L. N., Wei, J., Yan, B., Hing, P.** Friction and wear behaviour of carbon nitride films deposited on plasma nitrided Ti-6Al-4V. *Wear*, 2000, 237, 12 – 19.
2. **Celis, J.P., Drees, D., Huq, M.Z., Wu, P.Q., De Bonte, M.** Hybrid processes – a versatile technique to match process requirements and coating needs. *Surf. Coat. Tech.*, 1999, 113, 165 – 181.
3. **Batista, J.C.A., Godoy, C., Matthews, A.** Impact testing of duplex and non-duplex (Ti,Al)N and Cr–N PVD coatings. *Surf. Coat. Tech.*, 2003, 163–164, 353 – 361.
4. **Podgornik, B., Vižintin, J.** Tribology of thin films and their use in the field of machine elements. *Vacuum*, 2003, 68, 39 – 47.
5. **Gorokovsky, V.I., Bowman, C., Gannon, P.E., VanVorous, D., Voevodin, A.A., Muratore, C., Kang, Y.S., Hu, J.J.** Deposition and characterization of hybrid filtered arc/magnetron multilayer nanocomposite cermet coatings for advanced tribological applications. *Wear*, 2008, 265, 741 – 755.
6. **El-Hossary, F.M., Negm, N.Z., Abd El-Rahman, A.M., Hammad, M.** Duplex treatment of 304 AISI stainless steel using rf plasma nitriding and carbonitriding. *Mater. Sci. Eng. C*, 2009, 29, 1167 – 1173.
7. **Zukerman, I., Raveh, A., Landau, Y., Weiss, R., Shnek, R., Shneor, Y., Kalman, H., Klemberg-Saphieha, J.E., Martinu, L.** Tribological properties of duplex treated TiN/TiCN coatings on plasma nitrided PH15-5 steel. *Surf. Coat. Tech.*, 2007, 201, 6171 – 6175.
8. **Hernandez, M., Staia, M.H., Puchi-Cabrera, E.S.** Evaluation of microstructure and mechanical properties of nitrided steels. *Surf. Coat. Tech.*, 2008, 202, 1935 – 1943.
9. **Jaeger, G., Endler, I., Bartsch, K., Heilmaier, M., Leonhard, A.** Fatigue behaviour of duplex treated TiC_xN_{1-x}- and $Ti_{1-x}Al_xN$-hard coating steel compounds. *Surf. Coat. Tech.*, 2002, 150, 282 – 289.
10. **Podgornik, B., Vižintin, J.** Influence of substrate treatment on the tribological properties of DLC coatings. *Diamond and Related Materials*, 2001, 10, 2232 – 2237.
11. **Torres, R.D., Soares, P.C. Jr, Smitz, C., Siquera, C.J.M.** Influence of the nitriding and TiAlN/TiN coating thickness on the sliding wear behaviour of duplex treated AISI H13 steel. *Surf. Coat. Tech.*, 2010, 205, 5, 1381 – 1385.
12. **Guruvenket, S., Li, D., Klemberg-Sapieha, J.E., Martinu, L., Szpunar, J.** Mechanical and tribological properties of duplex treated TiN, nc-TiN/a-SiN_x and nc-TiCN/a-SiCN coating deposited on 410 low alloy stainless steel. *Surf. Coat. Tech.*, 2009, 203, 2905 – 2911.

13. **Alsaran, A., Çelik, A., Çelik, C., Efeoğlu, İ.** Optimization of coatings parameters for duplex treated AISI 5140 steel. *Mater. Sci. Eng. A*, 2004, 371, 141 – 148.
14. **Podgornik, B., Hogmark, S., Sandberg, O., Leskovsek, V.** Wear resistance and anti-sticking properties of duplex treated forming tool steel. *Wear*, 2003, 254, 1113 – 1121.
15. **He, J.L., Chen, K.C., Davison, A.** Improvements in the understanding and application of duplex coating systems using arc plasma technology. *Surf. Coat. Tech.*, 2005, 200, 1464 – 1471.
16. **Huang, S.W., Samandi, M., Brandt. M.** Evaluation of duplex coatings produced with a pulsed Nd:YAG laser and filtered arc. *Surf. Coat. Tech.*, 2002, 153, 31 – 39.
17. **Rudenja, S., Leygraf, C., Pan, J., Kulu, P., Talimets, E., Mikli, V.** Duplex TiN coatings deposited by arc plating for increased corrosion resistance of stainless steel substrate. *Surf. Coat. Tech.*, 1999, 114, 129 – 136.
18. **Recco, A.A.C., Oliveira, I.C., Massi, M., Maciel, H.S., Tschiptschin, A.P.** Adhesion of reactive magnetron sputtered TiN_x and TiC_y coatings to AISI H13 tool steel. *Surf. Coat. Tech.*, 2007, 202, 1078 – 1083.
19. **Majzoobi, G.H., Nemati, J., Rooz, A.J.N., Farrahi, G.H.** Modification of fretting fatigue behaviour of Al7075-T6 alloy by the application of titanium coating using IBED technique and shot peening. *Trib. Int.*, 2009, 42, 121 – 129.
20. **Pantleon, K., Kessler, O., Hoffmann, F., Mayr, P.** Induction surface hardening of hard coated steels. *Surf. Coat. Tech.*, 1999, 120 – 121, 495 – 501.
21. **Heidkamp, M., Kessler, O., Hoffmann, F., Mayr, P.** Laser beam surface hardening of CVD TiN-coated steels. *Surf. Coat. Tech.*, 2004, 188 – 189, 294 – 298.
22. **Pogrebnjak, A.D., Ruzimov, Sh.M., Alontseva, D.L., Żukowski, P., Karwat, C., Kozak, C., Kolasik, M.** Structure and properties of coatings on Ni base deposited using a plasma jet before and after electron a beam irradiation. *Vacuum*, 2007, 81, 1243 – 1251.
23. **Zenker, R., Sacher, G., Buchwalder, A., Liebich, J., Reiter, A., Häßler, R.** Hybrid technology hard coating – Electron beam surface hardening. *Workshop "Tribology and Surface Engineering"*, 28.-30.03.2007, Berlin.
24. **Sacher, G., Zenker, R.** Subsequent Heat Treatment of Hard Coated Steels by Electron or Laser Beam. *Workshop "Tribology and Surface Engineering"*, 28.-30.03.2007, Berlin.
25. **Öztarhan, A., Brown, J., Bakkaloglu, C., Watt, G., Evans, P., Oks, E., Nikolaev, A., Tek, Z.** Metal vapour vacuum arc ion implantation in Turkey. *Surf. Coat. Tech.*, 2005, 196, 327 – 332.

26. **Wang, L., Nam, K.S., Kwan, S.C.** Effect of plasma nitriding of electroplated chromium coatings on the corrosion protection C45 mild steel. *Surf. Coat. Tech.*, 2007, 202, 203 – 207.
27. **Czyrska-Filemonowicz, A., Buffat, P.A., Wierzchon, T.** Microstructure and properties of hard layers formed by duplex surface treatment containing nickel and phosphorous on a titanium-based alloy. *Scripta Materialia*, 2005, 53, 1439 – 1442.
28. **Wang, L., Kim, D.S., Nam, K.S., Kim, M., Kwon, S.C.** Microstructure of electroplated hard chromium coating after plasma nitrocarburizing. *Surf. Coat. Tech.*, 2005, 190, 151 – 154.
29. **Garbacz, H., Wieciński, P., Ossowski, M., Ortore, M.G., Wierzchoń, T., Kurzydłowski, K.J.** Surface engineering techniques used for improving the mechanical and tribological properties of the Ti6Al4V alloy. *Surf. Coat. Tech.*, 2008, 202, 2453 – 2457.
30. **Béjar, M.A., Schnake, W., Saowedra, W., Vildósola, J.P.** Surface hardening of metallic alloys by electrospark deposition followed by plasma nitriding. *Journal of Materials Processing Technology*, 2006, 176, 210 – 213.
31. **Lei, J., Zhuo, C., Tao, J., Jiang, S.** The effect of second-phase on the corrosion and wear behaviours of composite alloying layer. *Applied Surface Science*, 2008, 255, 2688 – 2696.
32. **Serres, N., Hlawka, F., Costil, S., Langlade, C., Machi, F.** Microstructure and mechanical properties of metallic NiCrSiB and composite NiCrSiB-WC layers manufactured via hybrid plasma / laser process. *Applied Surface Science*, 2011, 257, 12, 5132 – 5137.
33. **González, R., García, M.A., Peñuelas, I., Cadenas, M., del Rocío Fernández, Ma., Batter, A.H., Felgueroso, D.** Microstructural study of NiCrSiB coatings obtained by different processes. *Wear*, 2007, 263, 1 – 6, 619 – 624.
34. **Chen, H., Xu, C., Zhou, Q., Hutchings, J.M., Shipway, P.H., Liu, J.** Micro-scale abrasive wear behaviour of HVOF sprayed and laser remelted conventional and nanostructured WC-Co coatings. *Wear*, 2005, 258, 1 – 4, 333 – 338.
35. **Sidhu, B.S., Puri, D., Prakash, S.** Mechanical and metallurgical properties of plasma sprayed and laser remelted Ni-20Cr and Stellite-6 coatings. *Journal of Materials Processing Technology*, 2005, 159, 3, 347 – 355.
36. **Yilbas, B.S., Arif, A.F.M., Gondal, M.A.** HVOF-coating and laser treatment: three-point bending tests. *Journal of Materials Processing Technology*, 2005, 164 – 165, 954 – 957.
37. **Pokhmurska, A., Ciach, R.** Microstructure and properties of laser treated arc sprayed and plasma sprayed coatings. *Surf. Coat. Tech.*, 2000, 125, 1 – 3, 415 – 418.

38. **Zhang, S.-H., Cho, T.-Y., Yoon, J.-H., Fang, W., Song, K.-O, Li, M.-X., Joo, Y.-K., Lee, G.G.** Characterization of microstructure and surface properties of hybrid coatings of WC-CoCr prepared by laser heat treatment and high velocity oxygen fuel spraying. *Materials Characterization*, 2008, 59, 10, 1412 – 1418.
39. **Mateos, J., Cuetos, J.M., Vijande, R., Fernández, E.** Tribological properties of plasma sprayed and laser remelted 75/25 Cr_2C_3/NiCr coatings. *Trib. Int.*, 2001, 34, 5, 345 – 351.
40. **Wang, Y., Li, C.G., Tian, W., Yang, Y.** Laser surface remelting of plasma sprayed nanostructured Al_2O_3-13 wt%TiO_2 coatings on titanium alloy. *Applied Surface Science*, 2009, 255, 20, 8603 – 8610.
41. **Mateos, J., Cuetos, J.M., Fernández, E., Vijande, R.** Tribological behaviour of plasma-sprayed WC coatings with and without laser remelting. *Wear*, 2000, 239, 2, 274 – 281.
42. **Yuanzheng, Y., Youlan, Z., Zhengui, L., Yuzhi, C.** Laser remelting of plasma sprayed Al2O3 ceramic coatings and subsequent wear resistance. *Mater. Sci. Eng. A*, 2000, 291, 1 – 2, 168 – 172.
43. **Liang, G.Y., Wong, T.T., MacAlpine, J.M.K., Su, J.Y.** A study of wear resistance of plasma sprayed and laser-remelted coatings on aluminium alloy. *Surf. Coat. Tech.*, 2000, 127, 2 – 3, 232 – 237.
44. **Sidhu, B.S., Puri, D., Prakash, S.** Characterizations of plasma sprayed and laser remelted NiCrAlY bond coats and Ni3Al coatings on boiler tube steels. *Mater. Sci. Eng. A*, 2004, 368, 1 – 2, 149 – 158.
45. **Zhang, S.H., Yoon, J.H., Li, M.X., Cho, T.Y., Joo, Y.K., Cho, J.Y.** Influence of CO_2 laser heat treatment on surface properties, electrochemical and tribological performance of HVOF sprayed WC-24%Cr_2C_3-6%Ni coating. *Materials Chemistry and Physics*, 2010, 119, 3, 458 – 464.
46. **Yang, W., Li, M.** Effect of remelting process on characterization of air-plasma sprayed $Fe_{67.5}Ni_{23.5}B_9$ alloy coatings onto $_1Cr_{18}Ni_9Ti$ stainless steel. *Journal of Materials Processing Technology*, 2009, 209, 7, 3256 – 3263.
47. **Terčelj, M., Panjan, P., Urankar, I., Fajfar, P., Turk, R.** A newly designed laboratory hot forging test for evaluation of coated tool wear resistance. *Surf. Coat. Tech.*, 2006, 200, 3594 – 3604.
48. **Batista, J.C.A., Godoy, C., Buono, V.T.L., Matthews, A.** Characterization of duplex and non-duplex (Ti,Al)N and Cr–N coatings. *Mater. Sci. Eng. A*, 2002, 336, 39 – 51.
49. **Podgornik, B.** Coated machine elements – fiction or reality? *Surf. Coat. Tech.*, 2001, 146 – 147, 318 – 323.
50. **Klimek, K.S., Ahn, H., Seebach, I., Wang, M., Rie, K.-T.** Duplex processes applied for die-casting and forging tools. *Surf. Coat. Tech.*, 2003, 174 – 175, 667 – 680.

51. **De Las Heras, E., Egidi, D.A., Gorengia, P., González-Santamaría, D., Garsía-Luis, A., Brizuela, M., López, G.A., Flores Martines, M.** Duplex surface treatment of an AISI 316L stainless steel; microstructure and tribological behaviour. *Surf. Coat. Tech.*, 2008, 202, 2945 – 2954.
52. **Zeghni, A.E., Hashmi, M.S.J.** The effect of coating and nitriding on the wear behaviour of tool steels. *Journal of Materials Processing Technology*, 2004, 155 – 156, 1918 – 1922.
53. **Savisalo, T., Lewis, D.B., Luo, Q., Bolton, M., Hovsepian, P.** Structure of duplex CrN/NbN coatings and their performance against corrosion and wear. *Surf. Coat. Tech.*, 2008, 202, 1661 – 1667.
54. **Batista, J.C.A., Godoy, C., Pintaúde, G., Sinatora, A., Matthews, A.** An approach to elucidate the different response of PVD coatings in different tribological tests. *Surf. Coat. Tech.*, 2003, 174 – 175, 891 – 898.
55. **La Vecchia, G.M., Lecis, N.** Impact test and tribological behaviour of duplex-treated low-alloy steel. *Surf. Coat. Tech.*, 2010, 205, 2, 614 – 619.
56. **Kamminga, J.-D., Hoy, R., Janssen, G.C.A.M., Lugscheider, E., Maes, M.** First results on duplex coatings without intermediate mechanical treatment. *Surf. Coat. Tech.*, 2003, 174 – 175, 671 – 676.
57. **Chen, C.-Z., Li, Q., Leng, Y.-X., Chen, J.Y., Zhang, P.-C., Bai, B., Huang, N.** Improved hardness and corrosion resistance of iron by Ti/TiN multilayer coating and plasma nitriding duplex treatment. *Surf. Coat. Tech.*, 204, 2010, 3082 – 3086.
58. **Navinšek, B., Panjan, P., Gorenjak, F**. Improvement of hot forging manufacturing with PVD and DUPLEX coatings. *Surf. Coat. Tech.*, 137, 2001, 255 – 264.
59. **Forsich, C., Heim, D., Mueller, T.** Influence of the deposition temperature on mechanical and tribological properties of a-C : H : Si coatings on nitrided and postoxidized steel deposited by DC–PACVD. *Surf. Coat. Tech.*, 203, 2008, 521 – 525.
60. **Batista J.C.A., Joseph M.C., Godoy C., Matthews A.** Micro-abrasion wear testing of PVD TiN coatings on untreated and plasma nitrided AISI H13 steel. *Wear*, 249, 2002, 971 – 979.
61. **Yerokhin, A.L., Leyland, A., Tsotos, G., Wilson, A.D., Nie, X., Matthews, A.** Duplex surface treatments combining plasma electrolytic nitrocarburising and plasma-immersion ion-assisted deposition. *Surf. Coat. Tech.*, 2001, 142 – 144, 1129 – 1136.
62. **Lee, S.Y., Kim, S.D., Hong, Y.S.** Application of the duplex TiN coatings to improve the tribological properties of Electro Hydrostatic Actuator pump parts. *Surf. Coat. Tech.*, 2005, 193, 266 – 271.

63. **Podgornik, B., Vižintin, J., Wänstrand, O., Larsson, M., Hogmark, S., Ronkainen, H., Holmberg, K.** Tribological properties of plasma nitrided and hard coated AISI 4140 steel. *Wear*, 2001, 249, 254 – 259.
64. **Podgornik, B., Vižintin, J., Wänstrand, O., Larsson, M., Hogmark, S.** Wear and friction behaviour of duplex-treated AISI 4140 steel. *Surf. Coat. Tech.*, 1999, 120 – 121, 502 – 508.
65. **Liang, W., Yuzhou, G., Bin, X.** Plasma vapor deposition hard coating on pre-nitrided low alloy steel. *Surf. Coat. Tech.*, 2000, 131, 452 – 456.
66. **de Frutos, A., Arenas, M.A., Fuentes, G.G., Rodrígues, R.J., Martínez, R., Avelar-Batista, J.C., de Damborenea, J.J.** Tribocorrosion behaviour of duplex surface treated AISI 304 stainless steel. *Surf. Coat. Tech.*, 2010, 204, 1623 – 1630.
67. **Rahman, M., Haider, J., Dowling, D.P., Duggan, P., Hashmi, M.S.J.** Investigation of mechanical properties of TiN+MoS_x coating on plasma-nitrided substrate. *Surf. Coat. Tech.*, 2005, 200, 1451 – 1457.
68. **Zukerman, I., Raveh, A., Kalman, H., Klemberg-Sapieha, J.E., Martinu, L.** Thermal stability and wear resistance of hard TiN/TiCN coatings on plasma nitrided PH 15-5 steel. *Wear*, 2007, 263, 1249 – 1252.
69. **Luo, Q., Hasepian, P.E., Lewis, D.B., Münz, W.-D., Kok, Y.N., Cockrem, J., Bolton, M., Farinotti, A.** Tribological properties of unbalanced magnetron sputtered nano-scale multilayer coatings TiAlN/VN and TiAlCrYN deposited on plasma nitrided steels. *Surf. Coat. Tech.*, 2005, 193, 39 – 45.
70. **Podgornik, B., Vižintin, J., Ronkainen, H., Holmberg, K.** Friction and wear properties of DLC-coated plasma nitrided steel in unidirectional and reciprocating sliding. *Thin Solid Films*, 2000, 377 – 378, 254 – 260.
71. **Nie, X., Tsotos, C., Wilson, A., Yerokhin, A.L., Leyland, A., Matthews, A.** Characteristics of a plasma electrolytic nitrocarburising treatment for stainless steels. *Surf. Coat. Tech.*, 2001, 139, 135 – 142.
72. **Fu, Y., Du, H.** Effects of the counterface materials on the tribological characteristics of CN coating deposited on plasma-nitrided Ti-6Al-4V. *Mater. Sci. Eng. A*, 2001, 298, 16 – 25.
73. **Liu, Y., Meletis, E.J.** Tribological behaviour of DLC coatings with functionally gradient interfaces. *Surf. Coat. Tech.*, 2002, 153, 178 – 183.
74. **Donnet, C., Erdemir, A.** Historical developments and new trends in tribological and solid lubricant coatings. *Surf. Coat. Tech.*, 2004, 180 – 181, 76 – 84.
75. **Steiner, L., Bouvier, V., May, U., Hegadekatte, V., Huber, N.** Modelling of unlubricated oscillating sliding wear of DLC-coatings considering surface topography, oxidation and graphitisation. *Wear*, 2010, 268, 9 – 10, 1184 – 1194.

76. **Schaaf P.** Laser nitriding of metals. *Progress in Materials Science*, 2002, 47, 1, 1 – 161.
77. Description of production methods, used in Bodycote OY, http://www.bodycote.fi/fi/leftframe/Leftframeset_menetelm%E4t.htm, 23.04.2011. [in Finnish]
78. **Sivitski, A.** *Sliding Wear of PVD Hard Coatings: Fatigue and Measurement Aspects*. PhD Thesis. Tallinn University of Technology, Estonia, Tallinn, 2010.

ABSTRACT

During the duplex treatment, two or more surface treatment technologies are sequentially applied to obtain a composite, whose properties are higher than obtainable through an individual technology. Laser and electron beam surface treatment of coatings seems to be the most universal duplex treatment, as it allows to treat both thin and thick coatings. Laser and electron beam hardening improve the adhesion of a PVD or CVD coating by 1.2 – 3.3 times and surface hardness – by 1.2 – 2.3 times, depending on the substrate, whereas coating's distortion is minimal. Laser or electron beam treatment (remelting) improves the adhesion of thermal sprayed coatings by 1.05 – 3.4 times, however, hardness can as drop by 1.03 – 1.5 times, as rise by 1.1 – 2.2 times, depending on the sprayed material. Wear resistance of the remelted coatings also fluctuates 0.5 – 20 times in respect to the initial values. Nitriding/nitrocarburising in pair with a PVD/CVD coating remains the most popular duplex treatment. Nitriding of the substrate can improve the adhesion of a PVD/CVD coating by 1.2 – 19 times, sliding wear resistance – by 1.6 – 19.8 times, also it significantly improves the impact wear resistance.

In this work duplex treatment of thin (2 – 3 μm) PVD and thick (200 – 300 μm) thermal sprayed coatings is studied. The duplex treatments include the combinations of steel substrate plasma nitriding and subsequent PVD coating, PVD coating of a steel substrate and subsequent laser hardening and thermal spraying of a coating and subsequent laser treatment. PVD coated CS and CWTS were chosen for the laser hardening, nitradable low alloy steel was chosen for plasma nitriding and PVD single layer TiN (I generation), multilayer (Ti,Al)N-ML (II generation), gradient (Al,Ti)N-G and nanocomoposite multilayer FiVIc® (both – III generation) coatings' deposition. HVOFS Hardmetal and PS composite Ni- and Fe-based self-fluxing alloy-recycled hardmetal thermal sprayed coatings were chosen for laser treatment.

Microstructure and microhardness of all studied coatings and substrates were investigated. PVD coated steels were subjected to cyclic indentation, impact and sliding wear (nitrided ones) tests, laser treated TS coatings were subjected to cyclic indentation, impact wear and abrasive wear tests.

Microstructure studies and microhardness measurements demonstrated a formation of 80 – 100 μm hardened layer under the PVD TiN coated laser hardened CWTS and (Al,Ti)N coated CS. PVD (Al,Ti)N coated laser hardened CS demonstrated medium resistance to cracks' formation, TiN and Ti(C,N) coated laser hardened CS showed low resistance to cracking.

The nitrided layer with the thickness of 250 μm was observed in the nitrided specimens. Medium crack resistance was observed in the case of the III generation gradient PVD (Al,Ti)N-G coating. All other coatings demonstrated high susceptibility to cracking. The PVD I generation TiN coating demonstrated

the 1.1 – 1.3 higher impact wear resistance in comparison with the other coatings. The III generation FiVIc® coating demonstrated the 1.2 times lower wear, than the TiN coating, 1.4 times lower wear, than the (Ti,Al)N-ML coating, and 8.9 times lower wear, than the (Al,Ti)N-G coating.

Laser treatment of HVOFS hardmetal coating leads to the high degree of porosity of the near-surface layer, bringing the decrease in microhardness and lower wear resistance, than the reference material. Porous free structure was observed in the PS laser treated composite coatings, however, large chemical inhomogeinety of Ni-based self-fluxing alloy-recycled hardmetal composite coating was observed.

Laser treated HVOFS hardmetal coating demonstrated medium resistance to cracking and good resistance to impact wear.

The Ni-based composite coatings showed lower wear resistance in comparison with the Fe-based ones. The Ni-based composite coatings indicated higher abrasion wear at 30º impact angle and lower wear at 90º impact angle. Abrasive-erosion wear resistance of the Fe-based composite coatings was at the level of reference material at 30º impact angle and 1.5 times higher at 90º. The abrasive-erosion wear reistance of the Fe-based self-fluxing alloy composite coatings was approximately 1.5 times higher in comparison with the Ni-based ones.

Keywords: duplex treatment, coatings, PVD, thermal spraying, laser hardening, laser treatment

KOKKUVÕTE

Duplekspindamisel rakendatakse kahte või enamat pinnatöötlustehnoloogiat, et saada kombineeritud pindeid, millede omadused on kõrgemad võrreldes üksikpinnatehnoloogia kasutamisel saaduga. Laser- ja elektroonkiirtöötlus koos teiste pindamismoodustustega – duplekstöötlus võimaldab töödelda nii õhukesi kui pakse pindeid. Laser- ja elektroonkiirkarastus võimaldab tõsta aurustussadestatud pinnete naket 1.2 – 3.3 korda ja pinnakõvadust 1.2 – 2.3 korda minimaalse deformatsiooni juures. Laser/elektroonkiirpinnatöötlus võimaldab parandada termopihustatud pinnete naket 1.05 – 3.4 korda, kõvadus aga võib pärast töötlust kas langeda (1.03 – 1.50 korda), või ka tõusta 1.1 – 2.2 korda sõltuvalt pihustatud materjalist. Kulumiskindlus varieerub peale töötlust 0.5 – 20 korda võrreldes töötlemata olekuga. Kõige populaarsemaks duplekstöötluseks jääb nitriitimine/karbonitriitimine järgneva aurustussadestamisega. Aluse nitriitimine võimaldab tõsta aurustussadestatud pinde naket 1.2 – 19 korda, liugekulumiskindlust – 1.6 – 19.8 korda, sealjuures oluliselt paraneb löökkulumiskindlus.

Antud töös uuritakse õhukeste (2 – 3 μm) aurusstussadestatud ja paksude (200 – 300 μm) termopihustatud pinnete duplekstöötlust, kombineerides terasaluse plasmanitriitimist ja järgnevat aurustussadestust, aurustussadestusele järgnevat laserkarastust ning termopihustamist ja järgnevat lasertöötlust. Aurustussadestamisel alusmaterjaliks olid valitud süsinikteras ja külmtööriistateras laserkarastuseks ning nitriiditav madallegeerteras plasmanitriitimiseks. Õhukestest aursustussadestatud pinnetest olid valitud ühekihiline TiN (I põlvkond), mitmekihiline (Ti,Al)N-ML (II generatsioon), gradient- (Al,Ti)N-G ja nanokomposiitpinne FiVIC® (mõlemad – III põlvkond). Kiirleekpihustatud kõvasulampinne ja plasmapihustatud komposiitpinne Ni ja Fe baasil iseräbustuvast sulamist ja taaskasutatud kõvasulamist allutati lasertöötlusele.

Uuriti erinevate pinnete mikrostruktuuri ja mikrokõvadust valitud alustel. Tsüklilist indenteerimist (koormus 50 N, sagedus 50 Hz, 10^4 tsüklit) ja löökkulumise meetodit (koormus 16 N, sagedus 50 Hz, 10^4 – 10^7 tsüklit) kasutati aurustussadestuspinnatud laserkarastatud süsinikterase, nitriiditud aurustussadestuspinnatud madallegeerterase ja kiirleekpihustatud lasertöödeltud kõvasulampinde uurimisel. Kulutamismeetoditest kasutati liugkulutamistesti (koormus 10 N, sagedus 5 Hz) nitriiditud ja aurustussadestuspinnete korral. Abrasioonkulumisele katsetati (koormus 47/222 N, pöörlemiskiirus 200.8/238 min^{-1}, kestvus 3 min) aga kiirleek- ja plasmapihustatud lasertöödeldud pinded. Abrasiiverosioonile (abrasiivosakeste kiirus 80 m/s, kohtumisnurk 30º/90º) ja abrasiivlöökkulutamisele (abrasiivosakeste kiirus 80 m/s, kohtumisnurk 90º) allutati plasmapihustatud ning lasertöödeldud pinded.

Mikrostruktuuri ja mikrokõvaduse uuringud viitasid 80 – 100 μm karastatud kihi tekkele aurustussadestus- TiN pinde külmtööriistaterasel ja (Al,Ti)N pinde süsinikterasel. Karastatud kiht puudus aurustussadestus- TiN ja Ti(C,N) pinde korral süsinikterasel. Aurustussadestus- (Al,Ti)N pinne laserkarastatud süsinikterasel näitas keskmist vastupanu pragude tekkele, TiN ja Ti(C,N) pinded – madalat vastupanuvõimet.

Nitriiditud terasalusel ilmnes ligi 250 μm sügav nitriiditud kiht. III põlvkonna aurustussadestuspinne (Al,Ti)N-G näitas keskmist vastupanu pragude tekkele, ülejäänud pinded – madalat vastupanuvõimet pragunemisele. I põlvkonna TiN pinne näitas parimat löökkulumiskindlust võrreldes teiste pinnetega, samal ajal III põlvkonna FiVIc® pinne näitas parimat liugkulumiskindlust.

Lasertöödeldud kiirleekpihustatud kõvasulampinde struktuuris ilmnesid olulised muutused: pinnalähedases kihis tekkis kõrgpoorne ala, mis viis mikrokõvaduse vähenemiseni 2.2 korda ja kulumiskindluse languseni 6.2 korda võrreldes ainult pihustatud WC-17Co kõvasulampindega. Plasmapihustatud ja lasertöödeldud komposiitpinded olid poorivabad, kuigi suur struktuuri mittehomogeensus oli omane Ni baasil iseräbustuvast sulamist ja taaskasutatud kõvasulamist pindele.

Lasertöödeldud kiirleekpinne omas keskmist vastupanuvõimet pragude tekkele ja head vastupanuvõimet löökkulumisele.

Plasmapihustatud ja lasertöödeldud komposiitpinded Ni– ja Fe–sulamite baasil näitasid madalat abrasiivkulumiskindlust. Ni–sulami baasil komposiitpinded näitasid suuremat erosioonkulumist 30º kohtumisnurgal ja madalamat kulumist 90º kohtumisnurgal; Fe–sulami baasil komposiitpinded aga madalamat kulumist 30º kohtumisnurgal ja suuremat kulumist 90º juures. Abrasiivlöökkulumise tingimustes Ni–sulami baasil komposiitpinded näitasid suuremat ja Fe–sulami baasil väiksemat kulumist võrreldes etalonmaterjaliga (teras C45).

Töö järeldused on järgmised:

1. Terasaluse eelnitriitimine või järeltöötlus (laserkarastus) võimaldavad saada pinde all 100 – 250 μm paksust tugevdatud kihi. Laserkarastamisel saadud aluskihi kõvadus on 1.5 – 2 korda suurem karastamata terase omast, kusjuures tõus on märgatavam väiksema süsinikusisaldusega konstruktsiooniterase korral. Plasmapihustatud iseräbustuva sulami baasil komposiitpinde lasertöötlus võimaldab saada poorivaba struktuuri; suurim efekt on Fe–sulami baasil iseräbustuvate sulamite korral. Kiirleekkõvasulampinde lasertöötlus pole soovitav, kuna toob kaasa pooride ja pragude tekke, mis alandavad nii kõvadust kui ka abrasiivkulumiskindlust.
2. Parim vastupanu pragude tekkele oli demonstreeritud laserkarastatud või nitriiditud alusel (Al,Ti)N-G pinde korral. Lasertöödeldud kiirleekpinne omab keskmist vastupanuvõimet pragude tekkele.

3. Aurustussadestuspinnetest näitas I põlvkonna TiN pinne parimat löökkulumiskindlust (1.1 – 1.3 korda) võrreldes teiste pinnetega. Kiirleekpihustatud lasertöödeldud kõvasulampinne näitas head löökkulumiskindlust.
4. Aurustussadestusdupleksipinnete (plasmanitriitimine järgneva aurustus-sadestamisega) liugkulumiskindlus sõltub hõõrdetegurist. Aurustussadestatud III põlvkonna FiVIc® pinne näitas 1.2 korda madalamat kulumist, kui TiN pinne, 1.4 korda madalamat kulumist kui (Ti,Al)N-ML pinne ja 8.9 korda madalamat kulumist kui (Al,Ti)N-G pinne. Kiirleekpihustatud lasertöödeldud pinne näitas 6.2 korda suuremat abrasiivkulumist võrreldes võrdlusmaterjaliga. Plasmapihustatud lasertöödeldud Fe–sulami baasil iseräbustuvast sulamist komposiitpinded näitasid 1.1 – 1.9 korda paremat kulumiskindlust, kui Ni–sulami baasil iseräbustuvast sulamist komposiitpinded, välja arvatud erosioonkulumine 90º kohtumisnurgal, mil Ni baasil iseräbustuvast sulamist komposiitpinne osutus paremaks võrreldes Fe baasil sulamiga (1.1 korda).
5. Tulevaseks tööks on plaanitud järgmised tegevused:
   - laserkarastuse ja plasmanitriitimise mõju aurustussadestatud pinnete nakkele ja liugekulumiskindlusele;
   - kõva faasi koguse ja lasertöötluse parameetrite mõju uurimine termopinnete struktuurile ja omadustele;
   - dupleksipinnete potentsiaalsete kasutusalade määratlemine.

Võtmesõnad: dupleksitöötlus, pinded, aurustussadestus, termopihustus, laserkarastus, lasertöötlus

CURRICULUM VITAE

1. Personal data

   Name and surname Andrei Surzhenkov
   Date and place of birth 23.06.1983, Tallinn, Estonia

2. Contact information

   Address Ehitajate tee 5, 19086 Tallinn, Estonia
   Phone +372 5102198
   E-mail andrei.surzenkov@ttu.ee

3. Education

Educational institution	Year of graduation	Education (field of study/degree)
Tallinn University of Technology	2011	Faculty of Mechanical Engineering, Mechanical Engineering / PhD
Tallinn University of Technology	2007	Faculty of Mechanical Engineering, Product Development and Production Engineering / MSc.
Tallinn University of Technology	2005	Faculty of Mechanical Engineering, Product Development and Production Engineering / BSc.

4. Language competence/skills (fluent; average; basic skills)

Language	Level
Estonian	Fluent
Russian	Mother tongue
English	Fluent
German	Basic skills

5. Professional Employment

Period	Organization	Position
2008 – present	Tallinn University of Technology / Department of Materials Engineering	Researcher
2007	Tallinn University of Technology / Department of Materials Engineering	Engineer
2004 - 2007	Setton Ltd.	Technician-translator

6. Scientific work

Period of the project	Project name	Project no.
2008 – 2013	Hard coatings and surface engineering	SF0140091s08
2010 - 2012	Investigation in residual stresses in thermally sprayed and deposited coatings	ETF8459
2009 – 2011	Carbon nanotufibers based hard-lubricant tribological coatings	F9068
2008 - 2010	Optimization of tribological properties of PVD hard coatings	ETF7442
2008	Carbon nanotubes (CNT) based hard-lubricant tribological coatings	F8083
2007 - 2009	Modelling of wear resistance of composite materials and coatings	ETF7227
2003 – 2007	Wear resistant materials and wear	SF0142505s03

7. Main areas of scientific work/Current research topics

   a. Hard coatings and surface engineering SF0140091s08
   b. Investigation of residual stresses in thermally sprayed and deposited coatings ETF8459

8. Other research projects

   a. Graduate school “Functional materials and processes”, European Social Fund under project 1.2.0401.09 – 0079.
   b. Organizing conference Baltmattrib 2009, BF120, 2009.
   c. Graduate school “New manufacturing technologies and processes”, Socrates, 2007 – 2008.

ELULOOKIRJELDUS

1. Isikuandmed

Nimi ja perekonnanimi	Andrei Surzhenkov
Sünniaeg ja –koht	23.06.1983, Tallinn, Estonia
Kodakondsus	Eesti

2. Kontaktandmed

Aadress	Ehitajate tee 5, 19086 Tallinn, Eesti
Telefon	+372 5102198
E-post	andrei.surzenkov@ttu.ee

3. Haridus

Õppeasutus (nimetus lõpetamise ajal)	Lõpetamise aasta	Haridus (eriala/kraad)
Tallinna Tehnikaülikool	2011	Mehaanikateaduskond, Masina- ja aparaadiehitus/ tehnikateaduste doktor
Tallinna Tehnikaülikool	2007	Mehaanikateaduskond, Tootearendus ja tootmistehnika/ tehnikateaduste magister
Tallinna Tehnikaülikool	2005	Mehaanikateaduskond, Tootearendus ja tootmistehnika/ tehnikateaduste bakalaureus

4. Keelteoskus (alg-, kesk- või kõrgtase)

Keel	Tase
Eesti	Kõrgtase
Vene	Emakeel
Inglise	Kesktase
Saksa	Algaja

5. Teenistuskäik

Töötamise aeg	Tööandja	Ametikoht
2008 – käesolev hetk	Tallinna Tehnikaülikool / Materjalitehnika instituut	Teadur
2007	Tallinna Tehnikaülikool / Materjalitehnika instituut	Insener
2004 - 2007	Setton OÜ	Tehnik-tõlk

6. Teadustegevus

2008 – 2013	Kõvapinded ja pinnatehnika	SF0140091s08
2010 - 2012	Jääkpingete uurimine termopihustatud ja sadestatud pinnetes	ETF8459
2009 – 2011	Isemäärivad süsiniknanokiudude (CNF) tribopinded	F9068
2008 - 2010	Aurustussadestatud kõvapinnete triboloogia omaduste optimiseerimine	ETF7442
2008	Isemäärivad süsinikunanotoru (CNT) tribopinded	F8083
2007 - 2009	Komposiitmaterjalide ja -pinnete kulumiskindluse modelleerimine	ETF7227
2003 – 2007	Kulumiskindlad materjalid ja kulumine	SF0142505s03

7. Teadustöö põhisuunad

a. Kõvapinded ja pinnatehnika SF0140091s08
b. Jääkpingete uurimine termopihustatud ja sadestatud pinnetes ETF8459

8. Teised uurimisprojektid

a. Doktorikool "Funktsionaalsed materjalid ja tehnoloogiad", Euroopa Liit, Euroopa Sotsiaalfond, 2009 – 2010.
b. Teaduskonverentsi Baltmattrib 2009 korraldamine, BF120, 2009.
c. Doktorikool "Uued tootmistehnoloogiad ja -protsessid", Socrates, 2007 – 2008.

PAPER I

Surzhenkov, A.; Kulu, P.; Gregor, A.; Vuoristo, P.; Latokartano, J.; Rupponen, M. (2008). Laser Treatment of PVD Coated Carbon Steels and Powder Steels. *Materials Science (Medžiagotyra)*, 14 (4), 301 – 305.

ISSN 1392–1320 MATERIALS SCIENCE (MEDŽIAGOTYRA). Vol. 14, No. 4. 2008

Laser Treatment of PVD Coated Carbon Steels and Powder Steels

Andrei SURZHENKOV[1*], Priit KULU[1], Andre GREGOR[2], Petri VUORISTO[2], Jyrki LATOKARTANO[2], Mikko RUPPONEN[2]

[1]*Department of Materials Engineering, Tallinn University of Technology, Ehitajate tee 5, 19086 Tallinn, Estonia*
[2]*Laser Application Laboratory, Tampere University of Technology, Korkeakoulunkatu 6, 33101 Tampere, Finland*

Received 01 June 2008; accepted 29 June 2008

In the present study, the opportunities of laser beam treatment by the means of the 4 kW Nd:YAG laser are investigated. The studied materials are carbon steels C 45 and C22E (carburized), coated with the PVD coatings Ti(C,N), TiN and (Al,Ti)N, and powder steel Vanadis 6. The macrophotos of the laser beam treated surfaces were taken, the microstructures of the cross-sections of laser beam treated specimens were studied, and the microhardness profiles of the cross-sections of laser beam treated specimens were made. As these studies have shown, no signs of the influence of laser beam appear at the surface of the PVD coatings, until an energy input threshold is reached, after that the coating oxidizes and degrades. No hardened zones were found under the PVD coatings, except for (Al,Ti)N coating. In the case of steel Vanadis 6, three distinct zones can be seen. In the first zone, the carbide particles have dissolved, and a dendritic structure has appeared. In the second zone, the carbide particles remained, however, they were of smaller size in comparison with the initial structure. In the third zone, the initial structure remained. The growth of microhardness values was observed in the first and in the second zone, whereas bigger values were obtained in the second zone.

Keywords: laser beam treatment, PVD coatings, powder steels.

1. INTRODUCTION

The usage of hard physically vapour deposited (PVD) coatings has gained much acknowledgement as a way to remarkable improvement of tribological and corrosion resistance properties of a material. However, their application is restricted by the possibility of plastic deformation of the substrate [1 – 5], as the coatings themselves are very thin, and the load is to be carried by the substrate. To resist this, different pre- and after-treatments of the substrate are applied.

Among other techniques, laser beam treatment is attracting strong attention [6]. In comparison to other methods, it allows to obtain bigger substrate hardness values, than other heat treatment methods, lower distortion of the surface. In addition to that, laser beam treatment is highly localized [7].

The aim of this study was to investigate the opportunities of laser beam treatment of carbon steels with Ti(C,N), TiN and (Ti,Al)N PVD coatings, as well as powder steels.

2. EXPERIMENTAL

2.1. Preparation of the specimens

The chemical composition of steels, used in this work, is presented in Table 1. Specimens of four different sizes were used. Specimens, made of steel C 45, were machined to sizes of (30 × 30 × 5) mm and (15 × 25 × 5) mm. Specimens, made of steel C22E, had dimensions Ø 30 mm × 5 mm. Specimens, made of steel Vanadis 6, were of (25 × 30 × 5) mm size.

Specimens, made of steel C22E, were subjected to pack carburizing during 6 hours at the temperature of 900 ºC. The depth of the carburized layer was approximately 1 mm.

Specimens, made of steels C 45 and C22E, were grinded and polished using silicon carbide based grinding papers with grit sizes, gradually decreasing from 80 to 4000. Specimens, made of steel Vanadis 6, were polished with grinding papers with grit sizes gradually decreasing from 80 to 400.

The physical vapor deposition process was applied on specimens, made of steels C 45 and C22E. For the physical vapor deposition process, the PLATIT π^{80} hard-coating system was applied. The standard Ti(C,N) and (Al,Ti)N coatings were applied to specimens, made of steel C22E, and the standard Ti(C,N), (Al,Ti)N and TiN coatings were applied to the specimens, made of steel C 45. The thickness of the coatings equalled to 2,5 μm in all the cases.

2.2. Laser treatment stage

Laser beam treatment was performed using the Haas HL4006D 4 kW Nd:YAG laser with the wavelength of 1064 nm. The laser was operated in the CW mode, the dimensions of a laser spot were set as 4 mm × 9 mm. Treatment zone was shielded with argon at the flow rate of 20 l/min. Three passes without overlapping were applied to each specimen, treated at final sets of parameters. The principle scheme of a laser beam treatment is presented by Fig. 1. The final treatment parameters are brought at Table 2.

The choice of final parameters of treatment was partially dictated by [11], partially by the preliminary experiments' data. TiN and (Al,Ti)N coatings were treated, using lower laser beam power, to avoid their destruction.

*Corresponding author. Tel.: + 372-5102198; fax.: + 372-6202020.
E-mail address: *andrei.surzenkov@ttu.ee* (A. Surzhenkov)

Table 1. Chemical composition of the used steels

Steel grade	C, %	Si, %	Mn, %	Cr, %	Mo, %	V, %	P, %	S, %
C 45	0.42 – 0.50	0.17 – 0.37	0.50 – 0.80	–	–	–	< 0.035	< 0.035
C22E	0.17 – 0.24	0.17 – 0.37	0.40 – 0.70	–	–	–	< 0.035	0.020 – 0.040
Vanadis 6	2.6	1.0	0.4	6.8	1.5	5.4	–	–

Table 2. Final parameters of the laser treatment

Coating or steel grade	Steel grade of the substrate	Laser beam power, W	Scan speed, mm/min
Ti(C,N)	C22E	600	300
	C 45	600	300
(Al,Ti)N	C22E	500	300
	C 45	500	300
TiN	C 45	500	300
Vanadis 6	–	1000	300

2.3. Obtained data evaluation

Macrophotos of the laser beam treated surface were made using Canon EOS 350D camera. To reveal the microstructures of laser treated specimens' cross-sections, the latter were polished, etched with nital and studied under the Axiovert 25 (Carl Zeiss, Germany) optical microscope. In addition to that, the Vickers microhardness profiles were obtained applying the Buehler Micromet 2001 microhardness tester. The load was 0.3 kg.

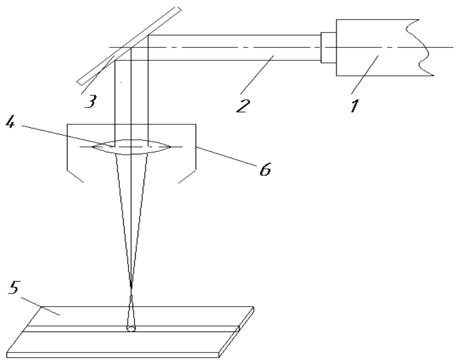

Fig. 1. The principle scheme of laser beam treatment: 1 – laser, which is operated in a pulsed or continuous wave mode, 2 – laser beam, 3 – turning mirror, 4 – optical system, 5 – specimen, 6 – nozzle for the gas feed

3. RESULTS AND DISCUSSION

3.1. Surface macrostructure

In the case of PVD coatings, no visible changes of the surfaces' conditions were noticed. However, when a certain threshold of energy input is exceeded, the coating is oxidized and removed from the substrate. Fig. 2 illustrates this case for the TiCN coating on carburized steel C22E.

In this case, three single passes at laser beam power values of 710 W, 650 W and 600 W (at Fig. 2, a, b and c respectively) at the constant speed of 300 mm/min were applied to the specimen. As it can be seen, degradation of the coating takes place in the middle of the laser beam treated zone. This can be explained by the different expansion coefficients of Ti(C,N) coating and the substrate. At the expense of that tensile stresses appear in the coating that leads to its degradation. Apart from that, the austenite-to-martensite transformation can be also partially responsible for the destruction of the coating, as the martensitic structure was found in the coating-free treated zone of the specimen, and the austenite-to-martensite transformation is followed by the size alterations.

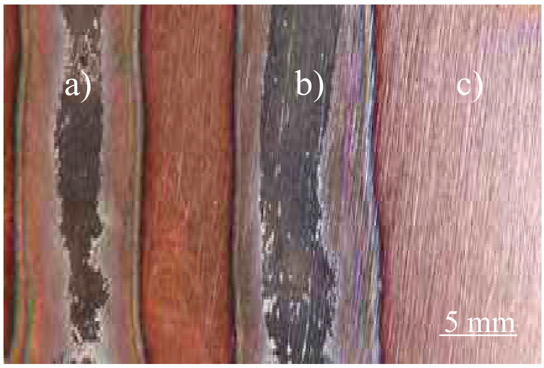

Fig. 2. The surface of laser beam treated Ti(C,N) coating, carried onto the carburized steel C22E. Scan speed 300 mm/min, laser beam power values: a) 710 W; b) 650 W; c) 600 W

Fig. 3. The surface of laser beam treated steel Vanadis 6. Scan speed 300 mm/min, laser beam power 1000 W

Fig. 3 represents the laser beam treated surface of steel Vanadis 6, where all three passes were completed, applying the final set of parameters. In this case, the surface melted significantly, whereas, as it can be seen, there is a clearly distinct border between the laser beam treatment zone and the surface, left untreated. In addition to that, it can be seen that at one edge the specimen has melted in a more dramatical way. The possible explanation for it is that the more melted zone appeared during the last pass, made by laser. In such case, the specimen is heated to a bigger extent, than at the beginning of treatment, thus the temperature in the zone of the third pass is higher.

3.2. Microstructure

Figs. 4 and 5 show the laser beam treated zones of carburized steel C22E specimens, which were coated with Ti(C,N) and (Al,Ti)N coatings, respectively. As it can be seen, no visible effect of treatment is present. The possible reason for it is that the temperature under the coating didn't exceed the phase transformation temperature.

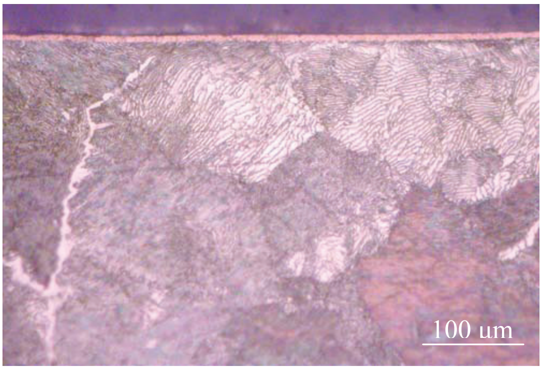

Fig. 4. Microstructure of laser beam treated carburized steel C22E, coated with the Ti(C,N) coating. Scan speed 300 mm/min, laser beam power 600 W

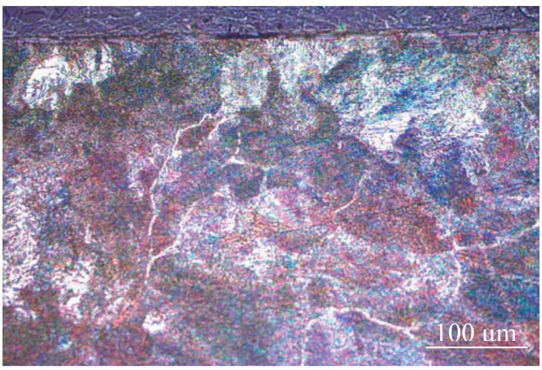

Fig. 5. Microstructure of laser beam treated carburized steel C22E, coated with the (Al,Ti)N coating. Scan speed 300 mm/min, laser beam power 500 W

Figs. 6 and 7 illustrate the laser beam treated zones of steel C 45, coated with Ti(C,N) and TiN PVD coatings, respectively. Neither in the first case nor in the second one any signs of phase transformation could be seen. The possible reason for it is that the phase transformation temperature has not been reached.

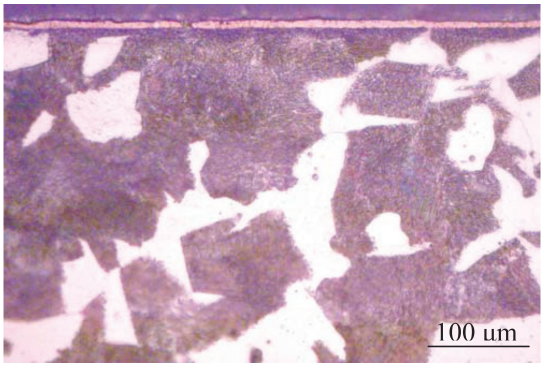

Fig. 6. Microstructure of laser beam treated steel C 45, coated with the Ti(C,N) coating. Scan speed 300 mm/min, laser beam power 600 W

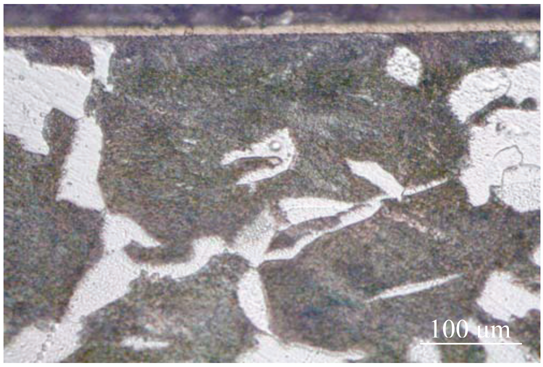

Fig. 7. Microstructure of laser beam treated steel C 45, coated with the TiN coating. Scan speed 300 mm/min, laser beam power 500 W

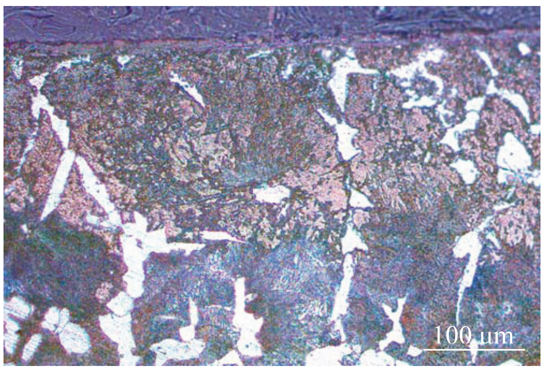

Fig. 8. Microstructure of the laser beam treated steel C 45, coated with the (Al,Ti)N coating. Scan speed 300 mm/min, laser beam power 500 W

Fig. 8 illustrates the structure of the laser beam treated steel C 45, coated with the (Al,Ti)N coating. The presence of small amounts of martensite can be seen. Such small amounts of martensite can be explained by an insufficient heating during the treatment. The reason, why such effect has not found place in the case of carburized steel C22E, can be the relatively large grains, which were not heated enough for the martensitic structures to appear.

Figs. 9 and 10 represent the microstructure of laser beam treated steel Vanadis 6. As it can be seen, two zones can be distinguished in the laser beam affected area. The first one, which is situated near the surface of the specimen, has a dendritic eutectic two-phase structure, whereas dendrites are mostly situated perpendicular to the direction of heating. This shows that in this case heat spreads rather by heat conductivity than by convection.

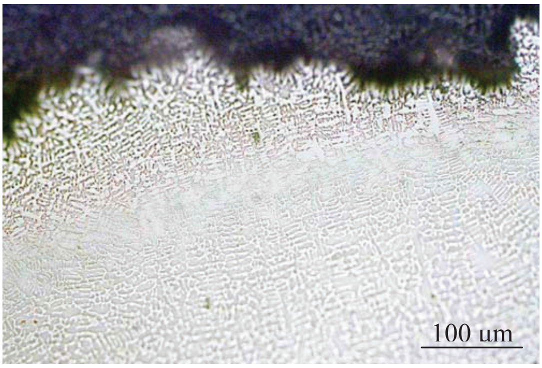

Fig. 9. Microstructure of the laser beam treated steel Vanadis 6. The first zone of the laser beam affected area. Scan speed 300 mm/min, laser beam power 1000 W

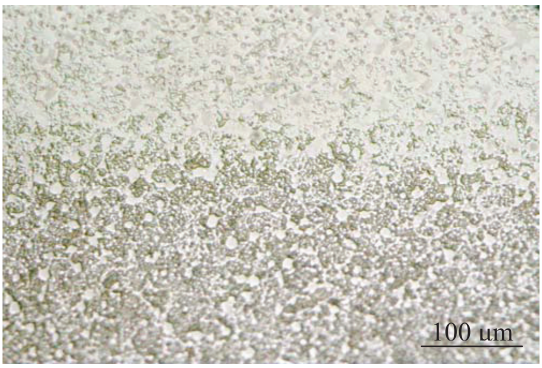

Fig. 10. Microstructure of the laser beam treated steel Vanadis 6. The second zone of the laser beam affected area. Scan speed 300 mm/min, laser beam power 1000 W

The second zone, situated near the untreated material, has a structure of the eutectic two-phase matrix with the dispersed carbide particles, whereas the latter are smaller than in the untreated material.

3.3. Microhardness

Fig. 11 represents the microhardness profiles of the cross-section of steel C22E laser beam treated specimens, coated with the Ti(C,N) and (Al,Ti)N coatings. In comparison, the microhardness profiles of the cross-sections of the untreated steel C22E specimens with the same coatings are brought.

As it can be seen, no hardening effect has found place. This can be explained by the insufficient heating by the laser beam.

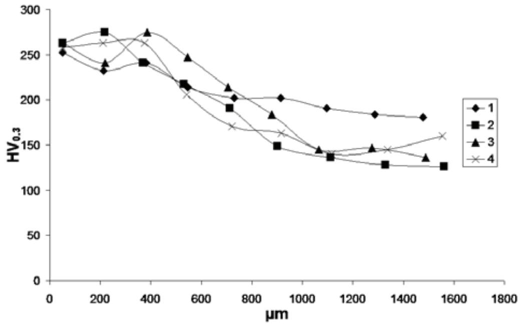

Fig. 11. The microhardness profiles of laser beam treated steel C22E specimens with PVD coatings: 1 – Ti(C,N), 2 – (Al,Ti)N, 3 – Ti(C,N), untreated, 4 – (Al,Ti)N, untreated

Fig. 12 shows the microhardness profiles of the cross-section of the laser beam treated steel C 45 specimens, coated with the coatings Ti(C,N), (Al,Ti)N and TiN coatings. In addition to them, the two horizontal lines illustrate the maximal and minimal microhardness values, obtained in the steel C 45 untreated specimens.

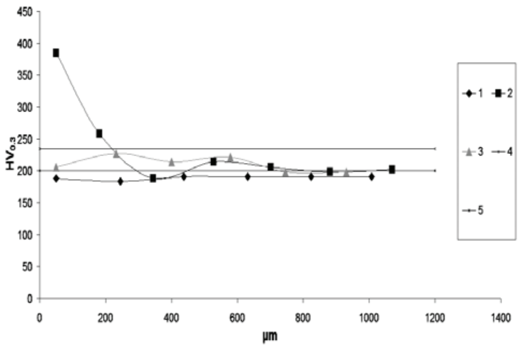

Fig. 12. The microhardness profiles of the laser beam treated steel C 45 specimens with the PVD coatings: 1 – Ti(C,N), 2 – (Al,Ti)N, 3 – TiN, 4 – C 45, untreated, maximal microhardness, 5 – C 45, untreated, minimal microhardness

As it can be seen, except for the specimen, coated with the (Al,Ti)N coating, where a hardened zone of about 200 μm appeared, no hardening effect can be seen. The possible reason for it is that the phase transformation temperature has not been reached in the majority of cases.

Fig. 13 represents the microhardness profile of the cross-section of the laser beam treated steel Vanadis 6.

As it can be seen, the depth of the hardened zone reaches 1400 μm, whereas the maximal microhardness value is approximately at the depth of 600 μm. Such distribution of the microhardness values can be explained by the fact that the microhardness of the eutectic, what formed at the top of the laser beam affected zone, has lower microhardness values than the structure in the middle of the laser beam affected zone. In its turn, it can be explained by the dissolution of carbides at the top of the laser beam affected zone, and the appearance of more

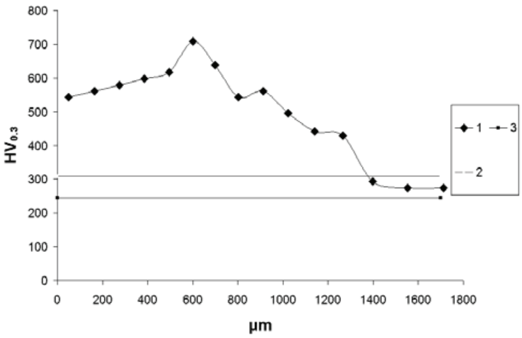

Fig. 13. The microhardness profile of the laser beam treated steel Vanadis 6 specimen: 1 – microhardness profile of the laser beam treated zone, 2 – steel Vanadis 6, untreated, maximal microhardness, 3 – steel Vanadis 6, untreated, minimal microhardness

dispersed carbides at the lower part of the laser beam affected zone.

4. CONCLUSIONS

1. No hardening effect is present in the steel C22E specimens with the given PVD coatings, treated at the current sets of parameters.
2. It is not recommended to carry out the laser beam treatment for the PVD Ti(C,N) coatings, being carried onto a carburized substrate, as the coating degrades before any hardening effect is achieved.
3. No signs of the hardening effect were found in the steel C 45 specimens with the Ti(C,N) and TiN coatings.
4. The depth of the hardened zone in the steel C 45 specimen with the (Al,Ti)N coating equaled to 200 µm, the maximal microhardness value was approximately 385 $HV_{0.3}$.
5. The depth of the hardened zone in the steel Vanadis 6 specimen was approximately 1400 µm, the biggest microhardness value in that zone equaled to approximately 710 $HV_{0.3}$.
6. It is recommended to avoid dissolution of carbides in the powder steel Vanadis 6 during the laser beam hardening, as it doesn't allow to obtain the maximal microhardness values.
7. The maximal microhardness values in the case of the steel Vanadis 6 appear, when the dispersed carbides are present in the structure.

Acknowledgments

The authors thank Endel Mens and Priidu Peetsalu from Tallinn University of Technology, as well as Eron Adolberg for the help during the preparation of the specimens and their investigation.

REFERENCES

1. **Batista, J. C. A., Godoy, C., Matthews, A.** Micro-scale Abrasive Wear Testing of Duplex and Non-duplex PVD (Ti,Al)N, TiN and Cr-N Coatings *Tribology International* 35 2002: p. 383.
2. **Batista, J. C. A, Godoy, C., Buono, V. T. L., Matthews, A.** Characterization of Duplex and Non-duplex (Ti,Al)N and Cr-N PVD Coatings *Materials Science and Engineering A* 336 2002: p. 40.
3. **Alsaran, A., Çelik, A., Çelik, C., Efeoğlu, İ.** Optimization of Coating Parameters for Duplex Treated AISI 5140 Steel *Materials Science and Engineering A* 371 2004: p. 141.
4. **Lee, S. Y.** Mechanical Properties of $TiN_x/Cr_{1-x}N$ Thin Films on Plasma Nitriding-assisted AISI H13 Steel *Surface & Coatings Technology* 193 2005: p. 55.
5. **De Las Heras, E., Egidi, D. A., Gorengia, P., González-Santamaria, D., Garsía-Luis, A., Brizuela, M., López, G. A., Flores Martinez, M.** Duplex Surface Treatment of an AISI 316L Stainless Steel; Microstructure and Tribological Behavior *Surface & Coatings Technology* 202: p. 2496.
6. **Sacher, G., Zenker, R.** Subsequent Heat Treatment of Hard Coated Steels by Electron or Laser Beam *German-Russian Workshop Tribology and Surface Engineering: Theory, Experiment, Technologies* Berlin University of Technology, March 28–30, 2007.
7. **Rykalin, N. N., Uglov, A. A., Zuev, I. V., Kockorah, A. N.** Laser and Electron Beam Treatment of Materials. Mashinostroyeniye, Moscow, 1985: p. 206 (in Russian).
8. Steels and Cast Irons. Standards (Grading, Composition, Properties). Matching. Ed. Kulu, P. Eesti Välismajanduse Teataja, Tallinn, 2001: pp. 17, 50 (in Estonian).
9. Eurometals. Steels, Cast Irons, Aluminum Alloys, Copper Alloys. Ed. Kulu, P. Tallinn, 2001: p. 1.154 (in Estonian).
10. Mechanical Production Engineer's Handbook. Vol. 1. Ed. Kosilova, A., Mestseryakov, R., Mashinostroenie, Moscow, 1986: p. 128 (in Russian).
11. **Adamiak, M., Dobrzański, L.** Microstructure and Selected Properties of Hot-work Tool Steel with PVD Coatings After Laser Surface Treatment *Applied Surface Science* 254 2008: pp. 4552 – 4556.
12. **Grigrorjants, A., Saphronov, A.** The Methods of Laser Beam Surface Treatment. Vysshaja shkola, Moscow, 1987 (in Russian).

Presented at the 17th International Conference
"Materials Engineering'2008"
(*Kaunas, Lithuania, November 06 – 07, 2008*)

PAPER II

Surzhenkov, A.; Allikas, G.; Gregor, A.; Zimakov, S.; Kulu, P.; Müller, H. (2008). Laser Treatment of Surfaces of Tool and PM steels and Steels with Coatings. *Proceedings of the 6th International Conference of DAAAM Baltic "Industrial Engineering"*: 24-26th April, 2008, Tallinn, Estonia. (Ed.) Küttner, R.. Tallinn University of Technology, 2008, 555 – 560.

6th International DAAAM Baltic Conference
INDUSTRIAL ENGINEERING”
24-26 April 2008, Tallinn, Estonia

LASER TREATMENT OF SURFACES OF TOOL AND PM STEELS AND STEELS WITH COATINGS

Surzhenkov A., Allikas G., Gregor A., Zimakov S., Kulu P., Müller H.

Abstract: Laser treatment of surfaces to improve their wear resistance was under the study. Specimens, made of plain carbon steel C45, tool steel Arne, PM steels Vanadis6 and Weartec® were laser hardened. HVOFS WC-17Co coating and PVD deposited TiN coating on steel substrates were treated applying CO_2 laser radiation, varying scan speed and power. The treated specimens were subjected to microhardness measurements and wear block-on-ring rubber wheel tests. The results of laser treatment showed that the microhardness values increased significantly in comparison with a conventional heat treatment. The wear resistance of all treated surfaces was lower, than in the case of conventional heat treatment methods.
Keywords: laser treatment, surface, steels, coatings.

1. INTRODUCTION

The purpose of this work was to study the potential of laser transformation hardening and laser treatment on four target groups: plain carbon steels, PM steels, steels with thermal sprayed coatings and physical vapor deposited coatings.

In the case of plain carbon steels and PM steels, the possibility of obtaining a harder and more wear resistant surface was researched, in the second case – the opportunity of enhancing these properties for the coating and the substrate, in the third one – the possibility of hardening the substrate steel.

2. EXPERIMENTAL

2.1 Studied materials and coatings

The materials studied include commercial conventional (C45, Arne) and powder metallurgy produced (PM) steels (Vanadis 6, Weartec®).

The chemical composition and initial microhardness of conventional and PM steels are shown in Tables 1 and 2.

The properties of high velocity oxy-fuel sprayed (HVOFS) WC-17Co coating and physical vapour deposited (PVD) TiN coating as well as the microhardness values of the substrates are given in Table 3.

2.2 Laser treatment

The used specimens were of 15 × 25 mm size, except for PVD TiN coated specimens, which had dimensions of 12 × 25 mm. For the current study, the CO_2 TRUMPF TLC 105 laser was applied. The wavelength equalled to 10.6 µm, the diameter of the laser spot – to 0.95 mm, focal length was –1 mm. The shield gas was N_2 at the pressure of 3 bars. No overlapping of laser passes was applied. The principle scheme of laser treatment is presented in Fig. 1.

The preliminary experiments were carried out in two stages. The task of the first stage was to find an optimal laser power value, the task of the second one – to find an optimal scan speed value. The parameters’ values were considered optimal, if they allowed the biggest microhardness values. Final parameters of laser treatment are brought in Table 4.

Table 1. Chemical composition (wt%), initial microhardness of plain carbon steels

Steel	C	Mn	Si	Cr	W	Others	HV0.3
C45	0.45	0.60	0.30	–	–	–	200–235
Arne	1.00	0.95	0.25	1.05	1.40	Cu < 0.30 Mo < 0.30 Ni < 0.35	220–230

Table 2. Chemical composition (wt%), initial microhardness of PM steels

Steel	C	Mn	Si	Cr	Mo	V	HV0.05
Vanadis 6	2.80	0.50	1.00	8.00	13.50	9.80	245 320
Weartec®	2.80	0.70	0.80	7.00	2.30	8.90	340 385

Table 3. Studied coatings and their properties

Type of coating	Substrate	Thickness of coating, μm	Microhardness	
			Substrate	Coating
HVOFS WC-17Co	C45	200	200–235 HV0.3	1400 HV0.3
	Arne	200	205–240 HV0.3	1350 HV0.3
PVD TiN	Vanadis 6	3	245–320 HV0.05	–

2.3 Microhardness measurement

The microhardness measurements in the case of preliminary experiments were carried out at the ZWICK 3212.002 measuring device. The applied load was 4.9 N for HVOFS WC-17Co coating and 2.0 N (the minimal possible) for steels and PVD TiN coatings.
The microhardness measurements, performed at specimens, treated at optimal parameters, were carried out at the Micromet 2001 measuring device. The applied load equalled to 2.9 N in the case of plain carbon steels and HVOFS WC-17Co coating and to 0.5 N in the case of PM steels and PVD TiN coating. Such choice was made on empirical basis. All measurements were started at 25 μm.

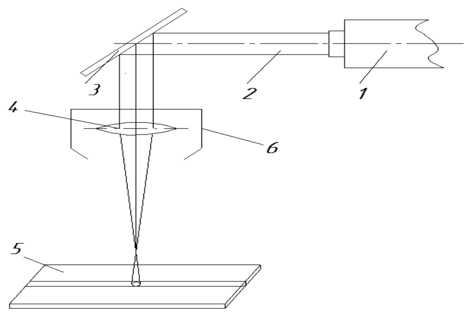

Fig. 1. The principle scheme of laser surface treatment of materials: 1 – laser, 2 – laser beam, 3 – turning mirror, 4 – optical system, 5 – specimen, 6 – nozzle for the gas feed

2.4 Abrasive wear testing

Abrasive wear tests were carried out using the block-on-ring rubber wheel scheme (standard ASTM G65-94). The diameter of ring equalled to 0.08 m, the force was 47 N, speed of rotation was 238.8 rpm, the mass of sand equalled to 1 kg. The experimental scheme of device is presented in Fig. 2

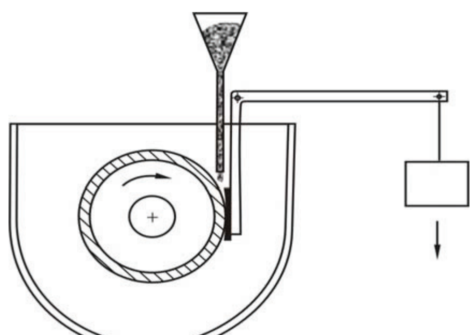

Fig. 2. The principle scheme of the block-on-ring (rubber wheel) abrasive wear tester

Table 4. Optimal parameters of laser treatment

Steel or coating	Power, W	Scan speed, mm/min
C45	300	250
Arne	345	250
Vanadis 6	300	750
Weartec®	225	750
HVOFS WC-17Co	495	300
PVD TiN	350	1200

The wear coefficient was calculated as

$$k = \frac{m_0 - m'}{\rho \cdot F \cdot t \cdot v \cdot r}, \text{ where} \qquad (1)$$

m_0 – initial weight of the specimen, kg,
m' – end weight of the specimen, kg,
ρ – density, kg/m^3,
F – force, N,
t – time of the experiment, s,
v – speed of rotation, rpm,
r – radius of the ring, m.

3 RESULTS AND DISCUSSION

3.1 Laser treatment of steels

3.1.1 Plain carbon steels

Figure 3 represents the microstructure of laser hardened plain carbon steel C45, which appeared during laser treatmtent along the surface. As can be seen from Fig. 3, the transformation zone has a distinct border. No visible crystalline structure is present in the upper part of the transformation zone, in the lower part of the transformation zone cementite seems to remain. In addition to that, it is possible to predict tempering effect at the overlapping place of two zones, as they are of different colour. The probable structures in the transformation zone are martensite near and inside the overlapping place in the upper part, and bainite.

Figure 4 shows the microstructure of laser hardened steel Arne. As can be seen, the laser transformation zone has a distinct border. No crystalline structure is observed neither in the transformation zone nor in the untreated steel, however, it can be assumed that the structure of the laser hardened zone consists of martensite and retained austenite in the upper part, and martensite, retained austenite and bainite in the lower part with possible presence of nitrides, which appeared due to reactions with the shield gas.

Figure 5 illustrates the microhardness distribution inside the transformation zone of the plain carbon steels' specimens.

As can be seen, microhardness values distribute in C45 and Arne steel specimens in a different way. The possible reasons for that can be the appearance of retained austenite in the surface layer of the laser transformation zone on case of steel C45

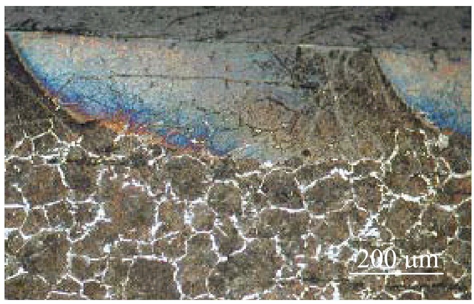

Fig. 3. The microstructure of laser hardened steel C45

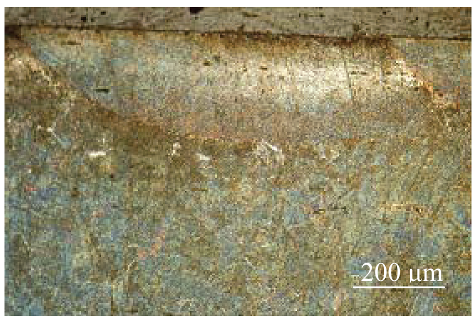

Fig. 4. The microstructure of laser hardened steel Arne

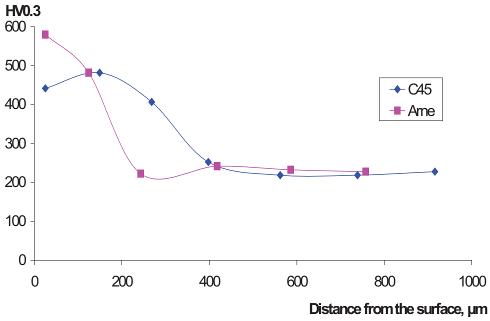

Fig. 5. Microhardness distribution inside the laser transformation hardened zone in C45 and Arne steel specimens

and saturation with nitrides, which appeared in reaction with the shield gas, of the surface layer of steel Arne with the simultaneous diffusion of alloying elements from the bottom subsurface layers.

3.1.2 PM steels

The microstructure of laser hardened steel Vanadis 6 is shown in Fig. 7. As it can be seen, no clear hardened zone is present, and there is no visible evidence of the hardening process.

The microstructure of laser hardened steel Weartec® is brought in Fig. 7. As it can be seen, an increase in the particle size near the surface can be remarked. However, no other evidence of the hardening effect can be seen.

Figure 8 represents the microhardness distribution inside the laser hardened zones of steels Vanadis 6 and Weartec®.

As it can be seen, the depth of the hardened zone reaches maximally 50 µm.

3.2. Laser treatment of coatings

3.2.1 HVOFS WC-17Co coatings

Figure 9 represents the microstructure of laser treated HVOFS WC-17Co coating.

As it can be seen, a transformation zone appears under the coating.

Figure 10 represents the microhardness distribution inside the laser treated zone.

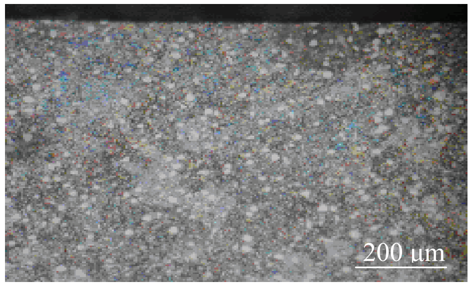

Fig. 6. Microstructure of laser hardened steel Vanadis 6

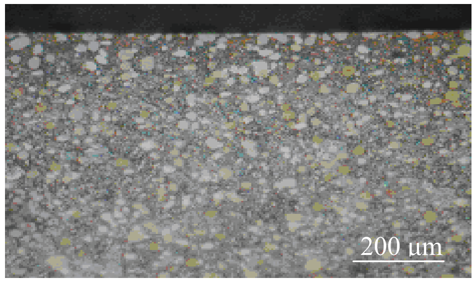

Fig. 7. Microstructure of laser hardened steel Weartec®

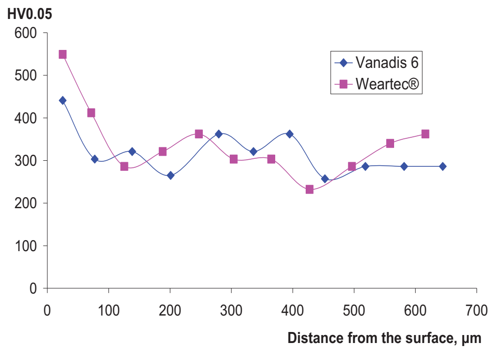

Fig. 8. Microhardness distribution inside the laser hardened zone in Vanadis 6 and Weartec® steel specimens

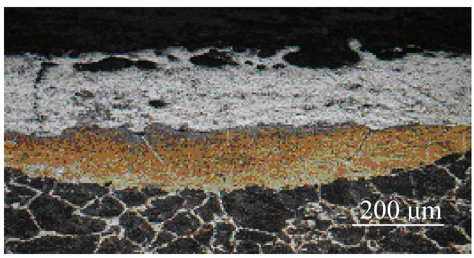

Fig. 9. Microstructure of laser treated HVOFS WC-17Co coating. Substrate – steel C45

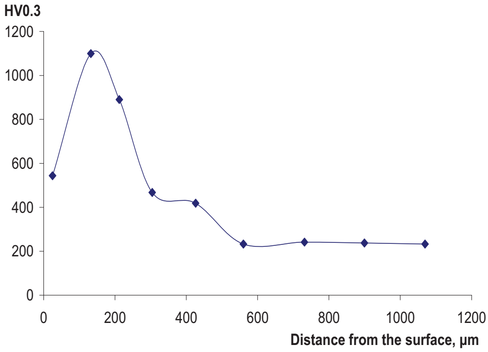

Fig 10. Microhardness distribution inside the laser treated zone of WC-17Co coated specimen

As it can be seen in Fig. 10, laser treatment causes drop in microhardness values in the coating. This can be explained by a burnout of the carbon and alloying elements and the decomposition of WC particles. In addition to that, an appearance of microcracks inside the coating was noticed.

3.2.2 PVD TiN coatings

The microstructure of the PVD TiN coated laser treated steel Vanadis 6 specimen is presented in Fig. 11.

As it can be seen, no visible changes in microstructure of the steel substrate can be observed.

Figure 12 shows the microhardness distribution inside the laser treated zone of PVD TiN coated steel Vanadis 6.

As it can be seen, laser treatment allows increasing the microhardness values of the substrate. However, the depth of the hardened zone doesn't exceed 50 µm.

4. ABRASIVE WEAR RESISTANCE

The results of wear abrasive experiments are shown in Fig. 13. PVD TiN coated specimens were not subjected to abrasive wear resistance, as they are to thin to show any positive results.

As can be seen, only laser-hardened steel Arne specimens show wear coefficient

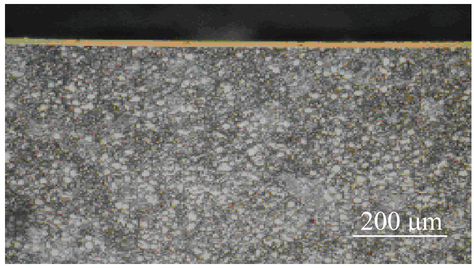

Fig. 11. Microstructure of laser treated PVD TiN coated specimen

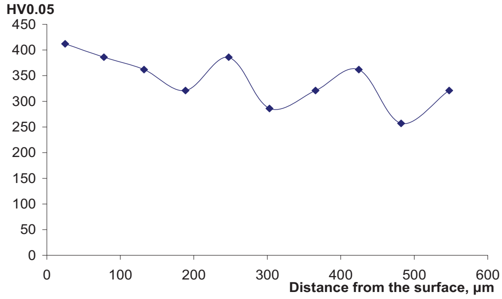

Fig.12. Microhardness distribution in the laser treated PVD TiN coated specimen

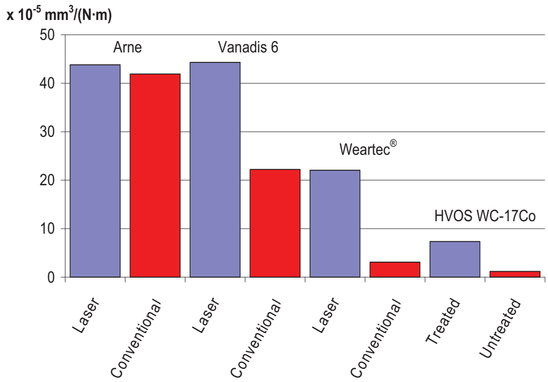

Fig. 13. Abrasive wear resistance of laser treated specimen in comparison with the conventionally treated or untreated ones

values, similar to that of conventionally hardened ones. The reasons for lower abrasive wear resistance in the case of PM steels can be too low hardened depth in comparison with conventional hardening. The lower abrasive wear resistance in the case of HVOFS WC-17Co coating correlates with the drop in microhardness, what can be seen in Fig. 10. As in the case of microhardness values, low abrasive wear resistance can be explained with the burnout of alloying elements, decomposition of WC particles and the appearance of microcracks.

5. CONCLUSIONS

Based on the obtained results, the next conclusions can be drawn:

1. Laser treatment allows enhancing remarkably the microhardness values of presented steels.
2. The microhardness of laser treated HVOFS WC-17Co coatings is lower that the microhardness of the untreated WC-17Co coating due to the changes in composition of coating.
3. Only a small hard zone appears under PVD TiN coating, thus it is doubtful, whether the purposes of the experiment are fulfilled.
4. Laser treatment reduces the abrasive wear resistance in all cases in comparison with conventional treatment.

6. ACKNOWLEDGEMENT

This research was supported by the scolarship from Erasmus. Authors thank the personnel of IFW, particularly Dr.-Ing. Habil. Günter Köhler, Dr.-Ing. Hartmut Müller, Dr.-Ing. Guntard Horn, Dr.-Ing. Jerke and Jörg Körner, as well as to Endel Mens, Priidu Peetsalu and Maksim Antonov from TUT.

7. REFERENCES

1. Grigoryants A.G., Saphronov A.N., *Methods of Surface Laser Treatment*, «Vyshaya shkola», Moscow, 1987. (in Russian)
2. Katsamas A.I., Haidemenopolous G.N., Surface hardening of low-alloy 15CrNi6 steel by CO_2 laser beam, *Surf. and Coat. Techn.*, 1999, **115**, 249 – 255.
3. Chiang Kwo-An, Chen Yong-Chwang, Laser surface hardening of H13 steel in the melt case, *Mater. Let.*, 2005, **59**, 1919 – 1923.
4. Senthi Selvan J., Subramanian K., Nath A.K., Effect of laser surface hardening on En18 (AISI 5135) steel, *Jour. of Mat. Proc. Techn*, 1999, **91**, 29 – 36.
5. Colaço R., Vilar R., Stabilisation of retained austenite in laser surface melted tool steels, *Mat. Scien. and Engin.* A, 2004, **385**, 123 – 127.
6. Pantelis D.I., Bouyiouri E., Kouloumbi N., Vassiliou P., Koutsomichalis A., Wear and corrosion resistance of laser surface hardened structural steel, *Surf. and Coat. Techn.*, 2002, **161**, 125 – 134.
7. Bochnowski W., Leitner H., Major Ł., Ebner R., Major B., Primary and secondary carbides in high-speed steels after conventional heat treatment and laser modification, *Mat. Chem. and Phys.*, 2003, **81**, 503 – 506.
8. Psakhie S.G., Technology of formation of an activated layer for enhanced microhardness and wear resistance, *Germ.-Russ. Worksh. "Trib. and Surf. Engin.: TET"*, Berlin University of Technology, 2007.
9. Sacher G., Zenker R., Subsequent heat treatment of hard coated steels by electron or laser beam, *Germ.-Russ. Worksh. "Trib. and Surf. Engin.: TET"*, Berlin University of Technology, 2007.
10. Rana J., Goswami G.L., Jha S.K., Mishra P.K., Prasad B.V.S.S.S., Experimental studies on the microstructure and hardness of laser-treated steel specimens, *Opt. & Las. Techn.*, 2007, **39**, 385 393.

8. CONTACT DATA.

The contact person: Andrei Surzhenkov, Ehitatajate tee 5, 19086 Tallinn, Estonia, phone no +372 6203353, e-mail andrei.surzenkov@ttu.ee

PAPER III

Surzenkov, A.; Kulu, P.; Tarbe, R.; Mikli, V.; Sarjas, H.; Latokartano, J. (2009). Wear resistance of laser remelted thermally sprayed coatings. *Estonian Journal of Engineering*, 15(4), 318 – 328.

Estonian Journal of Engineering, 2009, **15**, 4, 318–328 doi: 10.3176/eng.2009.4.09

Wear resistance of laser remelted thermally sprayed coatings

Andrei Surzhenkov[a], Priit Kulu[a], Riho Tarbe[a], Valdek Mikli[b], Heikki Sarjas[a] and Jyrki Latokartano[c]

[a] Department of Materials Engineering, Tallinn University of Technology, Ehitajate tee 5, 19086 Tallinn, Estonia; andrei.surzenkov@ttu.ee
[b] Centre for Materials Research, Tallinn University of Technology, Ehitajate tee 5, 19086 Tallinn, Estonia
[c] Laser Application Laboratory, Tampere University of Technology, Korkeakoulunkatu 10, FI-33720 Tampere, Finland

Received 3 September 2009, in revised form 4 November 2009

Abstract. Advantages of hard coatings and deposition technologies such as HVOF have opened new opportunities for the production of wear parts operating in an abrasive environment. Thermally sprayed hardmetal coatings are widespread in industrial applications for wear, but not usable under impact wear conditions. To widen the scope of thick hard coating applications, powder coatings, produced by plasma spraying and powder spray-fused coatings using laser remelting, were studied. Nickel- and iron-based self-fluxing alloy powders and WC-Co hardmetal powders were used as spray materials. The microstructure of coatings and the influence of heat treatment on the structure and composition of coatings as well as on the composition of the substrate were studied. The duplex-treated surfaces were tested under the conditions of abrasion and abrasive erosion and impact wear and the mechanisms of coating degradation were analysed. Prospects of coatings, containing thermal spray-fused iron-based metal-matrix WC-Co hardmetal for erosive wear conditions, are demonstrated. Based on the comparative studies of abrasive, erosive and impact wear resistance, recommendations for materials and coatings are formulated.

Key words: powder coatings, thermal spray, laser remelting, abrasion, erosion, abrasive impact wear.

1. INTRODUCTION

In terms of product lifetime of engineering materials and machine components, the surface is of prime concern. This involves wear behaviour and mechanical properties such as surface fatigue [1,2]. Thermally sprayed hardmetal coatings, also often called “carbide coatings”, are used widely in many industrial applications for wear, corrosion and high temperature protection [3]. Recent attention has focused on reduced consumption of existing resources and materials recycling. Therefore the application of composite powders, based on used (recycled) hardmetals for thermal spray is topical [4,5].

Wide use of thermally sprayed coatings gives evidence of the cost-effectiveness of self-fluxing alloys containing tungsten carbide (WC) particles, applied by the spray and fusion methods (flame, plasma and laser fusion). Some materials, most notably MCrSiB compositions, where M stands for either Ni, Co or Fe, can be fused by heating them up to the temperature of 1050 °C. Due to the brittleness of tungsten carbide, the impact wear resistance of the coatings is not high [4]. Because of their low porosity and high bond with the basic materials, the spray-fused composite coatings, containing WC-Co hard phase, can resist significant impact loads [6]. It has been shown that abrasive erosive and impact wear resistance of powder materials and coatings are not high [5,7,8]. Usage of the recycled hardmetal powder, produced by mechanical milling, causes high iron content in the powder (up to 20%) due to the intensive wear of the grinding media [9,10]. It is a factor, hindering their use in nickel-based compositions.

Following from the abovementioned, this work focuses on thermal spray-fusion for the production of high-performance surfaces, use of the deposition of hard coatings by thermal spray and subsequent laser treatment of powder composition, based on iron-based spray powder. To improve the impact wear resistance of plasma sprayed coatings, the following laser remelting was studied.

2. EXPERIMENTAL

2.1. Studied materials and coatings

For coatings, as a substrate, specimens of the size $50 \times 25 \times 10$ mm of plain carbon steel C45 were used. The composition and hardness of the steel are given in Table 1.

The composite powders for spray and fused coatings contained nickel- and iron-based powders as basic components. Table 2 shows the chemical composition of the self-fluxing alloy powders of the powder composites. With a spherical shape, their particle size was (+10 –45) and (+15 –53) µm for Fe- and Ni-based powders, respectively.

Table 1. Chemical composition and hardness of the substrate steel

Grade of the steel	Composition, wt%	Hardness HV1	
		Normalized	Hardened
C45	0.45 C; 0.60 Mn; 0.30 Si	200–235	480–515

Table 2. Chemical composition and particle size of the used self-fluxing spray powders

Type of the powder	Trade mark	Composition, wt%						Particle size, μm
		Cr	Si	B	C	Ni	Fe	
NiCrSiB (S)	1640–02*	7.5	3.5	1.6	0.25	bal.	2.5	+15 –53
NiCrSiB (H)	1660–02*	14.8	4.3	3.1	0.75	bal.	3.7	+15 –53
FeCrSiB	Grade 6A*	13.7	2.7	3.4	2.1	6.0	bal.	+10 –45
WC-Co	Rec VK**	WC – 75.6; Co – 11.5					12.9	+20 –63

* Powders of Höganäs AB, Bruksgatan 35, SE-263 83 Höganäs, Sweden; (S) – soft (380 HV), (H) – hard (780 HV).

** Experimental, TUT.

Nickel- and iron-based self-fluxing alloy powder compositions, containing 25 wt% of hardmetal particles, were used. WC-Co hardmetal powder, produced from used hardmetal by disintegrator milling, was employed [9,10]. Chemical composition of the hardmetal powder was the following (in wt%): WC – 75.6, Co – 11.5, Fe – 12.9. Powders had the particle size of (+20 –63) and –63 μm. Figure 1 illustrates the particle shape. Particles were primarily equiaxed in form and their microstructure showed a typical tungsten carbide based hardmetal structure.

2.2. Plasma spray and laser treatment of coatings

To depose a coating, plasma spray equipment RotAloy of Castolin Eutectic was applied. Plasma spraying parameters of the coatings are given in Table 3. Thickness of the coatings was about 0.2 mm. The plasma sprayed coatings were remelted using Nd: YAG laser Haas HL 4006 D of Trumpf with a wavelength of 1064 nm; the cross-section of the laser beam was 8 × 5 mm, overlapping – 50%. Parameters of laser remelting are provided in Table 3.

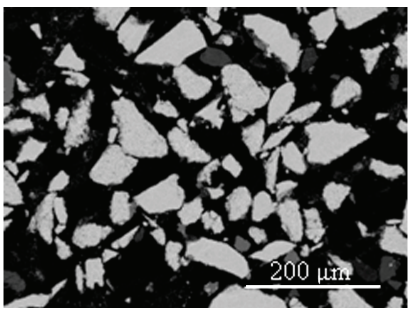

Fig. 1. Micrograph of hardmetal powder particles.

Table 3. Parameters of plasma spraying and laser remelting

Type of the coating	Power	Gas flow rates, l/min	Other parameters
Plasma spraying	–	Ar – 135 H_2 – 90	Spray current – 380 A, voltage – 150 V, powder feed rate – 30 g/min, spray distance – 100 mm
Laser remelting	I series – 1.75 kW for NiCrSiB compositions II series – 1.5 kW for FeCrSiB and NiCrSiB compositions	Ar – 20	Scan speed – 10 mm/s

2.3. Characterization of the coating structure, hardness and wear resistance

2.3.1. Microstructure of coatings

Coatings were characterized both in the sprayed condition and after laser remelting. Polished cross-sections were observed by the optical microscope using an Omnimet image analysis system and SEM. X-ray analysis (EDS) was performed to estimate changes in the composition of the metal matrix.

2.3.2. Determination of hardness

To determine surface hardness, measurements were made with a universal hardnessmeter Zwick 2.5/TS at a load from 1 to 100 N. The load was selected to obtain the size of indents comparable with the size of wear craters, formed by abrasive wear.

Microhardness measurements in the cross-section were carried out using the Micromet 2001 measuring device. The applied load was equal to 0.245 N. Low loads enabled us to measure the hardness of the metallic matrix as well as of the hardmetal particles in the matrix of the coating.

2.3.3. Abrasive wear testing

Abrasive block-on-ring wear (ABRW) abrasion tests were carried out using the block-on-ring rubber wheel scheme (ASTM standard G 65-94) (Fig. 2a). The diameter of the ring was 228.6 mm, the applied force was 222 N and the speed of rotation was 200.8 1/min (linear velocity 2.4 m/s). The parameters of the wear tests are given in Table 4. Abrasive erosive wear (AEW) and abrasive impact wear (AIW) of the coatings were studied with the experimental centrifugal-type wear testers CAK and DESI [7]. At AEW the velocity was 80 m/s, impact angles were 30° and 90°. By AIW tests a one-rotor system was used (Fig. 2c) [7]; the velocity was 80 m/s and the impact angle of abrasive particles with the specimen on the fixed pin surface was about 90°. Wear experiments ABRW and AEW with

(a) (b) (c)

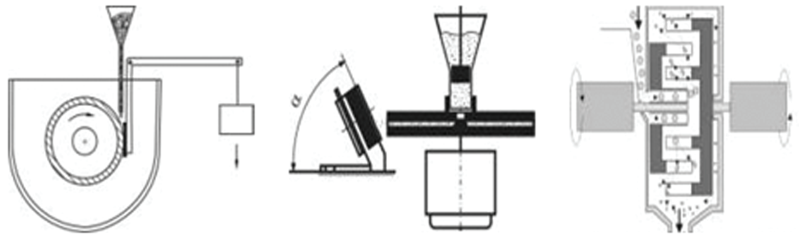

Fig. 2. Principal schemes of the block-on-ring wear tester (a), centrifugal-type erosion tester CAK (b) and disintegrator type impact wear tester DESI (c).

Table 4. Parameters of tribological tests

Type of the test	Velocity, m/s	The abrasive and the particle size, mm	Amount of the abrasive, kg
Abrasive block-on-ring wear (ABRW)	2.4	Quartz sand 0.1–0.3	1.5
Abrasive erosive wear (AEW)	80	Quartz sand 0.1–0.3	3
Abrasive impact wear (AIW)	80	Granite gravel 4–5.6	6

quartzite sand of fraction 0.1–0.3 mm were carried out. AIW tests were conducted with granite gravel of fraction 4.0–5.6 mm. Hardness of the quartzite and granite, measured at the polished cross-section, was 11.0 and 9.28 HV 0.05 GPa, respectively.

The mass loss of the specimens was determined and the wear coefficient at ABRW was calculated as

$$k = \frac{\Delta m}{\rho F t v r}, \tag{1}$$

where Δm is mass loss (kg), ρ is density (kg/m^3), F is force (N), t is time of the experiment (s), v is rotation speed (1/min) and r is the radius of the ring (m).

At AEW and AIW the mass loss of the specimens was determined and the volumetric wear rate I_v was calculated as

$$I_v = \frac{\Delta m}{\rho q}, \tag{2}$$

where Δm is mass loss (mg), q is quantity of the abrasive per specimen (kg) and ρ is sample density (mg/mm^3).

The relative volumetric wear resistance ε_v was determined for steel C45 as follows:

$$\varepsilon_v = I_v \big/ I_v^{C45}, \tag{3}$$

where I_v is the volumetric wear rate of the tested coating and I_v^{C45} is that of the reference steel C45.

3. RESULTS AND DISCUSSION

3.1. Structure, porosity and hardness of the coatings

The cross-sections of laser remelted plasma sprayed coatings are shown in Figs. 3 and 4.

NiCrSiB self-fluxing alloy forms a Ni-based matrix with WC hard particles (WC-Co hardmetal particles are practically dissolved in the Ni-based matrix). This was confirmed by the EDS analysis of the coating – different phase distribution in the coating is shown in Fig. 3b. Retained slag nests in the Ni-based coating were observed.

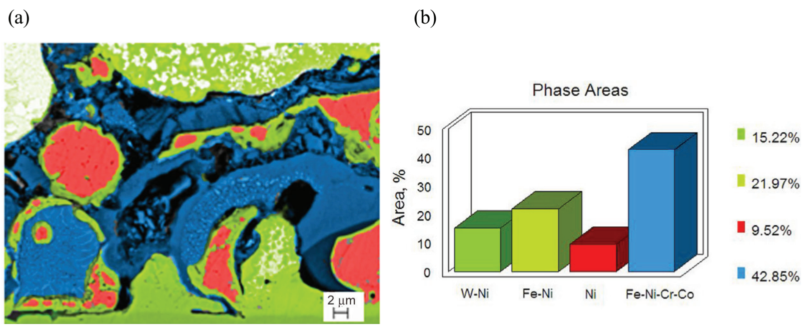

Fig. 3. Micrograph of the cross-section and composition of NiCrSiB(S)-based coating after laser remelting (a) and distribution of the elements (b).

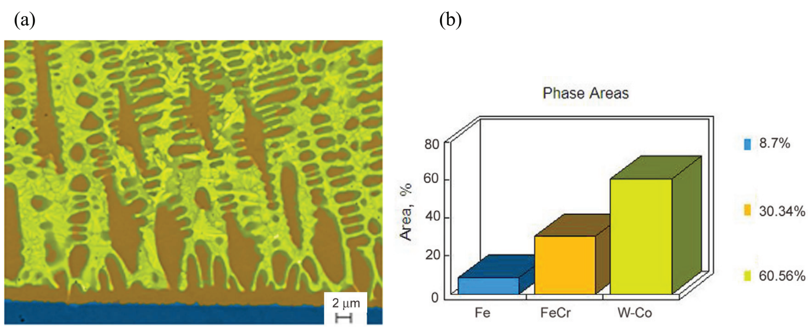

Fig. 4. Micrograph of the cross-section and composition of FeCrSiB-based coating after laser remelting: (a) microstructure; (b) distribution of the elements.

As it follows from Fig. 4, Fe-alloy based coating structure is a typical eutectic structure and more dense than the Ni-alloy based coating, where due to the high content of Fe (about 13%) large Fe-Cr dendrites and smaller W-Co dendrites are formed. The rate of solution of WC-Co in the metal matrix is higher in the Fe-alloy based coating – practically all WC-Co particles are dissolved in the iron-based matrix forming the (Fe-Cr) – (WC-Co) eutectic structure. The results of hardness measurements by both methods are brought in Table 5.

3.2. Wear resistance of spray-fused coatings

Results of abrasive wear tests (abrasion, erosion and impact wear) are given in Tables 6–8.

3.2.1. Abrasive block-on-ring wear resistance

By abrasion, the coatings studied demonstrated low wear resistance, the relative wear resistance is lower than one (0.5–0.9) (Table 6). Because the hardness of the abrasive is higher (about 11 GPa of the quartz sand) than that of the coating (about 3.0–5.6 GPa), intensive wear takes place as a result of microcutting or surface scratching. It was confirmed by the study of the worn surfaces (Fig. 5a).

Table 5. Hardness of spray-fused coatings on steel C45 ((WC-Co) of fraction +20 –63 μm)

Composition of coatings, wt%	Thickness, μm	Hardness HV, GPa	
		Surface HV1	(Metal matrix)/(hardmetal particles) HV 0.1
NiCrSiB(S) + 25 (WC-Co)	200	3.0–3.6	2.7–4.3/5.8–18.8
FeNiCrSiB + 25 (WC-Co)	200	4.4–5.6	4.9–6.8/7.7–9.4

Table 6. Abrasive block-on-ring wear (ABRW) resistance of coatings

Type of the coating and metal matrix	Condition and fraction, μm	Wear coefficient K, $mm^3/Nm \times 10^{-5}$	Relative wear resistance ε_v
NiCrSiB(S) + (WC-Co)	As-sprayed	36.1	0.18
	Laser remelted		
	–63	11.1/8.7*	0.58/0.74*
	+20 –63	13.5	0.48
NiCrSiB(H) + (WC-Co)	–63	8.4	0.76
FeCrSiB + (WC-Co)	As-sprayed	–	–
	Laser remelted		
	–63	8.8	0.73
	+20 –63	7.1	0.88

* I and II series.

(a) (b)

(1)

(2)

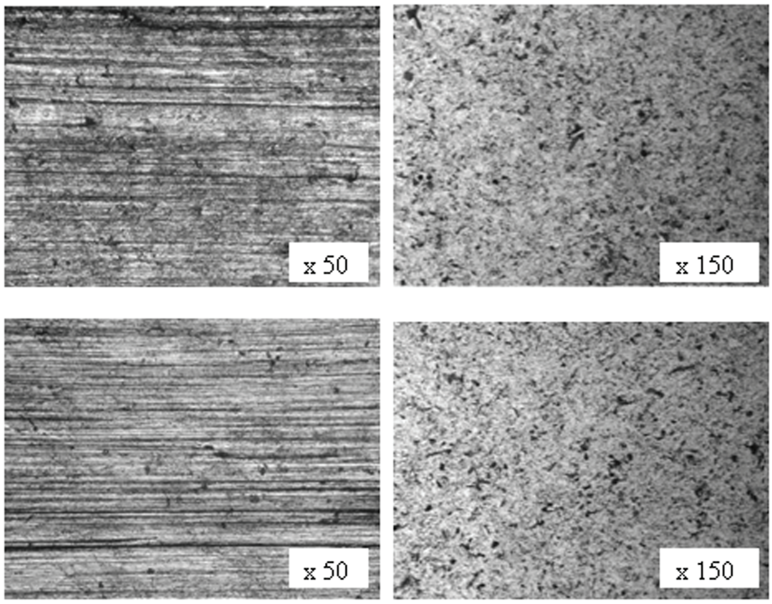

Fig. 5. Worn surfaces, topographigal images of (1) NiCrSiB(S) and (2) FeCrSiB-based coatings after wear: (a) ABRW; (b) AEW ($\alpha = 90°$).

3.2.2. Abrasive erosive wear resistance

Based on the studies of wear rate and wear mechanism of the coatings (Table 7), the wear resistance of Ni-based coatings at low impact angles is lower than the wear resistance of reference steel C45; Fe-based coating showed about 1.2 times higher wear resistance.

The first series (N = 1.75 kw) of the NiCrSiB-based coating demonstrated higher relative wear resistance at straight impact angle ($\alpha = 90°$). It may be explained by the high WC-Co particle solution rate in the Ni-based metal matrix due to different parameters of the laser remelting and the resulting lower brittleness of the composite. Higher erosion resistance of the FeCrSiB-based coatings, in comparison with the NiCrSiB-based coating at low impact angle ($\alpha = 30°$), can be explained by the higher hardness (about 1.5 times) and formation of a eutectic structure.

3.2.3. Abrasive impact wear

Impact wear resistance of the spray-remelted self-fluxing Ni-alloy based coating is practically at the level of the reference material – steel C45 (Table 8). Because of their low impact wear resistance, the HVOF sprayed coatings, based

Table 7. Abrasive erosive wear (AEW) resistance of coatings at different impact angles (hardmetal powder fraction +20 –63 μm) by impact angles of 30° and 90°

Type of the coating and metal matrix	Condition	Wear rate I_v, mm^3/kg		Relative wear resistance ε_v	
		30°	90°	30°	90°
NiCrSiB(S) + (WC-Co)	As-sprayed	447.6	–	0.1	–
	Laser remelted	25.3/33.2	25.7/29.7*	0.7/0.8	1.6/0.7*
NiCrSiB(H) + (WC-Co)	Laser remelted	22.1	25.3	0.8	1.6
FeCrSiB + (WC-Co)	Laser remelted	23.5	28.2	1.2	0.7

* I and II series.

Table 8. Abrasive impact wear (AIW) resistance of coatings

Type of the coating	Hard phase fraction, μm	Wear rate I_v, mm^3/kg	Relative wear resistance ε_v
NiCrSiB(S) + (WC-Co)	–63	55.7	1.03
	+20 –63	54.9	1.04
FeCrSiB + (WC-Co)	+20 –63	43.7	1.31

on a Ni-based alloy, and recycled hardmetal are not suitable for applications under impact wear conditions [7,11,12]. Spray-fused Fe-based coatings may offer an alternative for expensive powder steels and in some cases (under restoration of the working elements of milling devices) for traditional WC-Co hardmetals.

The absence of the correlation between the results of different wear tests can be explained by different wear mechanisms, namely by microcutting of the metal matrix in the case of abrasive wear, microcutting of the metal matrix and direct fracture of hard particles during abrasive erosive wear at low angles, micro-cutting or surface fatigue of the metal matrix and direct fracture of hard particles at the straight impact angle, surface fatigue of the metal matrix and direct fracture of hard particles during abrasive impact wear.

4. CONCLUSIONS

Iron-based self-fluxing alloys are more suitable for producing self-fluxing alloy-based composite coatings containing recycled WC-Co hardmetal powder in comparison with the nickel-based ones. Iron-based spray fusion coatings are of higher density and have a typical eutectic sturcture. Due to the laser remelting, the initial WC-Co hardmetal powder reinforcement is practically dissolved in the iron-based metal matrix. Due to the higher hardness of iron-based coatings they are more wear resistant by abrasion, but the iron-based coatings have lower erosive wear resistance by the straight impact than the Ni-based composite coatings. By abrasive impact wear, Fe-based coatings show better performance.

ACKNOWLEDGEMENTS

The authors are grateful to Petri Vuoristo from Tampere University of Technology and to the workers of Reneko Ltd., especially to Vyacheslav Kastyushin. This work was supported by the Estonian Ministry of Education and Research (target-financed project SF 01400091).

REFERENCES

1. Davis, J. R. (ed.). *Surface Engineering for Corrosion and Wear Resistance*. ASM International, 2001.
2. Bayer, R. G. *Wear Analysis for Engineers*. HNB, New York, 2002.
3. Karnerva, U., Lagerbom, J. and Vuoristo, P. Development of thermal spray powders for improved tribological and corrosive applications and cost-effective solutions. *Int. J. Mater. Product. Technol.*, 2007, **28**, 377–398.
4. Kleis, I. and Kulu, P. *Solid Particle Erosion. Occurrence, Prediction and Control*. Springer-Verlag, London, 2008.
5. Kivikytö-Reponen, P. *Correlation of Material Characteristics and Wear of Powder Metallurgical Metal Matrix Composites*. PhD Thesis, Helsinki University of Technology, 2006.
6. Kulu, P., Veinthal, R., Saarna, M. and Tarbe, R. Surface fatigue processes at impact wear of powder materials. *Wear*, 2007, **263**, 463–471.
7. Tarbe, R. *Abrasive Impact Wear: Tester, Wear and Grindability Studies*. PhD Thesis, Tallinn, TUT Press, 2009.
8. Veinthal, R., Tarbe, R., Kulu, P. and Käerdi, H. Abrasive erosive wear of powder steels and cermets. Forthcoming.
9. Tümanok, A., Kulu, P., Mikli, V. and Käerdi, H. Technology and equipment for production of hardmetal powders from used hardmetal. In *Proc. 2nd International DAAAM Conference*. Tallinn, 2000, 197–200.
10. Kulu, P., Käerdi, H. and Mikli, V. Retreatment of used hardmetals. In *Proc. TMS 2002 Recycling and Waste Treatment in Mineral and Metal Processing: Technical and Economic Aspects*. Lulea, 2002, vol. 1, 139–146.
11. Zimakov, S., Pihl, T., Kulu, P., Antonov, M. and Mikli, V. Applications of recycled hardmetal powder. *Proc. Estonian Acad. Sci. Eng.*, 2003, **9**, 304–316.
12. Kulu, P. and Zimakov, S. Wear resistance of thermal sprayed coatings on the base of recycled hardmetal. *Surface Coat. Technol.*, 2000, **130**, 46–51.

Lasersulatatud termopinnete kulumiskindlus

Andrei Surzhenkov, Priit Kulu, Riho Tarbe, Valdek Mikli,
Heikki Sarjas ja Jyrki Latokartano

Kõvapinnete ja kiirleekpihustamismooduste kasutuselevõtt võimaldab valmistada unikaalsete omadustega kuluvosi tööks abrasiivkulumise tingimustes. Termopihustatud kõvasulampinded on leidnud laialdast tööstuslikku kasutamist kulumisvastasel eesmärgil, kuid nimetatud pinded ei sobi tööks löökkulumise tingimustes. Laiendamaks paksude kõvapinnete kasutusvaldkondi, on käesolevas

töös uurimisobjektiks plasmapihustatud ja lasersulatatud pulberpinded. Pihustuspulbrina kasutati komposiitpulbrit iseräbustuva rauasulami baasil, mis kõvafaasina sisaldas 25 kaaluprotsenti taaskasutatavat WC-Co-kõvasulampulbrit.

Uuriti termotöötluse mõju nii pulberpinnete struktuurile ja koostisele kui ka alusmaterjali struktuurile ning omadustele. Pihustus-sulatuspindeid katsetati abrasiivkulumise (abrasioon ja erosioon) ning löökkulumise tingimustes ja uuriti pinnete kulumiskindlust ning kulumise mehhanismi. Selgitati välja raua baasil metallmaatriksiga ja WC-Co tugevdava faasiga pulberpinnete perspektiivsus abrasiiverosiooni tingimustes. Eri tingimustes (abrasioon, erosioon ja löökkulumine) läbi viidud pulberpinnete kulumiskindluse katsete tulemusena on esitatud soovitused pinnete valikuks.

PAPER IV

Kulu, P.; Saarna, M.; Sergejev, F.; Gregor, A.; Surženkov, A. (2010). Selection of coating systems and processes for different wear conditions. In: *Proceedings of 14th Nordic Symposium on Tribology*, NORDTRIB 2010, Storforsen, Sweden. Lulea University of Technology, 2010, 1 – 8.

Selection of coating systems and processes for different wear conditions

Priit Kulu, Mart Saarna, Fjodor Sergejev*, Andre Gregor, Andrei Surženkov.
Department of Materials Engineering, Tallinn University of Technology.
Corresponding authors' e-mail address: fjodor.sergejev@ttu.ee

Abstract: Advantages of hard coatings properties and deposition technologies, such as PVD and thermal spraying, in combination with different substrate materials have provided new opportunities for production of wear parts, operating in various complicated wear conditions.
Such a wide nomenclature makes it difficult to find best suiting coating–substrate systems for desired wear applications. Current systematic study will give knowledge for better understanding of this matter and allow selecting the appropriate coating.
The following coatings systems were under the study:

- hard thin PVD coatings on hardmetals and cermets, high-speed steels and nitrided steels;
- hard thick thermal sprayed (HVOF sprayed) coatings on steel.

From the processes following coatings deposition and treatment methods were used:

- physical vapour deposition (PVD) of TiN, TiAlN and laser hardening;
- plasma nitriding and PVD;
- thermal spraying and laser cladding.

Coated and duplex treated surfaces were subjected to the different types of wear: abrasive, indentation surface fatigue and impact wear (surface fatigue wear). The wear resistance and mechanisms of surface degradation were studied. The recommendations of coating systems selection for different service conditions are proposed.

Key words: PVD, thermal spraying, duplex treatment, wear resistance, selection of coating systems.

1. INTRODUCTION

The use of thin hard physically vapour deposited (PVD) films on a relatively soft substrate material is often limited due to their brittleness. Unsupported coating tends to fail by intensive cracking and final chipping (or delamination). To wider their applications areas, not only by use of the hardmetal and high-speed steel substrates, the use of coating followed heat treatment is proposed [1, 2]. The production of gradient coatings using nitridizing process with following hard coatings (duplex coatings) on nitriding steels is also very prospective [3]. A subsequent heat treatment of the hard coated low-tempering steels by using high-energy beams, especially laser beam for substrate hardening, causes a notable improvement of its loads supporting abilities [4].

Another group of protective coatings are the "so-called" thick hard coatings. Thermal sprayed, for example such as deposited by high velocity oxygen fuel (HVOF) process, hardmetal coatings are very prospective for wear protection and provide good wear and corrosion resistance [5]. WC-Co hardmetals are the most widely used materials for different wear applications due to their excellent combination of high wear resistance and good strength-toughness properties.

The use of hard coatings at impact wear modes refers to resistance for plastic deformation, direct brittle and fatigue fracture as these are dominating mechanisms of failure and there is a controversy between the hardness and fracture toughness.

Well known Vickers indentation method (also referred as the Palmqvist method) is used for determination of fracture toughness as well as the cracking resistance [6]. The characterisation of thin hard coatings endurance is widely made with use of the indentation methods [7]. Same techniques were used in the current study.

2. EXPERIMENTAL PART

2.1. Coating-substrate systems

Three different substrate–coatings systems: hardmetal–coating, high-speed PM (powder metallurgy) steel-coating and nitrided steel–coating was investigated. The hardmetal and heat treated steel samples of size 20x20x5 mm^3 were diamond grinded and polished to desired surface roughness. Two different PVD coatings, monolayer TiN and multilayer TiAlN-ML, were deposited using the PLATIT π80. The properties of substrates and coatings are given in Tables 1 and 2.

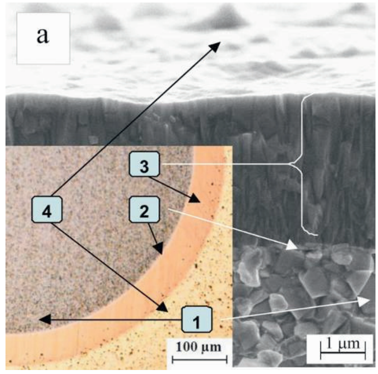

Figure 1. SEM image of the TiN PVD coatings cross-section: 1– HM substrate; 2 – Ti adhesion layer; 3 – TiN coating; 4 – coating surface with microdroplets.

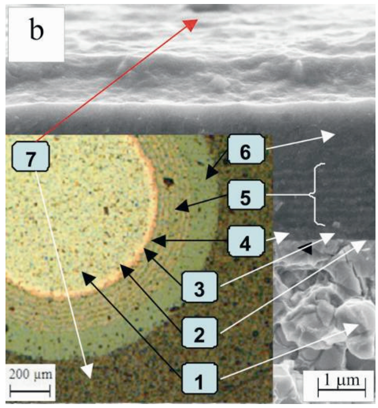

Figure 2. SEM image of the TiAlN-ML multilayer PVD coatings cross-section: 1– HM substrate; 2 – Ti adhesion layer; 3 – TiN layer; 4 – TiAlN layer; 5 – TiAlN/AlN multilayer coating; 6 – TiAlN coating; 7 – coating surface with microdroplets.

The microstructures of coated systems were observed using the SEM (Zeiss EVO MA15). The thicknesses of the PVD coatings are measured by Kalotester KaloMax®, and were about 2.3 µm for both coatings.

Table 1. Substrate materials and their properties.

Type of substrate	Designation	Condition	Surface hardness HV	Modulus of elasticity E, GPa	Surface roughness R_a, µm
Hardmetal (HM)	H10 (WC-10wt%Co)	As produced	1555 HV0.3	590	0.20
High-speed steel (HSS)	Vanadis 6	Hardened	840 HV0.01	210	0.46
Nitrided steel (NS)	38CrMoAl8	Nitrided	850 HV0.01	250-300	0.50

Table 2. Studied PVD coatings.

Type of coatings	Substrate	Coating, thickness, µm	Coating hardness, GPa	Surface roughness R_a, µm
TiN, monolayer	NS, HM, HSS	2.3	28.0 ± 0.6	0.08
TiAlN, multilayer	NS, HM, HSS	2.3	19.9 ± 1.2	0.10

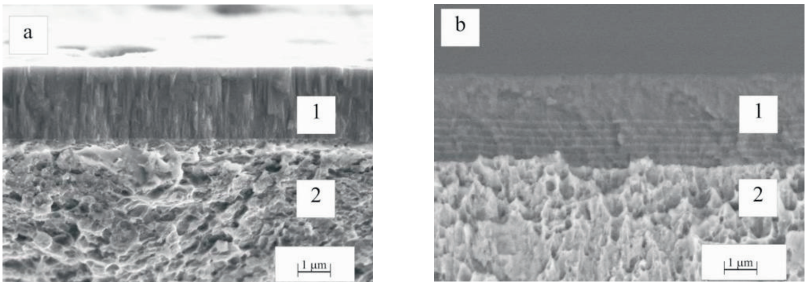

Figure 3. SEM images of fractured surface of coatings on nitrided steel: a – TiN; b – TiAlN-ML; 1 – PVD coating; 2 – nitrided layer.

The cross-sections of TiN and TiAlN-ML coatings on hardmetal and duplex specimens are given in Fig. 1-2 and 3, correspondently.

The substrate material and coating surface roughness were measured by a surface roughness measuring instrument of Taylor Hobson Ltd. Surtronic 3+ with an accuracy of 2% (see Tables 1-3).

The thick WC-17Co hardmetal coating (Tafa 1343), with 17 weight percent of cobalt binder, was produced by (HVOF) spraying technique, with Tafa JP 5000 on substrate steel EN C45 (or 1C45 by DIN EN 10083). Laser hardening of coated specimens was performed using the Haas HL 4006 D 4 kW Nd: YAG laser.

Table 3. Studied HVOF sprayed coatings.

Type of coating	Substrate	Coating thickness, µm	Coating surface hardness, HV0.2	Surface roughness R_a, µm
WC-17Co (Tafa 1343)	Steel C45 laser hardened	200/177*	750–1080	0.05

* Thickness of the laser hardened zone

Vickers microhardness of coating was measured using 0.1 – 0.2 N loads. The microstructures of the coating in as sprayed condition and laser hardened coating are shown in Fig. 4.

The hardness of such treated HVOF (see Table 3) coating is lower than thin PVD TiN or TiCN, but may be prospective for wear resistant applications.

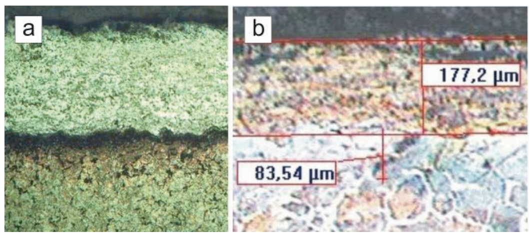

Figure 4. Microstructure of cross-section of HVOF sprayed WC-17wt%Co coating on steel C45 substrate: a – as sprayed; b – laser hardened.

2.2. Coatings adhesion testing

The quality of the adhesive bonding between coatings and substrate materials was estimated by Rockwell adhesion test (Rockwell “C” indentation test) [8]. Tests were performed on hardness tester Zwick 8150 at load of 1471 N (150 kgf). Indentations were made in a direction perpendicular to the specimen surface. The indented samples were then analysed with an optical microscope and results were classified into the standard categories from Class 0 (best bonding) to Class 3 (complete delamination).

2.3. Abrasive wear testing

The resistance to abrasion wear rate was measured according to ASTM G65-94 dry sand/rubber wheel test scheme (block-on-wheel). The diameter of the rubber disk was reduced to 80 mm for testing of $5 \times 20 \times 20 mm^3$ sized samples. The applied force was 18.64 N with circumferential velocity of 2 $m \times s^{-1}$.The identical sand particles were used as abrasive in all tests as the most common naturally occurring one (SiO_2, mean size 0.1 mm, feed rate 300 $g \times min^{-1}$).

To quantify the weight loss during abrasion experiments, the specimens were ultrasonically cleaned in acetone and weighed before and after the tests to the nearest of 0.01mg using GR-202, A&D Instruments balance.

2.4. Cracking resistance – indentation surface fatigue testing

An indentation at a single point technique was used to evaluate the cracking resistance (indentation surface fatigue) of the coatings. Vickers diamond indenter and Instron 8800 servo hydraulic fatigue test system were exploited (Fig. 5).

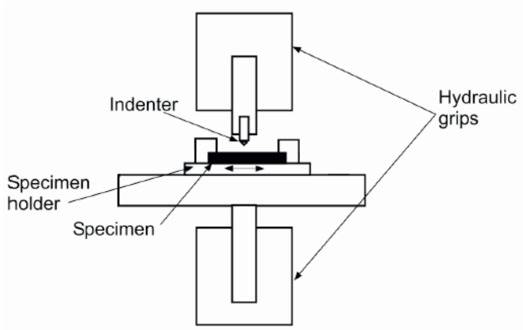

Figure 5. The schematic representation of the indentation surface fatigue tester.

The qualitative evaluation criteria's (from 0 to VI – to delamination) of the cracking resistance of the coatings (see Table 5) were considered and examined by optical microscopy and SEM.

The number of indentation cycles varied from 1 up to 10 000 and total indenting load of 100 (low) and 500 N (high) was applied with stress ratio R = 0.1, sinusoidal loading pattern and with loading frequency of 0.5 – 15 Hz.

2.5. Impact wear testing

The impact wear testing was performed on impact wear tester (Fig. 6) designed and produced in TUT (Tallinn University of Technology). The special design using ball indenters up to 30 mm (12 mm in current study) in diameter enables to study the flat-to-flat contact behaviour of coatings what is characteristic to tools in forming operations, blanking and etc.

Table 5. Crack types and crack evaluation criteria.

Evaluation criteria						
0	I	II	III	IV	V	VI
Crack type						
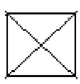	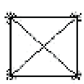	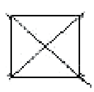	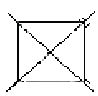	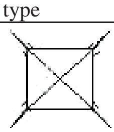	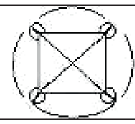	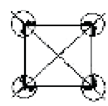
Very weak SRC*, emanated from the edge and around the corners	Weak SRC*	Medium SRC* and weak RC** – beginning of RC** formation	Medium SRC* and medium RC** – propagation of weak RC**	Medium SRC* and strong RC**	Medium RC**, delamination of coating in the corners of indent and cone (ring) cracks at the periphery of indent	Strong RC** and delamination of the coating around the corners of indent or perimeter

* SRC – secondary radial crack; ** RC – radial cracks

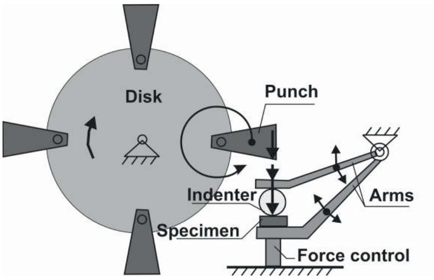

Figure 6. Schem of the impact wear tester.

The dynamic load is transferred from the hammers that are connected to, and accelerated by the rotating disk. The transferred energy depends on speed and mass of hammers and can be adjusted. Hammers fastened on the periphery of the disk allow increasing the frequency at least up to 100 Hz (25 Hz in current study).

The force measurement system (force sensor) with the protection from overloading was used for monitoring of the contact parameters. Applied force was equal to 16 N, with speed of hammer at the impact point was 2.75 m×s^{-1}. In the current study, the cyclic loading limited by 1 × 106 – 1 × 107 cycles since it is often used by authors active in the area of surface fatigue study of PVD coatings [9, 10] and during that number of cycles most of the characteristic fatigue failure modes take place.

3. RESULTS AND DISCUSSION

3.1. Mechanical properties of coating-substrate systems

The microhardness values of the substrates were measured using Vickers pyramid at loads of 0.1–2 N (0.01–0.2 kgf) see Figs. 7-8.

Hardness distribution of coated nitrided steel given in Fig. 7 shows that the core microhardness of the plasma nitrided substrate is 350 HV0.01 and the microhardness of the nitrided surface, having case depth of approximately 300 μm, is around 850 HV0.01 e.g. the surface hardness is increased by a factor of 2.4.

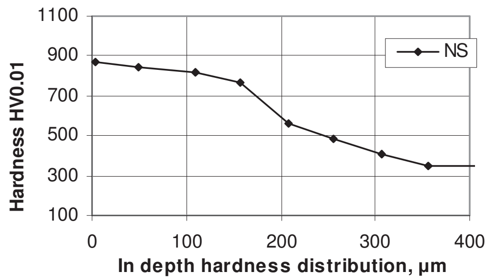

Figure 7. The hardness distribution of nitrided steel (NS) substrate (38CrMoAl8).

The hardness distribution in HVOF sprayed WC-Co coated sample, brought in Fig. 8, shows that laser treatment does not affect the microhardness of the substrate, which stays at the same level as the one of the sprayed coating. The microhardness of the laser treated coating ranges from 750 HV0.2 to 1080 HV0.2, whereas no clear influence of the laser treatment can be tracked.

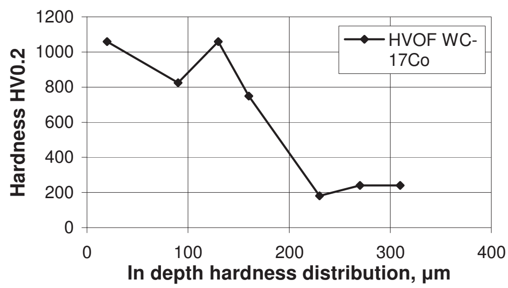

Figure 8. The hardness distribution in laser treated HVOF sprayed WC-Co samples.

3.2. Adhesion test

The results of the adhesion test of TiN and TiAlN-ML coatings on nitrided steel substrate are presented by micrographs in Figs. 9-10. The type and the volume of a failure zone indicate to film adhesion and its brittleness, which corresponds to the microstructure and the mechanical properties of the coatings.

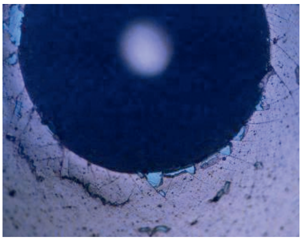

Figure 9. Micrograph of the adhesion test of TiN PVD coating on nitrided steel (NS) at 20 x magnification.

Coatings of higher hardness and lower Young's modulus (higher H/E ratio, TiAlN-ML) withstand the load without adhesive delamination of the coating, but with nucleation of long conical cracks (Class 1). In case of TiN coating, considerable amount of long radial cracks of 100 – 150 µm were generated, causing the partial adhesive delamination of coating that is a typical behaviour of TiN coating under loading (Class 2).

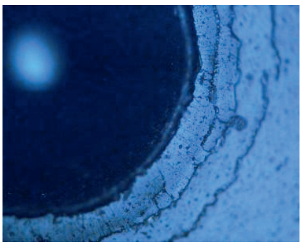

Figure 10. Micrograph of the adhesion test of TiAlN-ML PVD coating on nitrided steel (NS) at 20 x magnification.

The structural defects presented on the surface, such as microdroplets, pores and non-metallic inclusions, simplify chipping/delamination process.

3.3. Abrasive wear rate, indentation surface fatigue and impact wear resistance

It has been recognized that the ranking of materials according to their hardness and elastic modulus *H*/*E* ratio can provide extremely close agreement to their ranking in terms of wear behaviour [1, 11]. The abrasive wear mode is commonly "not suitable" for thin hard PVD coatings. In case of TiN and TiAlN-ML the performance of coatings with higher *H*/*E* ratio corresponds to lower endurance when an adhesive wear mechanism dominates, see Table 6. Although the performance of studied coating systems deposited on HM and HSS drills is quit good [1].

Table 6. Wear rating parameters [12, 13]

Coating	Elastic recovery parameter, H/E	Resistance to plastic deformation, H^3/E^2	Abrasive wear rate, mg×km^{-1}
TiN	0.064	0.114	2.38
TiAlN-ML	0.066	0.087	1.83
WC-17Co	0.022	0.005	3.61

For the abrasion test results the weight loss is given with respect to the weight of abrasive and the sliding distance correspondingly. The volumetric loss was not calculated due to the gradient structure of the coatings. Multilayer coatings have advantage in structure dependent stress distributions in wear resistance. This leads to abrupt brittle fracture of TiN and WC-Co coatings with formation of long radial and cone cracks. The quasi-plastic damage mode prevails for multilayer coatings and in our case for TiAlN-ML. Recently new assessment criteria for hard coatings was proposed – resistance of coating to plastic deformation H^3/E^2 [14].

The results of cyclic indentation surface fatigue resistance of two hard PVD coatings – TiN and TiAlN-ML coatings on HSS and NS substrates are given in Figs. 11-12. After the first indentation, mostly contact region model of coating deformation was presented due to indenting load of 100 N and 500 N applied after 10 000 indentations.

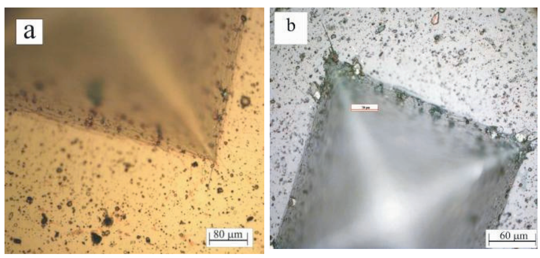

Figure 11. Impression on HSS at 500 N load: a – TiN; b - TiAlN.

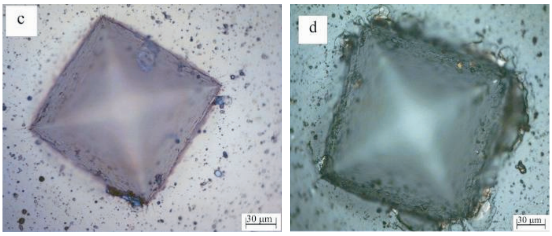

Figure 12. Impression of on NS at 100 N load: c- TiN; d - TiAlN.

PVD hard coatings performed similarly up to 100 indentations. At 1 000 indentations some perimeter delamination was observed in case of TiAlN-ML. This became even more apparent at 10 000 indentations as shown on Fig. 11b.

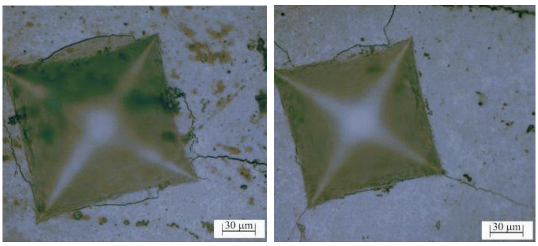

Figure 13. Impression of WC-17Co on C45 at 100 N load: after 1 000 indentations (left); after 10 000 indentations (right).

HVOF sprayed coating exhibited no delamination but cone cracks starting from 100 indentations and radial cracks at 10 000 cycles (Fig. 13).

Multilayer TiAlN (ML) on NS coating has shown the highest indentation surface fatigue and impact wear (surface fatigue wear, see Fig. 14) resistance compared to that of TiN monolayer and thick HVOF spayed WC-Co coatings.

These results can be explained by greater elastic recovery ability (higher H/E and lower E/H ratios) of TiAlN-ML coating [12, 15]. Although, the mechanical properties of substrate play important role in cyclic loading, especially at high loads. During the impact test there is a stress gradient, depending on the elastic modulus ratio between the coating and substrate.

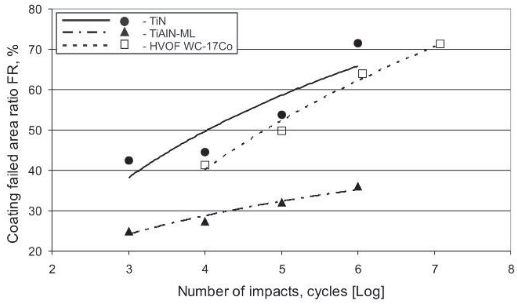

Figure 14. Coatings failure diagram under 80 mJ impacts.

The stress ratio between the coating and substrate can be determined based on the rearranged Hook equation [16]:

$$\frac{\sigma_c - \sigma_s}{\sigma_s} = \frac{E_c - E_s}{E_s} \qquad (1)$$

where σ_c – is the stress applied to coating;
σ_s – is the stress applied to substrate;
E_c – is the coating elastic module;
E_s – is the substrate elastic module.

According to Eq. (1), the stress gradient would be zero if where is no different between coating and substrate elastic modules (E_c=E_s). Therefore, the smaller the difference between the coating and substrate elastic moduli, the lower is the stress gradient, the higher is the wear resistance in impact (cyclic) conditions. The matrix for studied coatings-substrate systems is shown in Table 7.

Table 7. Differences between coating and substrate elastic modulus matrix

Coating/Substrate	Harmetal (HM)	High-speed steel (HSS)	Nitrided steel (NS)
TiN	-0.26	1.09	0.59
TiAlN-ML	-0.49	0.43	0.09
WC-17Co	-0.19	1.29	0.75

The better performance of duplex-coated systems can be explained by much lower magnitude of the tensile stresses in the loaded area due to compressive subsurface stresses (from the nitriding treatment) in combination with compressive stresses in the film (produced by the ion plating technique). This explains the better impact resistance of duplex coatings in comparison to their non-duplex rivals [16].

4. CONCLUSIONS

The recommendations of coating systems selection for different service conditions are proposed:

- to withstand low loads the greater elastic recovery ability (higher H/E ratio) of coating must be achieved;
- to assure best resistance of coating to plastic deformation or high loads the H^3/E^2 ratio must be maximized;
- elastic modulus mismatch between the coating and substrate must be lowest for cyclic loading.

In current study the TiAlN-ML multilayer on hardmetal (HM) substrate is best suitable for high loads tribological application (abrasive wear, sliding wear, impact wear – surface fatigue). The same multilayer coating most endurable at low loads if combined with nitrided steel (NS) substrate.

ACKNOWLEDGEMENTS

This work was supported by the Estonian Ministry of Education and Research (project SF 0140091s08) and the Estonian Science Foundation (grant No. 7889).

REFERENCES

1. Santos, S. C. et al. Tribological characterisation of PVD coatings for cutting tools, Surf. Coat. Tech., 2004, 184, 141–148.
2. VDI 3198:1992-08, Coating (CVD, PVD) of Cold Forging Tools. VDI-Verlag, Düsseldorf, 1991.
3. McGuire, G. E., Rossnagel, S.M., Bunshah, R., F. Handbook of Hard Coatings, Noyes Pub., 2001.
4. Sacher, G., Zenker, R. Subsequent heat treatment of hard coated steels by electron on laser bean, German – Russian Workshop “Tribology and Surface Engineering: theory, experiment, technologies”, Berlin University of Technology, 28-30 March, 2007.
5. Karneva, U., Laberbom, J., Vuoristo, P. Development of thermal spray powders for improved tribological and corrosive applications and cost-effective solutions. Int. J. Mater. Product. Technol., 2007, 28, 377-398.
6. Palmqvist, S. The work for the formation of a crack during Vickers indentation as a measure of the toughness of hard metals. Arch. Eisenhüttenwes, 1962, 33, 629–634.
7. Richter, J. Application of Vickers indentation for assessment of PVD TiN coated new nonledeburitic high-speed steels. Surf. Coat. Tech., 2003, 162, 119–130.
8. CEN/TS 1071-8:2004. Methods of test for ceramic coatings - Part 8: Rockwell indentation test for evaluation of adhesion.
9. Bouzakis, K.-D., Siganos, A. Fracture initiation mechanisms of thin hard coatings during the impact test, Surf. Coat. Tech., 2004, 185, 150-159.
10. Bouzakis, K.-D. et al. The influence of the coating thickness on its strength properties and on the milling performance of PVD coated inserts, Surf. Coat. Tech. 2003, 174 –175, 393–401.
11. Leyland, A., Matthews, A. On the significance of the H/E ratio in wear control: a nanocomposite coating approach to optimised tribological behaviour, Wear, 2000, 246, 1-11.
12. Antonov, M. et al. Assessment of gradient and nanogradient PVD coatings behaviour under erosive, abrasive and impact wear conditions, Wear,2009, 267, 5-8, 898-906.
13. Surzhenkov, A. et al. Wear resistance of laser remelted thermally sprayed coatings, Estonian Journal of Engineering, 2009, 15, 318-328.
14. Musil, J. et al. Relationships between hardness, Young’s modulus and elastic recovery in hard nanocomposite coatings, Surf. Coat. Tech., 2002, 154, 304–313.
15. Sivitski, A. et al. Application of the indentation method for cracking resistance evaluation of hard coatings of tool steels, Estonian Journal of Engineering, 2009, 15, 4, 309-317.
16. Batista, J.C.A. et al. An approach to elucidate the different response of PVD coatings in different tribological tests, Surf. Coat. Tech., 2003, 174 – 175, 891–898.

PAPER V

Surzhenkov, A., Põdra, P., Adoberg, E., Sergejev, F., Saarna, M., Viljus, M., Mikli, V., Kulu, P. Comparative analysis of the duplex I–III generation PVD coatings. *Materials Science (Medžiagotyra)* (accepted for presentation).

Comparative Study of the PVD I–III Generation Coatings on the Plasma Nitrided Steel.

Andrei SURZHENKOV[1*], Priit PÕDRA[2], Fjodor SERGEJEV[1], Mart SAARNA[1], Eron ADOBERG[1], Valdek MIKLI[4], Mart VILJUS[4], Priit KULU[1]

[1] *Department of Materials Engineering, Tallinn University of Technology, Ehitajate tee 5, 19086 Tallinn, Estonia*
[2] *Department of Mechatronics, Tallinn University of Technology, Ehitajate tee 5, 19086 Tallinn, Estonia*

Abstract. In the current study, the cracking, impact and sliding wear resistance of the PVD single layer TiN (I generation), multilayer (Ti,Al)N-ML (II generation), gradient (Al,Ti)N-G and multilayer nanocomposite FiVIc® (both – III generation) coatings on the nitrided low alloy steel 42CrMo4 are analysed. The cyclic indentation test (normal load50 N, 10,000 cycles) was carried out to determine the cracking resistance of the coatings. Impact wear test was performed at the normal load 16 N, strokes' frequency 25 Hz, 10^4 – 10^7 strokes. Sliding wear test was applied, using the block-on-plate scheme, Ø 10 mm Al_2O_3 ball as the counterbody, at the normal load of 10 N, the frequency 5 Hz, the amplitude 10 mm and the test duration 10 min. Best resistance to cracks' formation is demonstrated by the gradient (Al,Ti)N-G coating, showing medium radial cracks' formation, whereas delamination of the coating can be observed in other cases. 1.6 – 1.7 times higher impact wear resistance is shown by the TiN coating in comparison with the other coatings. The FiVIc® coating demonstrates lightly better resistance to sliding wear in comparison with the TiN and (Ti,Al)N-ML coatings due to a lower coefficient of friction. The worst sliding wear resistance is observed in the case of the (Al,Ti)N-G coating due to a high affinity of the coating's and counterbody's materials.

Keywords: duplex treatment, PVD coating, I–III generation, cracking resistance, impact wear, sliding wear

1. INTRODUCTION

Plasma nitriding of a steel substrate has been successfully applied to improve the mechanical properties of a surface layer under I generation single component [1-5] and multicomponent [2,6-9], as II generation multilayer [10,11], as III generation nanocomposite [12] PVD hard coatings. However, no holistic picture of the different generations of PVD coatings [13] on a nitrided substrate is available. In this paper, the comparative analysis of the I-III generations of PVD coatings is made, the resistance of the coatings to cyclic impact loading, impact wear and sliding wear are studied.

2. EXPERIMENTAL

2.1 Substrate preparation

Low-alloy steel 42CrMo4 was chosen as the substrate. Chemical composition and microhardness of steel are brought in Table 1. Specimens were milled to the dimensions of 50 × 25 × 10 mm and subjected to hardening (850 °C, oil) and tempering (500 °C, 2 h). Prior to nitriding the specimens were grinded to the surface finish of Ra = 0.8.

Table 1. Chemical composition of steel 42CrMo4

Steel grade	Chemical composition, wt%	Hardness, HV0.05
42CrMo4	0.38 – 0.45 C, 0.60 – 0.90 Mn, ≤ 0.40 Si, 0.035 P, 0.035 S, 0.90 – 1.20 Cr, 0.15 – 0.30 Mo	315 – 345

2.2 Plasma nitriding

Plasma nitriding using process Plasnit® [14] was carried out at Bodycote OY (Finland). The temperature of the process equalled to 500 … 520 °C, the pressure – to 1 … 10 mbar.

2.3 PVD coating process

The I generation TiN coating, the II generation (Ti,Al)N-ML coating and the III generation (Al,Ti)N-G and FiVIc® coatings were chosen as the objectives of the study. Before the coatings' deposition, a layer of thickness 0.02 mm was grinded down from the nitrided surface in order to remove the 'white layer' [15]. The coatings were deposited using the Platit π80 hardcoating unit. The parameters of coatings' deposition are brought in Table 2 and their thickness and mechanical properties – in Table 3.

2.4 Microstructure studies

Cross-section of a specimen was polished, etched with the 3% nital and studied under the optical microscope (OM) Axiovert 25. Distribution of chemical elements inside the nitrided zone was determined by the means of energy dispersive spectroscopy (EDS) at the scanning electron microscope EVA 25 (Carl Zeiss)

* Corresponding author, tel.: +3725102198, e-mail: andrei.surzenkov@ttu.ee

Table 2. Parameters of deposition of the PVD coatings

Coating	Type	Bias voltage, V	Ti-Al/ AlSi cathode arc current, A	Pressure, 10^{-3} mbar	Temp., °C	Ar flow, sccm	N_2 flow (sccm)	C_2H_2 flow (sccm)
TiN	Monolayer	–75 … –120	100– 125 / -	8	450	6	200	–
(Ti,Al)N-ML	Multilayer	–60 … –150	85 – 125 / 65 – 115	8-15	475	6	200	–
(Al,Ti)N-G	Gradient	–60 … –150	60 – 125 / 52 – 130	4-12	430 – 450	6	150 – 200	–
FiVIc® (NaCo® + DLC)	Multilayer + nanocom-posite	–75 … –150	82 – 125 / 65 – 100	9-12	435 – 475	6	150 – 200	7 – 39

Table 3. Thickness and mechanical properties of the deposited PVD coatings

Coating	Thickness, µm	Nanohard-ness (GPa)	Modulus of elasticity (GPa)	E/H ratio	H^3/E^2 ratio	Coefficient of friction
TiN	2.3	28.5	438	0.065	0.121	0.55
(Ti,Al)N-ML	3.1	19.9	301	0.066	0.086	0.6
(Al,Ti)N-G	3.0	23.8	336	0.071	0.119	0.7
FiVIc®	2.0	29.0	323	0.090	0.233	0.15

2.5 Microhardness measurements

Vickers microhardness at the load of 0.49 N was measured at the polished cross-section of a specimen, beginning from the coating surface towards the middle part in order to determine the case depth. Micromet 2001 (Buehler) microhardness tester was used in the measurements.

2.6 Cyclic indentation testing

To estimate the cracking resistance of the coatings, cyclic indentation at a single point technique was used. Instron 8800 servo hydraulic fatigue test system with the Vickers diamond indenter were applied for this purpose. The scheme of the testing device is brought at Figure 1. All coatings were subjected to 10,000 indentation cycles at the load 50 N. After the testing, the imprints were studied under the optical microscope Axiovert 25. Cracking resistance was estimated by the qualitative evaluation criteria (from weak craking 0 to VI – delamination) [16].

2.7 Impact wear testing

To study the wear resistance of the coatings at the dynamic loads, wear tests were performed at the impact wear tester, designed at TUT [16]. The scheme of the experimental device is brought in Figure 2. The load of 16 N was applied at the stroke frequency of 25 Hz. The linear speed of hammers equalled to 2.75 m/s. The number of strokes varied in the range of 10^4 – 10^6, each next number of cycles was 10 times bigger than the previous. The impact wear scars were studied under theoptical microscope Axiovert 25 with the help of the computer program Buehler Omnimet. The dependence of the indentation stress σ vs. the indentation depth δ was calculated on the base of the measurements' results.

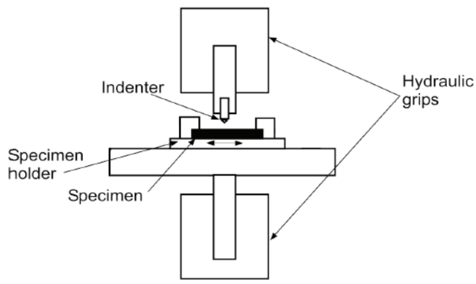

Figure 1. Schematic representation of the cyclic indentation tester [16]

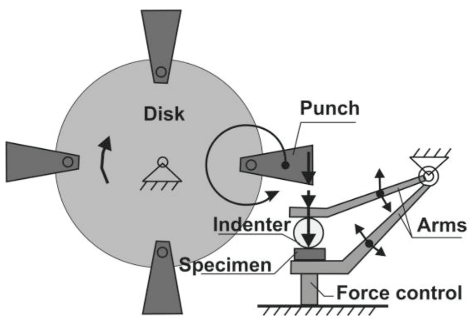

Figure 2. Scheme of the impact wear tester [16]

2.8 Sliding wear testing

Sliding wear resistance of the coatings was tested, applying the ball-on-plate scheme on the Wasau tribometer. The Ø 10 mm Al_2O_3 ball was used as the counterbody, the normal load was 10 N, the frequency – 5 Hz, the amplitude of movement – 10 mm, the duration of the test – 10 min. Each coating was tested 3 times at the same specimen. After the sliding wear test, the depth of the wear scars was determined applying the Mahr profilometer. The average of the measurements' results and the standard deviation were calculated.

3. RESULTS AND DISCUSSION

3.1 Microstructure studies

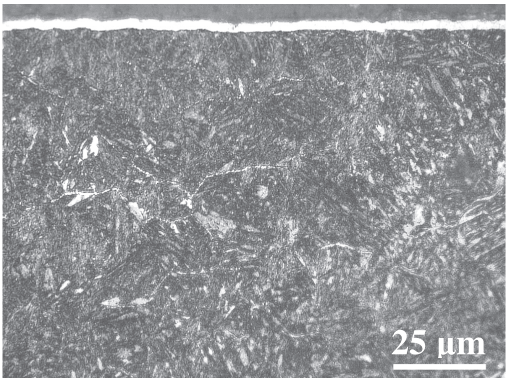

Figure 3. Microstructure of the plasma nitrided PVD coated specimen (TiN coating)

Microstructure of a plasma nitrided specimen is shown in Fig. 3. No white layer can be observed, thus it can be concluded it has been completely removed during grinding. The observed diffusion layer has an eutectic microstructure with the inclusion of carbide particles. Taking into consideration that the nitriding temperature was lower than the phase transition temperature, the observed microstructure has most probably remained after the heat treatment. The structure contains the α phase (Fe(N)) and γ' (Fe_4N) phase, as well as nitrides and carbonitrides [15].

3.2 Microhardness measurements

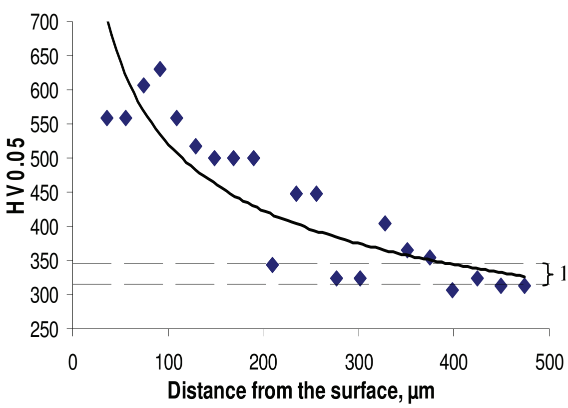

Figure 4. Microhardness distribution inside the nitrided zone of the PVD coated steel (TiN coating); 1- initial microhardness

Microhardness measurements (Fig. 4) show that the depth of the nitrided zone equals to at least 250 µm, which is in correspondence with the nitrogen's diffusion depth, reported by the manufacturer [14]. The decrease in the microhardness values is caused by the reduction of the nitrogen's content in the nitrided layer.

3.3 Cyclic indentation testing

Results of indentation tests are brought in Fig. 5.

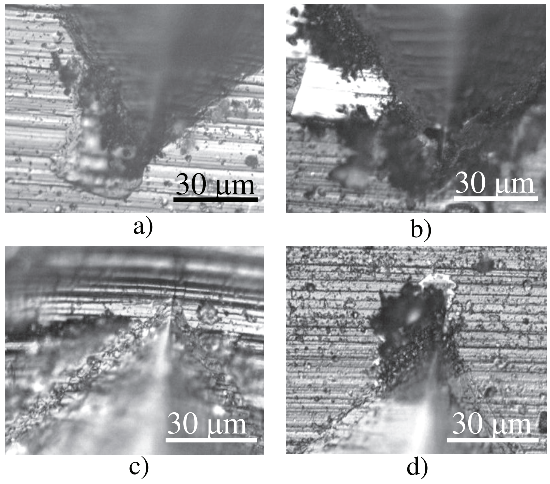

Figure 5. Impressions' corners at the PVD coated plasma nitrided steel after 10,000 indentation cycles: a – TiN, VI class; b – (Ti,Al)N-ML, VI class, c – (Al,Ti)N-G, III class, d - FiVIc®, VI class

As seen at Fig. 5, the PVD coating of the I generation (TiN), II generation ((Ti,Al)N-ML) and III generation (FiVIc®) coatings deformed according to the upfit model (delamination around the corners of the imprint without or with minor cracks' formation). According to the crack evaluation criteria, the crack resistance of these coatings can be estimated as the VI criteria. The best cracking resistance was demonstrated by the PVD III generation (Al,Ti)N-G coating, what can be related as the III criteria (medium radial cracking). The reason for such behaviour of coatings can be related to the differences in chemical compositions of coatings and the substrate, which were minimal in the case of (Al,Ti)N-G coating.

3.4 Impact wear testing.

The impact wear behaviour of coatings depends on the their mechanical properties. The II-III generation PVD coatings demonstrate similar impact wear resistance. The best impact wear resistance is demonstrated by the PVD I generation TiN coating (1.6 – 1.7 times higher than the remaining ones). Such response to the impact wear can be explained by the higher value of modulus of elasticity of the TiN coating, what allows it to resist the deformation during impact better, and similar values of the modulus of elasticity of other coatings.

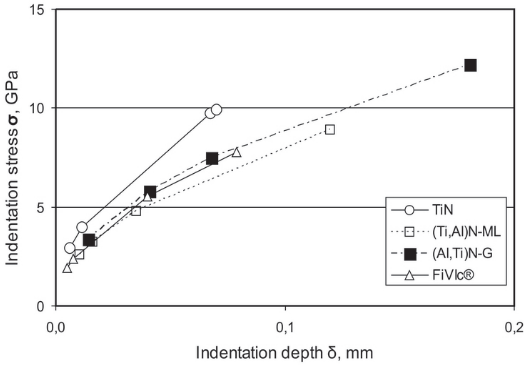

Figure 6. Comparison of the indentation depth of the PVD coatings on the plasma nitrided steel

3.5 Sliding wear resistance.

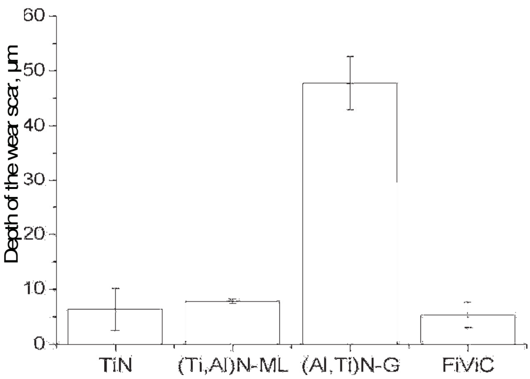

Figure 7. Depths of the wear track on the PVD I-III generations coatings on the nitrided steel

The PVD I generation TiN, II generation (Ti,Al)N-ML and III generation FiVIc® coatings demonstrated similar wear resistance, whereas the lowest average wear value was shown by the FiVIc® coating (1.2 times lower than the TiN and 1.4 times lower, than the (Ti,Al)N-ML coating (Fig. 7)). This fact can be explained by the lowest coefficient of friction of all studied coatings. The highest wear value, demonstrated by the PVD III generation (Al,Ti)N-G coating (8.9 times higher than the FiVIc® one) may be caused by the relatively high Al content in the coating, what, considering the material of the counterbody, may lead to a higher wear.

The smoothest wear scar's profile is obtained in the case of FiVIc® coating (Fig. 8 d), what indicates the smallest amount of abrasive particles, formed during the process. This fact can be explained by the low CoF of DLC layer at the surface of the coating, what prevents the formation of a large amount of wear debris. As it can be seen from Fig. 8, d, the width of the wear scar on the FiVIc® coating is also the smallest among the others, what is a prove of effective support of the underlying nanocomposite NaCo® layer.

Most steepest wear scar's profile was obtained for the (Al,Ti)N-G coating, what is a sign of more brittle

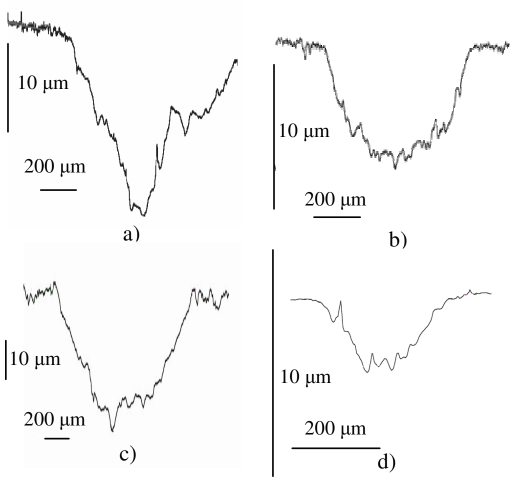

Figure 8. Profiles of the wear scars: PVD a – TiN, b – (Ti,Al)N-ML, c – (Al,Ti)N-G, d - FiVIc® coating

nature of it, what is confirmed by the bigger grooves at the bottom of the scar (Fig. 8, c).

4. CONCLUSIONS.

1. The hard 250 µm deep nitrided zone, consisting of Fe(N), Fe_4N, nitrides, carbonitrides and carbides, has formed during the nitriding process. The microhardness of the nitrided zone varied in the range 450 – 630 HV0.05.
2. The PVD III generation (Al,Ti)N-G coating demonstrated the best cracking resistance (III class of the cracking evaluation criteria) in comparison with the other coatings (VI class of the cracking evaluation criteria) due to the biggest affinity of the chemical composition between the coating and the substrate.
3. The 1.6 – 1.7 times higher impact wear resistance was demonstrated by the PVD I generation TiN coating in comparison with the other studied coatings due to the highest modulus of elasticity
4. The PVD III generation FiVIc® coating showed the 1.2 – 8.9 better wear resistance in comparison with the other studied coatings due to the lowest coefficient of friction.
5. Lowest wear, shown by the FiVIc® coating, is explained a combination of a low friction DLC layer at the surface and tough supportive nanocomposite NaCo® layer. The highest wear, observed on the (Al,Ti)N-G coating, is caused by the biggest affinity of the coating's material to the counterbody's material and by a more brittle nature of the coating.

Acknowledgements

Authors express their sincere acknowledgement to M.-M. Nanits, M. Hiiemaa and A. Põlder from the Department of Mechatronics, Tallinn University of Technology, for their help with the profilometer measurements. This work was supported by the Estonian Ministry of Education and Research, project SF0140091s08.

References

1. **Lee S.Y., Kim S.D., Hong Y.H.** Application of the duplex TiN coatings to improve the tribological properties of Electro Hydrostatic Actuator pump parts. *Surf. Coat. Tech.* 193 2005: pp. 266-271.
2. **Batista J.C.A., Godoy C., Buono V.T.L., Matthews A.** Characterization of duplex and non-duplex (Ti,Al)N and Cr–N coatings. *Mater. Sci. Eng. A* 336 2002: pp. 39-51.
3. **Chekour L., Nouveau C., Chala A., Djouadi M.-A.** Duplex treatment of 32CrMoV13 steel by ionic nitriding and triode sputtering: application to wood machining. *Wear* 255 2003: pp.1438-1443.
4. **Staia M.H., Pérez-Delgado E.S., Sancher C., Castro A., Le Bourhis E., Puchi-Calbera E.S.** Hardness properties and high-temperature wear behaviour of nitrided AISI D2 tool steel, prior and after PAPVD coating. *Wear* 267 2009: pp. 1452-1461.
5. **Panjan P., Čekada M., Kirn R., Soković M.** Improvement of die-casting tools with duplex treatment. *Surf. Coat. Tech.* 180-181 2004: pp. 561-565.
6. **Batista J.C.A., Godoy C., Pintaúde G., Sinatora A., Matthews A.** An approach to elucidate the different response of PVD coatings in different tribological tests. *Surf. Coat. Tech.* 174-175 2003: pp. 891-898.
7. **Jaeger G., Endler I., Bartsch K., Heilmaier M., Leohnardt A.** Fatigue behaviour of duplex treated TiC_xN_{1-x} and $Ti_{1-x}Al_xN$-hard coating steel compounds. *Surf. Coat. Tech.* 150 2002: pp. 282-289.
8. **Podgornik, B., Vižintin, J., Wänstrand, O., Larsson, M., Hogmark, S., Ronkainen, H., Holmberg, K.** Tribological properties of plasma nitrided and hard coated AISI 4140 steel. *Wear* 249 2001: pp. 254 – 259.
9. **Podgornik, B., Vižintin, J., Wänstrand, O., Larsson, M., Hogmark, S.** Wear and friction behaviour of duplex-treated AISI 4140 steel. *Surf. Coat. Tech.* 120 – 121 1999: pp. 502 – 508.
10. **Terčelj M., Panjan P., Urankar I., Fajfar P., Turk R.** A newly designed laboratory hot forging test for evaluation of coated tool wear resistance. *Surf. Coat. Tech.* 200 2006: pp. 3594-3604.
11. **Rahman M., Haider J., Dowling D.P., Duggan P., Hashmi M.S.J.** Investigation of mechanical properties of TiN+MoS_x coating on plasma-nitrided substrate. *Surf. Coat. Tech.* 200 2005: pp. 1451-1457.
12. **Guruvenket S., Li D., Klemberg-Sapieha J.E., Martinu L., Szpunar J.** Mechanical and tribological properties of duplex treated TiN, nc-TiN/a-SiN_x and nc-TiCN/a-SiCN coating deposited on 410 low alloy stainless steel. *Surf. Coat. Tech.* 203 2009: pp. 2905-2911.
13. **Donnet C., Erdemir A.** Historical developments and new trends in tribological and solid lubricant coatings. *Surf. Coat. Tech.* 180-181 2004: pp. 76-84.
14. Description of production methods, used on Bodycote OY, http://www.bodycote.fi/fi/leftframe/Leftframeset_menetelm%E4t.htm, 24.04.2011 [in Finnish].
15. **Schaaf P.** Laser nitriding of metals. *Progress in Materials Science* **47 2002: pp.1-161.**
16. **Kulu, P., Saarna, M., Sergejev, F., Gregor, A., Surženkov, A.** (2010). Selection of coating systems and processes for different wear conditions. *Proceedings of 14th Nordic Symposium on Tribology*, NORDTRIB 2010, 08.06 - 11.06.2010, Storforsen, Sweden: pp. 1 - 8.

DISSERTATIONS DEFENDED AT TALLINN UNIVERSITY OF TECHNOLOGY ON *MECHANICAL AND INSTRUMENTAL ENGINEERING*

1. **Jakob Kübarsepp**. Steel-bonded hardmetals. 1992.
2. **Jakub Kõo**. Determination of residual stresses in coatings & coated parts. 1994.
3. **Mart Tamre**. Tribocharacteristics of journal bearings unlocated axis. 1995.
4. **Paul Kallas**. Abrasive erosion of powder materials. 1996.
5. **Jüri Pirso**. Titanium and chromium carbide based cermets. 1996.
6. **Heinrich Reshetnyak**. Hard metals serviceability in sheet metal forming operations. 1996.
7. **Arvi Kruusing**. Magnetic microdevices and their fabrication methods. 1997.
8. **Roberto Carmona Davila**. Some contributions to the quality control in motor car industry. 1999.
9. **Harri Annuka**. Characterization and application of TiC-based iron alloys bonded cermets. 1999.
10. **Irina Hussainova**. Investigation of particle-wall collision and erosion prediction. 1999.
11. **Edi Kulderknup**. Reliability and uncertainty of quality measurement. 2000.
12. **Vitali Podgurski**. Laser ablation and thermal evaporation of thin films and structures. 2001.
13. **Igor Penkov**. Strength investigation of threaded joints under static and dynamic loading. 2001.
14. **Martin Eerme**. Structural modelling of engineering products and realisation of computer-based environment for product development. 2001.
15. **Toivo Tähemaa**. Assurance of synergy and competitive dependability at non-safety-critical mechatronics systems design. 2002.
16. **Jüri Resev**. Virtual differential as torque distribution control unit in automotive propulsion systems. 2002.
17. **Toomas Pihl**. Powder coatings for abrasive wear. 2002.
18. **Sergei Letunovitš**. Tribology of fine-grained cermets. 2003.
19. **Tatyana Karaulova**. Development of the modelling tool for the analysis of the production process and its entities for the SME. 2004.
20. **Grigori Nekrassov**. Development of an intelligent integrated environment for computer. 2004.
21. **Sergei Zimakov**. Novel wear resistant WC-based thermal sprayed coatings. 2004.
22. **Irina Preis**. Fatigue performance and mechanical reliability of cemented carbides. 2004.

23. **Medhat Hussainov**. Effect of solid particles on turbulence of gas in two-phase flows. 2005.

24. **Frid Kaljas**. Synergy-based approach to design of the interdisciplinary systems. 2005.

25. **Dmitri Neshumayev**. Experimental and numerical investigation of combined heat transfer enhancement technique in gas-heated channels. 2005.

26. **Renno Veinthal**. Characterization and modelling of erosion wear of powder composite materials and coatings. 2005.

27. **Sergei Tisler**. Deposition of solid particles from aerosol flow in laminar flat-plate boundary layer. 2006.

28. **Tauno Otto**. Models for monitoring of technological processes and production systems. 2006.

29. **Maksim Antonov**. Assessment of cermets performance in aggressive media. 2006.

30. **Tatjana Barashkova**. Research of the effect of correlation at the measurement of alternating voltage. 2006.

31. **Jaan Kers**. Recycling of composite plastics. 2006.

32. **Raivo Sell**. Model based mechatronic systems modeling methodology in conceptual design stage. 2007.

33. **Hans Rämmal**. Experimental methods for sound propagation studies in automotive duct systems. 2007.

34. **Meelis Pohlak**. Rapid prototyping of sheet metal components with incremental sheet forming technology. 2007.

35. **Priidu Peetsalu**. Microstructural aspects of thermal sprayed WC-Co coatings and Ni-Cr coated steels. 2007.

36. **Lauri Kollo**. Sinter/HIP technology of TiC-based cermets. 2007.

37. **Andrei Dedov**. Assessment of metal condition and remaining life of in-service power plant components operating at high temperature. 2007.

38. **Fjodor Sergejev**. Investigation of the fatigue mechanics aspects of PM hardmetals and cermets. 2007.

39. **Eduard Ševtšenko**. Intelligent decision support system for the network of collaborative SME-s. 2007.

40. **Rünno Lumiste**. Networks and innovation in machinery and electronics industry and enterprises (Estonian case studies). 2008.

41. **Kristo Karjust**. Integrated product development and production technology of large composite plastic products. 2008.

42. **Mart Saarna**. Fatigue characteristics of PM steels. 2008.

43. **Eduard Kimmari**. Exothermically synthesized B_4C-Al composites for dry sliding. 2008.

44. **Indrek Abiline**. Calibration methods of coating thickness gauges. 2008.

45. **Tiit Hindreus**. Synergy-based approach to quality assurance. 2009.

46. **Karl Raba**. Uncertainty focused product improvement models. 2009.

47. **Riho Tarbe**. Abrasive impact wear: tester, wear and grindability studies. 2009.

48. **Kristjan Juhani**. Reactive sintered chromium and titanium carbide- based cermets. 2009.

49. **Nadežda Dementjeva**. Energy planning model analysis and their adaptability for Estonian energy sector. 2009.

50. **Igor Krupenski**. Numerical simulation of two-phase turbulent flows in ash circulating fluidized bed. 2010.

51. **Aleksandr Hlebnikov**. The analysis of efficiency and optimization of district heating networks in Estonia. 2010.

52. **Andres Petritšenko**. Vibration of ladder frames. 2010.

53. **Renee Joost**. Novel methods for hardmetal production and recycling. 2010.

54. **Andre Gregor**. Hard PVD coatings for tooling. 2010.

55. **Tõnu Roosaar**. Wear performance of WC- and TiC-based ceramic-metallic composites. 2010.

56. **Alina Sivitski**. Sliding wear of PVD hard coatings: fatigue and measurement aspects. 2010.

57. **Sergei Kramanenko**. Fractal Approach for Multiple Project Management in Manufacturing Enterprises. 2010.

58. **Eduard Latõsov**. Model for the Analysis of Combined Heat and Power Production. 2011.

59. **Jürgen Riim**. Calibration Methods of Coating Thickness Standards. 2011.

60. **Andrei Surženkov**. Duplex Treatment of Steel Surface. 2011.